Isotope geology and Miocene magmatic evolution along the northern border of the Menderes Massif (NW Anatolia, Turkey)

Dissertation

zur Erlangung des Grades eines Doktors der Naturwissenschaften

der Geowissenschaftlichen Fakultät
der Eberhard Karls Universität Tübingen

vorgelegt von

ALTUĞ HASÖZBEK

aus İzmir/Türkei

2010

Tag der mündlichen Prüfung: 21.07.2010

Dekan: Prof. Dr. Peter Grathwohl

1. Berichterstatter: Prof Dr. Dr. h.c. Muharrem Satır

2. Berichterstatter: Prof Dr. Burhan Erdoğan

3. Berichterstatter: Prof Dr. Wolfgang Siebel

Contents

Acknowledgements……. IV

Abstract / Zusammenfassung……..... V

Introduction and aims of the study……..... 1

Geological overview……....4

Summary of the publications…….. 8

References…….. 22

Supplementary

Chapter 1: Early Miocene granite formation by detachment tectonics or not?

A case study from the northern Menderes Massif (Western Turkey) 17

Chapter 2: Early Miocene post-collisional magmatism in NW Turkey:

geochemical and geochronological constraints……...48

Chapter 3: Al-in hornblende thermobarometry and petrogenesis of the

Alaçam granite in NW Anatolia Turkey)…….76

Acknowledgements

I would like to send my sincere appreciation to my supervisors Prof Dr. Dr. h. c. Muharrem Satır, Prof. Dr. Burhan Erdoğan and Prof. Dr. Wolfgang Siebel for their supervision and motivation that supported me throughout this study. Their point of view in geology and their patience gave me a chance to expand my geological background both in the fields, isotope geology and analytical techniques. I also would like to thank Dr. Erhan Akay for his support and his views in every step of this study. I'm also grateful to Prof. Dr. Osman Candan, Prof. Dr. Günay Çifci, Dr. Talip Güngör, Dr. İsmail İşintek, Dr. Ersin Koralay, and Dr. Cüneyt Akal, G. Deniz Doğan for their helps to make me feel more motivated and strong during hard steps of my study. Profs. A. İ. Okay, P. Bons and G. Topuz are also thanked for their constructive comments on my manuscripts. My thanks also go to Dr. Wenzel for his help during electron microprobe analysis and Dr. Schulz for his help during CL analyses. I would also express my thanks to all of the kind people who are working in Department of Geochemistry in Tübingen University, Department of Geology and Vocational School of Higher Education of Torbalı in Dokuz Eylül University, İzmir (Turkey). Especially my thanks go to Dr. Taubald, E. Reitter, G. Bartholomä, Dr. Kibaroglu, K. Akbayram, Dr. Sunal, Dr. Shang, B. Steinhilber, G. Stoschek, J. Zöldföldi, S. Eroğlu, V. Leno, and U. Wahl for their friendship and invaluable technical help at the Tübingen University, C. T. Akdag, H. Elçi and Dr. Kılınç for their friendly support at Dokuz Eylül University. I am also so grateful to have meet C. Thomson and J. Thomson in the last months of my PhD for their friendly support and corrections of the English text.

This study was financially supported by projects of the scientific and Technical Research Council of Turkey (TUBITAK) - project no: 104Y036, the Graduate School and Applied Science of Dokuz Eylül University - project no: 2009.KB.Fen.074, and DAAD (Deutscher Akademischer Austausch Dienst). I'm also grateful to the people of these organizations for their supports.

Finally, I wish to thank my family for their trust and support during my academic studies. This PhD thesis is especially dedicated to memories of my mother Nesrin Hasözbek, my father Rüştü Hasözbek, and to the one (whoever you may be) who makes 'the Blue' possible.

Abstract

In the Aegean region, complex geodynamic processes including subduction, continent-continent collision, and back-arc extension occurred from the Eocene to the present time. In NW Anatolia (Turkey), the products of these events are widely exposed. Especially, Miocene granites along the northern border of the Menderes Massif demonstrate prominent geologic features associated with these complex geodynamic events. In order to determine the magmatic evolution of the northern boundary of the Menderes Massif and to understand its tectono-magmatic position in the Aegean region, during and after the collision of the Anatolide-Tauride platform with the Sakarya Continent, two regions in NW Anatolia (Simav and Alaçam regions) were examined by detailed mapping, geochemical, isotopic and geochronological studies.

After the closure of the Neo-Tethys and the collision of the Menderes Platform with the Sakarya Continent during the Cretaceous, a nappe package consisting of four main tectonic zones was formed in NW Anatolia. These are: (1) Menderes metamorphics, (2) Meta-ophiolithic nappe complex, (3) Afyon Zone, and (4) Bornova Flysch Zone. This nappe package, stacked together by the collision, was intruded and stitched by Early Miocene granitic plutons that constitute a NE-SW trending magmatic belt that evolved in a thick continental crust. In the Simav region, Eğrigöz and Koyunoba granites are intrusive to the Menderes Metamorphics and Afyon Zone. In the Alaçam region, the Alaçam granite shows clear cross-cutting relations with the Menderes Massif, Afyon Zone, and Bornova Flysch Zone. The Eğrigöz, Koyunoba, and Alaçam are undeformed magmatic bodies and present similar geological, geochemical, isotopic, and geochronological features. They are shallow-seated bodies (2-7 km), granite-granodiorite and monzogranite in composition, and are I-type, calc-alkaline in nature. Their Sr-Nd-Pb-O isotopes are in line with derivation from lower-to middle crustal source lithologies. It can be demonstrated that crustal assimilation during the magma generation played an important role. Radiogenic age determinations from the granites show that the U-Pb zircon crystallization ages are between 19.4 ± 4.4 Ma for the Eğrigöz granite, 21.7 ± 1.0 Ma for the Koyunoba granite, 20.0 ± 1.4 Ma, and 20.3 ± 3.3 Ma for the Alaçam granite and from its related stock. Mica cooling ages of 18.77 ± 0.19 Ma for the Eğrigöz granite and early Miocene (20.01 ± 0.20 Ma and 20.17 ± 0.20 Ma) cooling ages of the Alaçam granite and its related stocks were also obtained by Rb-Sr (whole rock, biotite)

analyses which indicate rapid cooling. Moreover, U-Pb zircon ages from the country rocks of the Miocene granites yield 30.04 ± 0.56 Ma for a metagranite of the Menderes Massif in Simav region and 314.9 ± 2.7 Ma for gneissic granite of the Afyon Zone in the Alaçam region, which were both previously interpreted as a sheared part of the Miocene Eğrigöz and Alaçam granites.

Field occurrences, geochemical, isotopic characteristics and geochronological data obtained from the Eğrigöz, Koyunoba and Alaçam granites show close similarities with other Oligo-Miocene granitoids in northwestern Anatolia. It is concluded that all granitoids from this belt emplaced along an E-W trending regional zone in a compressional regime, rather than representing individual bodies related to local, north-dipping, low-angle detachment faults, as suggested in previous papers.

Zusammenfassung

Seit dem Eozän finden in der Ägäis komplexe geodynamische Prozesse statt, die Subduktion, Kontinent-Kontinent Kollision und Dehnung im Back-arc Bereich umfassen. In Nordwest Anatolien (Türkei) sind die Produkte dieser Ereignisse weiträumig aufgeschlossen. Insbesondere weisen miozäne Granite entlang des Nordrandes des Menderes Massivs markante geologische Merkmale auf, die mit diesen komplexen geodynamischen Prozessen in Verbindung stehen. Um die magmatische Entwicklung des Nordrandes des Menderes Massivs während und nach der Kollision der Anatolisch-Tauridischen Platte mit dem Sakarya Kontinent nachzuvollziehen, wurden zwei Regionen in Nordwest Anatolien (Simav Region und Alaçam Region) mittels ausführlicher Kartierung sowie geochemischer, isotopischer und geochronologischer Analysen untersucht.

Nach der Schließung der Neotethys, der Bildung der Izmir-Ankara Zone und der Kollision der Menderes Platte mit dem Sakarya Kontinent während der Kreide, kam es zu großräumigen Deckenbildungen. Die Decken können folgendermaßen untergliedert werden: (1) Menderes Metamorphite, (2) ein metaophiolitischer Deckenkomplex, (3) die Afyon Zone und (4) die Bornova Flysch Zone. Im Untermiozän intrudierten in dieses Deckenpaket granitische Plutone, die einen magmatischen Gürtel bilden und sich vom Nordost nach Südwest erstrecken. Dieser Prozeß bewirkte eine Verdickung der kontinentalen Kruste. In der Simav-Region intrudierten die Eğrigöz und Koyuonba-Granit in die Menderes Metamorphite und die Afyon Zone. In der Alaçam Region zeigt der Alaçam Granite klare Intrusivkontakte sowohl zu den Menderes Metamorphiten, als auch der Afyon und der Bornova Flysch Zone. Bei all diesen Graniten handelt es sich undeformierte magmatische Körper, die im Miozän entstanden sind und das Schwerpunktthema der vorliegenden Dissertation bilden. Die Granite ähneln sich in ihren geologischen, geochemischen, isotopischen und geochronologischen Merkmalen. Es handelt sich um flach intrudierte Körper (2-7 km Tiefe) von granit-granodioritischer und monzogranitischer Zusammensetzung (I-Typ Granite), die eine kalkalkaline Affinität vorweisen. Die Sr-Nd-Pb-O Isotopenzusammensetzung weist auf eine tief- bis mittelkrustalen Herkunft der Schmelzen hin. Es kann gezeigt werden, dass Krustenassimilation während der Magmenbildung eine wichtige Rolle gespielt hat. Isotopische Altersbestimmungen an den Graniten zeigen, dass das Kristallisationsalter bei 19.4 ± 4.4 Ma für den Eğrigöz Granit und bei 21.7 ± 1.0 Ma für den Koyuonba Granit liegt

und bei 20.0 ± 1.4 Ma und 20.3 ± 3.3 Ma für den Alaçam Granit. Abkühlungsalter von 18.77 ± 0.19 Ma für den Eğrigöz Granit und solche von 20.01 ± 0.20 Ma und 20.17 ± 0.20 Ma für den Alaçam Granit wurden mittels Rb-Sr Analysen (Gesamtgestein und Biotit) erhalten. Die Isotopendaten deuten auf eine schnelle Abkühlung der Magmen hin. Darüber hinaus wurde das Umgebungsgestein der Granite, welches zuvor als deformierte Randfazies gedeutet wurde, auf 30.04 ± 0.56 Ma (Metagranit des Menderes Massivs in der Simav Region) und 314 ± 2.7 Ma (Metagranit der Afyon Zone in der Alaçam Region) datiert.

Die Geländebeobachtungen, geochemische Charakteristika und geochronologische Daten der Eğrigöz, Koyunoba und Alaçam Granite zeigen große Ähnlichkeiten mit anderen Oligo-Miözänen Granitoiden aus Nordwest Anatolien. Es wird daraus geschlossen, dass alle Granitoide dieses Gürtels entlang einer Ost-West streichenden regionalen Zone während eines kompressionalen Regimes intrudierten und nicht, wie in vorhergehenden Publikationen behauptet, als individuelle Körper, die im Zusammenhang mit lokalen, nach Norden einfallenden, flach winkligen Abscherzonen (sog. detachment faults) stehen.

Introduction and aims of this study

The Africa-Eurasia convergent zone in the Aegean region is characterized by complex geodynamic processes resulting from subduction, back-arc extension, and continent-continent collision from the end of the Cretaceous to present day. In the Aegean region, HP-LT metamorphic rocks, post-collisional magmatic belts and back-arc extension related volcanic fields are widely exposed. To demonstrate the complex geodynamic scenario of the Africa-Eurasia convergent zone in the Aegean region, western Anatolia is one of the key areas.

In western Anatolia, the internal stratigraphy, magmatic and metamorphic evolution of the Menderes Massif and its neo-tectonic exhumation history have been studied extensively (Akkök 1983; Şengör et al. 1984a; Satır and Friedrichsen 1986; Erdoğan 1992; Erdoğan and Güngör 1992; 2004; Hetzel et al. 1995a; Bozkurt and Satır 2000; Satır & Taubald 2001; Candan et al. 2001; Whitney & Bozkurt 2002; Ring et al. 2003; Seyitoğlu et al. 2004; Catlos & Çemen 2005; Whitney et al 2005; 2008; Çemen et al. 2006; Westaway 2006; Catlos et al. 2010; Bozkurt et al 2010). The uplift of the massif was first proposed to occur along high-angle normal faults during the neotectonic period by which graben structures of Western Anatolia were formed (Şengör and Yılmaz, 1981; Şengör et al. 1984a; 1984b; Dora et al. 1990; 1995; Yılmaz 1997). Since the early 1990's an alternative model has arisen suggesting that extensional low-angle normal faults were effectively active during the neo-tectonic period and that tectonic denudation was the cause of the exhumation (Verge 1993; Bozkurt and Park 1994; Hetzel et al. 1995a; 1995b; Lips et al. 2001; Ring et al. 2003; Seyitoğlu et al. 2004; Purvis and Robertson 2004; Çemen et al. 2006; Catlos et al. 2010; Bozkurt et al. 2010) that led to assigning the Menderes Massif as a metamorphic core complex. In this model, the boundary between the high-grade metamorphic Menderes Massif and tectonically overlying less or nonmetamorphic units was suggested as an extensional detachment zone. Along this regional scale extension related zone in NW Anatolia, most of the granitoids with its related volcanic counterparts were previosly interpreted as a result of this tectonic event and related to the formation of core complexes (Okay and Satır 2000; Işık and Tekeli 2001; Işık et al. 2004; Seyitoğlu et al. 2004; Ring and Collins 2005; Thomson and Ring 2006; Erkül, 2009).

In NW Anatolia, the closure of the Neo-Tethys resulted in progressive collision of the Tauride-Anatolide Platform with the Sakarya Continent. This process was associated with widespread post-collisional, alpine-type magmatism. The generation of pre- (subduction-related), syn-, and

post-collisional magmatism is well documented and most authors suggest a southward retreat of the African lithospheric plate (Hellenic subduction zone) (Dilek & Altunkaynak 2009; Jolivet & Brun 2010; Stouariti et al. 2010) as the ultimate cause of this magmatism. Arc migration resulted in the emplacement of granitoids both in the Balkan region, Aegean islands and NW Anatolia. In NW Anatolia, Oligo-Miocene magmatism comprises subvolcanic and plutonic rocks which form a NW trending belt close to the northern border of the Menderes Massif (Akay 2009). According to previous works, two types of emplacement are suggested for the Miocene granitoids: **(1)** Recent model puts forward the idea that the Miocene granites emplaced syn-kinematically along an extensional detachment fault at ca. 23-20 Ma (Okay and Satır 2000; Işık and Tekeli 2001; Işık et al. 2004; Seyitoğlu et al. 2004; Ring and Collins 2005; Thomson and Ring 2006; Erkül 2009). (2) In an alternative model, a regional compressional regime was proposed for the Miocene granites and their volcanic equivalents along a magmatic belt instead of an individual extensional zone (Genç 1998; Altunkaynak and Yılmaz 1998; Karacık and Yılmaz 1998; Yılmaz 1997; Yılmaz et al. 2001; Akay 2009).

Due to the controversial emplacement models for the Miocene granites, which are mainly used as evidence for the formation of the core complexes and to understand the geodynamic evolution of the NW Anatolia, we focused on two main regions along the northern border of the Menderes Massif. In these regions, the tectonic belts of the Menderes Massif, Afyon Zone and Bornova Flysch zone are intruded by Miocene granitoids. These regions are: **(1)** Simav region (Kütahya), **(2)** Alaçam region (Balıkesir). Limited number of studies have been carried out so far in these regions (Akdeniz and Konak 1979 a, b; Akkök 1983; Dora et al. 1990; 1995; Işık and Tekeli 2001; Işık et al. 2004; Seyitoğlu et al. 2004; Ring and Collins 2005; Thomson and Ring 2006; Özgenç and İlbeyli 2008; Akay 2009; Erkül 2009). This thesis focuses on the evolution of the Eğrigöz and Koyunoba granites in the Simav region, and the Alaçam granite with its related stocks in the Alaçam region. An important aim of this thesis is to find arguments whether or not **(1)** low-angle normal faults caused the Miocene magmatism, and **(2)** the Eğrigöz, Koyunoba and Alaçam granites are genetically related with a low-angle detachment zone along the northern border of the Menderes Massif.

In order to elucidate the emplacement problem of the early Miocene granitic intrusions in the northern Menderes Massif, we remapped both the Simav and Alaçam regions and obtained U-Pb zircon ages from the granites, and from a metagranitic body of the Menderes Massif and the Afyon Zone. ^{207}Pb-^{206}Pb single zircon evaporation ages were obtained from a gneissic rock of

the Menderes Massif. In addition to that, three Rb-Sr biotite ages from the Eğrigöz and Alaçam granites were obtained. Al-in hornblende barometry calculations were performed to evaluate the emplacement depth of the Miocene Alaçam granite. This thesis is divided into three chapters to discuss the Miocene magmatic evolution of the northern margin of the Menderes Massif in the light of new geological, mineralogical, isotopic and geochronological evidence.

Geological overview

In NW Anatolia, nappe packages formed during the collision of the Tauride-Anatolide Block to the south and the Sakarya Continent to the north. These nappe packages which are exposed in both study areas (Simav region, Alaçam region) comprise from south to north, **(1)** A high-to-medium grade metapelite association (the Menderes Massif) (Akdeniz and Konak 1979 a, b; Akkök 1983; Dora et al. 1990), **(2)** a HP-LT belt tectonically overlying the Menderes Massif along its northern border (the Afyon Zone) (Okay et al. 1996; Candan et al. 2005), and **(3)** an internally sheared flysch (the Bornova Flysch Zone) tectonically overlying the Menderes metamorphics and the Afyon Zone along its northwest margin (Okay et al. 1996).

Metamorphic associations of the Menderes Massif are widely exposed in NW Anatolia and can be divided into three sub-massifs: **(1)** southern sub-massif, **(2)** central sub-massif, and **(3)** northern sub-massif (Bozkurt et al. 1993; 1995 and references therein). The study regions are located within the northern sub-massif which is dominated by gneiss-schist-marble associations and metagranites and these high-grade units of the massif are tectonically overlain by less metamorphosed rocks of the Afyon Zone.

Originally, the Afyon zone was separated as an individual tectonic zone by Okay (1984). In previous studies, the Afyon zone was interpreted to have been formed under greenschist facies conditions (Okay, 1984; Okay et al. 1996). However, recent papers suggest that a HP-LT metamorphism took place in the central parts of the zone (Candan et al. 2005). In the Simav region, the Afyon zone consists of metadetrital and metavolcanic rock lithologies. These rocks grade into metacrystalline basement rocks outside of the study area. In both regions, the Afyon zone is conformably overlain by strongly recrystallized limestones known as Budağan Limestone (Kaya, 1972). The Menderes Massif and the Afyon Zone are tectonically overlain by the slightly deformed Bornova Flysch Zone representing the Izmir-Ankara Zone. This zone comprises ophiolitic and carbonate blocks embedded in slightly sheared sandstone and mudstone matrix. In both study regions, the nappe packages are intrusively cut by the Miocene granitic bodies and their volcanic counterparts. These granites are: **(1)** Eğrigöz and Koyunoba granites (Simav region), **(2)** Alaçam granite and its related stocks (Alaçam region).

1. *Eğrigöz and Koyunoba granites*

Eğrigöz and Koyunoba granites crop out along the northern part of the Simav village (Kütahya) in the northern Menderes Massif. These granites constitute the Simav Magmatic Complex with their volcanic counterparts (Akay, 2009). The long axis of these granitoids extends approximately in a NNE-SSW direction. The Eğrigöz granite is 18 x 32 km, and the Koyunoba granite is 10 x 18 km in diameter. Both granites are generally light pinkish and gray; in places light brownish in color and strongly altered. They are mostly granitic to monzonitic in composition and penetrated by aplite and pegmatite dykes. The texture of the granites is holocrystalline and partly porphyritic to granophyric with well defined myrmekitization and perthitization in feldspars. At the margins of the granitoids, the texture is fine grained, grading into a coarser grained texture towards the center of the plutons. The sizes of pink colored orthoclase phenocrystals may reach up to 0.5-2 cm.

Contacts between granites and the basement country rocks are clearly intrusive and at the contacts they are undeformed. Close to the contact, the Eğrigöz and Koyunoba granites contain augen gneisses of the Menderes Massif as enclaves. Along the intrusive boundary, both granites display minor deformation structures such as fracture cleavage and lineation. These deformed zones, not more than 1-5 m in width, gradually pass into undeformed granite toward the central part of the bodies. Moreover, the Eğrigöz and Koyunoba granites engulfed boulders of the Menderes Massif and the Afyon Zone as roof pendants. The presence of such large roof pendants (ca. 3 x 4 km) inside the granites indicate shallow crustal emplacement of these granites.

2. *Alaçam granite and its related stocks*

The Alaçam granite and its related stocks are exposed in the southeastern part of the Dursunbey town (Balıkesir) along the northern Menderes Massif. The granite has an elongated shape and extends approximately in a NNW-SSE direction, and the dimension of the granite is about 5 x 12 km. The granite is mostly gray in color, and displays typical holocrystalline and in places porphyritic in texture. The lithological features of the Alaçam granite show similarities to the Eğrigöz and Koyunoba granites.

The granite and its related stocks exhibit cross-cutting relations with the Menderes Massif, Afyon Zone and Bornova Flysch Zone. No deformation is observed with the exception of a slightly deformed microgranitic endocontact which is probably related to rapid cooling.

An ongoing debate along the northern Menderes Massif is, whether the Miocene granites are related to a regional extensional event or not. In previous models (Işık and Tekeli 2001; Işık et al. 2004; Seyitoğlu et al. 2004; Ring and Collins 2005; Thomson and Ring 2006; Erkül, 2009), the boundary between the high-grade metamorphic Menderes Massif and the tectonically overlying less or nonmetamorphic units was suggested as an extensional detachment zone and some of the main evidences presented for this model are: **(1)** Synkinematic granite intrusions emplaced into footwall rocks with upward, gradual change in texture from undeformed to sheared granites and a low-angle normal sense of shear and brittle deformed overprint (Işık and Tekeli 2001; Işık et al. 2004; Seyitoğlu et al. 2004), **(2)** $^{40}Ar/^{39}Ar$ ages of mylonitic gneisses in the footwall rocks and U-Th-Pb (SIMS) dates of leucogranite dykes demonstrating close age agreement with the so-called syn-kinematic granitoids and **(3)** Thermo-chronologic evidence for rapid cooling that was interpreted as a result of tectonic denudation by low-angle normal faulting rather than erosion (Işık and Tekeli 2001; Işık et al. 2004; Seyitoğlu et al. 2004; Ring and Collins 2005; Thomson and Ring 2006; Erkül, 2010). According to these studies, the Eğrigöz, Koyunoba, Alaçam granites are interpreted to have been formed along an extensional detachment zone separating the Menderes Massif in the footwall and metapelites of the Afyon Zone or ophiolitic melange in the hanging wall. However, contact relations and the relative ages of the assembly of different tectonic and stratigraphic successions in the study areas set some important limitations on the tectono-magmatic models of the northern margin of the Menderes Massif.

The different slices of the nappe package (Menderes Massif, Afyon Zone, Tavşanlı Zone, and Bornova Flysch Zone) formed along the suture zone between the Tauride-Anatolide Block and the Sakarya Continent. They tectonically overlay the different units (gneisses, schists or marbles) of the Menderes Massif (Kaya 1981; Başarır and Konuk 1981; Candan 1988; Erdoğan and Güngör 1992; Yılmaz et al. 1994, Akay, 2009). Therefore, the exhumation of the basement units must have started prior to the emplacement of the nappe packages along the İzmir-Ankara Suture Zone. With the ongoing compression, the thrusting of nappe packages was accompanied and followed by a considerable thickening. When the Miocene Eğrigöz, Koyunoba and Alaçam granites intruded, the paleotopography was underlain by metapelites-metarhyolites of the Afyon

Zone or the Menderes metamorphic rocks. The middle-late Miocene cover succession, and a considerable part of the young granites and their volcanic phases were eroded after Early Miocene and this erosion is still continuing at the present time.

Summary of the publications

Three chapters form the general framework of this thesis. Miocene magmatic evolution of the Menderes Massif is their primary focus. The first chapter deals with the Simav region and presents new geological, geochronological and geochemical data for the Eğrigöz, and Koyunoba granites and basement rocks. The second chapter explores the geochemical and geochronological constraints of the post-collisional Alaçam granite with its country rocks in Alaçam region. The last chapter bears on the emplacement mode and isotopic signatures of the Alaçam granite and sheds further light on the Miocene magmatic evolution of the region.

Chapter 1: Early Miocene granite formation by detachment tectonics or not? A case study from the northern Menderes Massif (Western Turkey) - published in Journal of Geodynamics -

This paper focuses on the Eğrigöz and Koyunoba granites and explores the question whether their formation is related to a syn-extensional event or not. The paper contains new geological observation from granites and their country rocks, and new geochronological and geochemical constraints.

Eğrigöz and Koyunoba granites are shallow-seated, I-type, calc-alkaline, post-collisional granitic bodies. They are associated with their subvolcanic-volcanic sequences which crosscut the Menderes Massif, Afyon Zone and the tectonic contact between them.

Major, trace and rare earth element compositions show geochemical differences between the Miocene granites (Eğrigöz and Koyunoba) and a metagranite of the Menderes Massif. The latter was previosly interpreted as a mylonitic upper part of the undeformed granites (Işık and Tekeli 2001; Işık et al. 2004; Seyitoğlu et al. 2004; Ring and Collins 2005; Thomson and Ring 2006). According to the geochemical signatures of the metagranite, Ba, Rb and V contents in metagranite samples are remarkably different from the samples of the Eğrigöz and Koyunoba granites. The undeformed granites are clearly I-type in nature, whereas ASI values of most metagranite samples indicate an S-type affinity. Compared to the REE patterns of the undeformed granites, the metagranites are more enriched in light rare earth elements (LREE) ($[La/Yb]_N$ = 8-38.4), and less enriched in heavy rare earth elements (HREE) ($[Gd/Yb]_N$ = 0.8-

5.0). Besides, negative Eu anomalies observed in the undeformed granites ($0.7 < Eu/Eu^* < 1.3$) are not seen in the metagranites ($0.6 < Eu/Eu^* < 0.8$)

Geochronological analyses were performed on samples which were collected close to the intrusive boundaries of the granites with the basement rocks. The age relation between gneisses, metagranites of the Menderes Massif and the Eğrigöz and Koyunoba granites was evaluated by U-Pb (zircon) and $^{207}Pb/^{206}Pb$ (single zircon evaporation) geochronology. $^{207}Pb/^{206}Pb$ evaporation ages between 607-501 Ma and U-Pb zircon ages of 543 ± 10 Ma and 30.04 ± 0.56 Ma were obtained for two gneiss samples and a metagranite of the Menderes Massif, respectively. U-Pb zircon analyses yield crystallization ages of 21.7 ± 1.0 Ma for the Koyunoba granite and 19.4 ± 4.4 Ma for the Eğrigöz granite. A cooling age of 18.77 ± 0.19 Ma for the Eğrigöz granite was obtained by Rb-Sr (whole rock, biotite) analyses.

All the data presented in this paper point out that the Early Miocene I-type granites (Eğrigöz and Koyunoba) are part of a NW-SE trending magmatic belt. Moreover, the metagranites and the undeformed Eğrigöz and Koyunoba granites are not genetically related with each other. Granite emplacement related to a low angle detachment fault is not supported by our new geological, geochronological and geochemical data.

Chapter 2: Early Miocene post-collisional magmatism in NW Turkey: geochemical and geochronological constraints - published in International Geology Review -

This paper offers new geochemical and geochronological constraints of the Alaçam granite. The Alaçam region is situated along the northern Menderes Massif and close to the Simav region. Due to this proximity and the geological resemblance, the Alaçam region played an important role to understand the magmatic evolution of the northern massif. The Alaçam granite stitches into four different tectonic zones which were formed after the Alpine collision of the Menderes platform and Sakarya Continent.

The Alaçam granite and its related stocks exhibit typical I-type characteristic. The geochemical features of the granite show close similarities with the Eğrigöz and Koyunoba granites. The Alaçam granite shows enrichment in light REEs (LREEs) relative to heavy REEs (HREEs). In

LREEs a distinctive negative trend is clear, and a clear flat pattern is observed in HREEs. Negative Eu, Sr, and Nb anomalies are also characteristic for the Alaçam granite.

In previous studies, the gneissic granites and the metarhyolites of the Afyon tectonic zone have been interpreted as the sheared parts of the Alaçam granite (Seyitoğlu et al. 2004; Erkül, 2009). Such interpretation implies a crustal-scale detachment zone and an extensional regime during emplacement. A similar intrusion mode was postulated for other granites situated along the northern margin of the Menderes Massif (e.g. Eğrigöz and Koyunoba granites). However, we determined U-Pb zircon ages of 314.9 ± 2.7 Ma from a gneissic granite sample of the Afyon Zone and 20.0 ± 1.4 Ma and 20.3 ± 3.3 Ma from the Alaçam granite and its related stocks demonstrating that these rocks have no genetic relation with each other. Rb-Sr biotite ages of the granite and its stocks are 20.01 ± 0.20 Ma and 20.17 ± 0.20 Ma, suggesting fast cooling at a shallow crustal level.

Geological, geochemical and geochronological characteristics show that the Early Miocene Alaçam granite is similar to numerous EW-trending plutons of NW Anatolia. This granite with its stock bears post-collisional geochemical features and is interpreted as a product of Alpine-type magmatism along the İzmir-Ankara Suture Zone in NW Turkey and seems to have no genetic relation to the detachment zone.

<u>Chapter 3:</u> Al- in-hornblende thermobarometry and petrogenesis of the Alaçam granite in NW Anatolia (Turkey) - submitted to the Turkish Journal of Earth Sciences -

In this paper, the intrusion depth and the isotopic compositions of the Alaçam granite were investigated. The exact emplacement depth of the Miocene granites along the northern border of the Menderes Massif is still a subject of debate. Previous estimates on the granites emplacement depth were mainly based on geological features. However, the exact emplacement depth is important for understanding the general emplacement mode of the Miocene granites. The new Al-in-hornblende data and isotopic compositions of the Alaçam granite give rise to re-consider the general mode of the Miocene magmatic activity and cast doubt on the hypothesis that magmatism was triggered by extensional tectonic processes.

Three samples from the main body of the Alaçam granite were analyzed for Al-in-hornblende barometry. Chemical compositions of the rims and cores of the amphiboles do not differ from each other. Fe^{3+}/Fe^* ratio ranges from 0.20 to 0.37. Total-Al content is between 0.942 and 1.609 cations per formula unit and all cores and rims of the A-site occupancy range from 0.295 to 0.555. Pressure calculations for amphibole compositions (rim and core) fall in the range between 0.60 and 2.07 kbar. By using a conversion factor of 1 kbar = 3.7 km of crust (Tulloch & Challis 2000), the intrusion depth of the Alaçam granite can be estimated between 2-7 km. Our data is also compatible with the other Oligo Miocene granitoids in NW Anatolia (Kavaklar, Çavuşlu, Eybek plutons) (Ghassab 1994). In earlier studies, the emplacement depth of the granitoids was evaluated from geodynamic observation and various researchers have suggested a large scale crustal extension related emplacement model for the granitoids in the Aegean Sea and NW Anatolia (e.g. Cyclades Miocene plutonic suites, Eğrigöz, Alaçam granites in NW Anatolia) (Isik & Tekeli 2001; Bozkurt 2004; Seyitoglu *et al.* 2004; Jolivet & Brun 2010; Stouraiti *et al.* 2010). The extension model gave rise to consider an intrusion depth at the brittle-ductile transition zone. In general, crustal-scale detachment zones form and evolve in the middle to lower crust (Ramsay 1980; Coward 1984). The location of the transition zone between elastico-frictional (ductile) and quasi-plastic (brittle) behavior would define an emplacement depth of these granitoids between ca. 15-20 km (Sibson 1977). However, our new Al-in-hornblende thermobarometry from amphiboles of the Alaçam granite is inconsistent with this geodynamic model.

In the Aegean Sea, both I-type and S-type granitoids crop out with their volcanic counterparts. The petrogenetic nature of the Tinos, Ikeria, Naxos, Paros, Krokos granitoids were previously studied in detail (Stouariti et al. 2010 and references therein). In general, these studies show that these Aegean magmatic suites are derived from crustal meta-sedimentary sources (Altherr & Siebel 2002 and references therein). Stouariti et al. (2010) proposed that three end members (metasedimentary crustal source, marble, and amphibolite) contributed to magma formation. Miocene granitoids also occur along the northern and southern parts of the İzmir-Ankara Suture Zone. Close age similarities, geochemical and geological features of the NW Anatolian granite and Aegean granitoids give rise to speculate that this magmatism is closely related with each other. Initial isotopic signatures of the Alaçam granite are $^{87}Sr/^{86}Sr(I) = 0.70865\text{-}0.70915$, $e_{Nd}(I) = -5.8$ to -6.4, $\delta^{18}O = 9.5\text{-}10.5$, $^{206}Pb/^{204}Pb = 18.87\text{-}18.90$. These characteristics indicate a crustal source and its derivation from an older meta-crustal protolith. When compared with the Aegean granitoids, the isotopic compositions of the Alaçam granite are distinctly different.

New Al-in-hornblende barometry isotopic data of the Alaçam granite and its related stocks do not substantiate previously suggested extension related model for both the Aegean Islands and NW Anatolia magmatism. The emplacement depth and the crustal source signatures imply a compression regime for the formation of the Early Miocene granites along the northern border of the Menderes Massif.

References

Akay, E., 2009. Geology and petrology of the Simav Magmatic Complex (NW Anatolia) and its comparison with the Oligo-Miocene granitoids in NW Anatolia; implications on Tertiary tectonic evolution of the region. Int J Earth Sci, 98:1655-1675

Akdeniz, A., Konak, N., 1979a. Geology of Simav-Emet-Tavşanlı-Dursunbey-Demirci area. Report of the Mineral Research and Exploration Institute 108 p (in Turkish with English abstract)

Akdeniz, N., Konak, N., 1979b. Rock units of the Menderes Massif and setting of the metabasic and metaultramafic rocks around Simav. Geol Soc Turk Bull 22: 175-184

Akkök, R., 1983. Structural and metamorphic evolution of the northern part of the Menderes Massif: new data from the Derbent area and their implication for the tectonics of the massif. J Geol 91: 342-350

Altherr, R., & Siebel, W. 2002. I-type plutonism in a continental back-arc setting: Miocene granitoids and monzonites from the central Aegean Sea, Greece. Contrib Mineral Petrol, 143: 397-415

Altunkaynak, Ş., Yılmaz, Y., 1998. The Mount Kozak magmatic complex, Western Anatolia. J Volcanol Geotherm Res 85: 211-231

Başarır, E., Konuk, Y.T., 1981. Crystalline basement and allocthon units of Gümüldür region. Bull Geol Soc of Turk 24: 1-6

Bozkurt, E., Park G.R., 1994. Southern Menderes Massif: an incipient metamorphic core complex in western Anatolia, Turkey. J Geol Soc 151: 213-216

Bozkurt, E., Satır, M., 2000. The southern Menderes Massif (western Turkey): geochronology and exhumation history. Geol. J. 35: 285-296

Bozkurt, E., Park, R. G., & Wınchester, J. A. 1993. Evidence against the core-cover interpretation of the southern sector of the Menderes Massif, West Turkey. Terra Nova 55: 445-451

Bozkurt, E., Winchester, J.A., Park, R.G., 1995. Geochemistry and tectonic significance of augen gneisses from the southern Menderes Massif (West Turkey). Geol Mag 132: 287-301

Bozkurt, E. 2004. Granitoid rocks of the southern Menderes Massif (southwestern Turkey): field evidence for Tertiary magmatism in an extensional shear zone. Int J Earth Sci, 93: 52-71

Bozkurt, E., Satır, M., Buğdaycıoğlu, Ç., 2010. (in review). Dating a detachment fault by Rb-Sr geochronology:a case study from the Simav detachment fault and its tectonic implications for the evolution of the northern Menderes Massif (Western Turkey). Tectonophysics

Candan, O., 1988. Petrography, petrology and mineralogy of the area between Demirci and Borlu (Northern flank of the Menderes Massif). PhD Thesis, Dokuz Eylül University, Engineering Faculty, Department of Geological Engineering 125 p (in Turkish with English abstract, unpublished)

Candan, O., Dora, O.Ö., Oberhänsli, R., Çetinkaplan, M., Partzsch, J.H., Warkus, F.C., Dürr, S., 2001. Pan-African high-pressure metamorphism in the Precambrian basement of the Menderes Massif, W Anatolia, Turkey. Int J Earth Sci 89: 793-811

Candan, O., Çetinkaplan, M., Oberhänsli, R., Rimmele, G., Akal, C., 2005. Alpine high-P/low-T metamorphism of the Afyon Zone and implications for the metamorphic evolution of Western Anatolia, Turkey. Lithos 84: 102-124

Catlos, J.E., Baker, C., Sorensen, S.S., Çemen, İ., Hançer, M., 2010. Geochemistry, geochronology, and cathodoluminescence imagery of the Salihli and Turgutlu granites (central Menderes Massif, western Turkey): implications for Aegean tectonics. Tectonophysics 488: 110-130

Catlos, E.J., Çemen, İ., 2005. Monazite ages and rapid exhumation of the Menderes Massif, western Turkey. Int J Earth Sci. 94: 204-217

Coward, M. P., 1984. Precambrian crust: examples from NW Scotland and southern Africa and their significance, in Kröner, A., and Greiling, R., (Eds), Precambrian tectonics ilusturated. Stuttgart, Schweizerbartsche Verlangsbuchhandlung (Nägele u. Obermiller), 207-235

Çemen, İ., Catlos, E.J., Gögüş, O., Özerdem, C., 2006. Postcollisional extensional tectonics and exhumation of the Menderes massif in the Western Anatolia extended terrane, Turkey. In: Dilek, Y., and Pavlides, S. (eds), Postcollisional tectonics and magmatism in the Mediterranean region and Asia: Geol Soc Am Spec 409: 353-379

Dilek, Y. & Altunkaynak, S. 2009. Geochemical and temporal evolution of Cenozoic magmatism in western Turkey: mantle response to collision, slab breakoff, and lithospheric tearing in an orogenic belt. Geol Soc London Spec Pub (In: van Hinsbergen, D. J. J., Edwards, M. A. & Govers, R., (Eds)) 311: 213-234

Dora, O. Ö., Kun, N., Candan, O., 1990. Metamorphic history and geotectonic evolution of the Menderes Massif. IESCA Proc 2: 102-115

Dora, O. Ö., Candan, O., Dürr, H., Oberhänsli, R., 1995. New evidence on the geotectonic evolution of the Menderes Massif. In: Pişkin Ö, Ergün M, Savaşçın MY, Tarcan G (eds) IESCA Proc, 53-72

Erdoğan, B., 1992. Problem of core-mantle boundary of Menderes Massif. Geosound 20: 314-315

Erdoğan, B., Güngör, T., 1992. Stratigraphy and tectonic evolution of the northern margin of the Menderes Massif. Bulletin of the Turkish Association of the Petroleum Geologists 2: 1-20

Erdoğan, B., Güngör, T., 2004. The problem of the core-overlie boundary of the Menderes Massif and an emplacement mechanism for regionally extensive gneissic granites. Turkish J of Earth Sci 13: 15-36

Erkül, F., 2009. Tectonic significance of synextensional ductile shear zones within the Early Miocene Alaçam granites, Northwestern Turkey. Geol Mag 147: 611-637

Genç, S.C., 1998. Evolution of the Bayramiç magmatic complex, northwestern Anatolia. J Volcanol Geotherm Res 85: 233-249

Ghassab, T.R., 1994. Alpidsche Entwicklunsgechichte des Kazdag Massivs und der angrenzenden Granitoide (Biga Halbinsel, NW-Türkei): Eine geologische, geochemische und geochronologische Studie. Diplomarbeit. Tubingen Uni. pp 106 (in German-unpublished)

Hetzel, R., Passchier, C.W., Ring, U., Dora, O.Ö., 1995a. Bivergent extension in orogenic belts: the Menderes Massif (southwestern Turkey). Geol 23: 455-458

Hetzel, R., Ring, U., Akal, C., Troesch, M., 1995b. Miocene NNE-directed extensional unroofing in the Menderes Massif, SW Turkey. J Geol Soc Lond 152: 639-654

Holland, T. & Blundy, J. 1994. Non-ideal interactions in calcic amphiboles and their bearing on amphibole-plagioclase thermometry. Contrib Mineral Petrol 116: 433-47

Işık, V., Tekeli, V., 2001. Late orogenic crustal extension in the northern Menderes Massif (Western Turkey): evidence for metamorphic core complex formation. Int J Earth Sci 89: 757-765

Işık, V., Tekeli, O., Seyitoğlu, G., 2004. The $^{40}Ar/^{39}Ar$ age of extensional ductile deformation and granitoid intrusion in the northern Menderes core complex: implications for the initiation of extensional tectonics in western Turkey. J Asian Earth Sci 23: 555-566

Jolivet, L., & Brun, J. P. 2010. Cenozoic geodynamic evolution of the Aegean. Int J Earth Sci, 99: 109-138

Karacık, Z., Yılmaz, Y., 1998. Geology of the ignimbrites and the associated volcano-plutonic complex of the Ezine are, northwestern Anatolia. J Volcanol Geotherm Res 85: 251-264

Kaya, O., 1972. Tavşanlı yöresi ofiyolit sorununun ana çizgileri. Bull Geol Soc Turk 15/1: 26-108 (in Turkish with English abstract)

Kaya, O., 1981. Latest Cretaceous underthrusting and faulting in west Anatolia: with particular reference to ultramafic rocks and Menderes Massif. TUBİTAK Nat Sci J, Atatürk special issue. 15-36

Lips, A.L.W., Cassard, D., Sözbilir, H., Yılmaz, H., Wijbrans, J.R., 2001. Multistage exhumation of the Menderes Massif, western Anatolia (Turkey). Int J Earth Sci 89: 781-792

Okay, A.İ., 1984. Distribution and characteristics of the northwest Turkey blueschists. In Robertson A.H.F and Dixon J.A (Eds.), The Geological Evolution of the Eastern Mediterranean. Geol Soc Lond, Special Pub, 17: 455-466

Okay, A. İ Satır, M., 2000. Coeval plutonism and metamorphism in a latest Oligocene metamorphic core complex in northwest Turkey. Geol Mag 137: 495-516

Okay, A.İ., Tansel, İ., Tüysüz, O., 2005. Obduction, subduction and collision as reflected in the Upper Cretaceous-Lower Tertiary sedimentary record of western Turkey. Geol Mag 138: 117-142

Okay, A.İ., Satır, M., Maluski, H., Siyako, M., Monie, P., Metzger, R., Akyüz, S., 1996. Paleo- and Neo-Tethyan Tethyan events in northwestern Turkey: Geologic and geochronologic constraints. In: A. Yin and M. Harrison (Eds.) The Tectonic Evolution of Asia. Cambridge University Press 420-441

Özgenç, İ., İlbeyli, N., 2008. Petrogenesis of the late Cenozoic Eğrigöz granite in western Anatolia, Turkey: Implications for magma genesis and crustal processes. Int Geol Rev 50: 375-391

Purvis, M., Robertson, A.H.F., 2004. A pulsed extension model for the Neogene-Recent E-W trending Alaşehir graben and the NE-SW trending Selendi and Gördes basins, western Turkey. Tectonophysics 391: 171-201

Ramsay, J. G. 1980. Shear zone geometry: a review. J Structural Geol, 2: 83-99

Ring, U., Collins, S.A., 2005. U-Pb SIMS dating of synkinematic granites: timing of core-complex formation in the northern Anatolide belt of western Turkey. J Geol Soc Lond 162: 289-298

Ring, U., Johnson, C., Hetzel, R., Gessner, K., 2003. Tectonic denudation of a late Cretaceous-Tertiary collisional belt: regionally symmetric cooling patterns and their relation to extensional faults in the Anatolide belt of western Turkey. Geol Mag 148: 421-441

Satır, M., Friedrichsen, H., 1986. The origin and evolution of the Menderes Massif, W-Turkey: a rubidium/strontium and oxygen isotope study. Geol Rundsch 75: 703-714

Satır, M., Taubald, H., 2001. Hydrogen and oxygen isotopeevidence for fluid-rock interactions in the Menderes Massif, western Turkey. Int J Earth Sci 89, 812-821

Seyitoğlu, G., Işık, V., Çemen, İ., 2004. Complete Tertiary exhumation history of the Menderes Massif, western Turkey: an alternative working hypothesis. Terra Nova 16: 358-364

Sibson, R. H. 1977. Fault rocks and fault mechanisms. J Geol Soc Lond, 133: 191-213

Stouraiti, C., Mitropoulos, P., Tarney, J., Barreiro, B., Mcgrath, A. M., & Baltatzis, E. 2010. Geochemistry and petrogenesis of late Miocene granitoids, Cyclades, southern Aegean: Nature of source components. Lithos, 114, 337-352

Şengör, A.M.C., Yılmaz, Y., 1981. Tethyan evolution of Turkey; A plate tectonic approach: Tectonophysics 75: 181-241

Şengör, A.M.C., Yılmaz, Y., Sungurlu, O., 1984a. Tectonics of the Mediterranean Cimmerides: nature and evolution of the western termination of Paleo Tethys. In: Dixon JE, Robertson AHF (eds). The geological evolution of the eastern Mediterranean. Spec Publ Geol Soc Lond 17: 119-181

Şengör, A.M.C., Satır, M., Akkök, R., 1984b. Timing of tectonic events in the Menderes Massif, western Turkey: implications for tectonic evolution and evidence for Pan-African basement in Turkey. Tectonics 3: 93-707

Thomson, S.N., Ring, U., 2006. Thermochronologic evaluation of postcollision extension in the Anatolide orogen, western Turkey. Tectonics 25: 1-20

Tulloch, A. J., & Challis, G. A. 2000. Emplacement depths of Paleozoic-Mesozoic plutons from western New Zealand estimated by hornblende-Al geobarometry. New Zealand J Geol Geophys, 43: 555-567

Verge, N.J., 1993. The exhumation of the Menderes Massif metamorphic core complex of Western Anatolia. Terra abstr: 5: 249

Westaway, R., 2006. Cenozoic cooling histories in the Menderes Massif, western Turkey, may be caused by erosion and flat subduction, not low-angle normal faulting. Tectonophysics 412: 1-25

Whitney, D., Teyssier, C., Kruckenberg, S.C., Morgan, V.L., Iredale, L.J., 2008. High-pressure–low-temperature metamorphism of metasedimentary rocks, southern Menderes Massif, western Turkey. Lithos 101: 218-232

Whitney, D.L., Bozkurt, E., 2002. Metamorphic history of the southern Menderes Massif, western Turkey. Geol Soc Am Bull 114: 829-838

Whitney, D.L., Teyssier, C., Vanderhaeghe, O., 2005. Gneiss domes and crustal flow. In: Whitney, D.L, Teyssier, C., Siddoway, C.S. (Eds.), Gneiss Domes in Orogeny: Geol Soc Am Spec 380: 15-33

Yılmaz, Y., 1997. Geology of western Anatolia active tectonics of northwestern Anatolia-The Marmara poly-project. A multidisciplinary approach by space-geodesy, geology, hydrogeology, geothermics and seismology, Univ. Press Zurich. 31-53

Yılmaz, Y., Altunkaynak, Ş., Karacık, Z., Gündoğdu, N., Temel, A., 1994. Development of neo-tectonic related magmatic activities in western Anatolia. Int Vol Congr, Ankara, Abstract: 13

Yılmaz, Y., Genç, Ş.C., Karacık, Z., Altunkaynak, Ş., 2001. Two contrasting magmatic associations of NW Anatolia and their tectonic significance. J Geod 31: 243-271

Supplementary

Chapter 1: *Early Miocene granite formation by detachment tectonics or not? A case study from the northern Menderes Massif (Western Turkey)*

Altuğ Hasözbek · Erhan Akay · Burhan Erdoğan · Muharrem Satır · Wolfgang Siebel

A. Hasözbek
Institut für Geowissenschaften, Universität Tübingen,
Wilhelmstrasse 56, D-72074 Tübingen, Germany
E-mail: altug.hasoezbek@student.uni-tuebingen.de
Tel: +49-7071-2973156
Fax: +49-7071-295713

E. Akay · B. Erdoğan
Dokuz Eylul University, Engineering Faculty,
Department of Geological Engineering,
Tınaztepe, 35160 Buca, Izmir, Turkey

M. Satır · W. Siebel
Institut für Geowissenschaften, Universität Tübingen,
Wilhelmstrasse 56, D-72074 Tübingen, Germany

Published in Journal of Geodynamics

Idea:	40%
Problem:	50%
Production of Data:	70%
Evaluation and Interpretation:	70%
Preparation of the manuscript:	70%

Abstract

The northern border of the Menderes Massif is dominated by gneiss-schist-marble associations and metagranites. The high-grade units of the massif are tectonically overlain by a meta-platform sequence of the Afyon Zone and the Cretaceous-early Tertiary HP/LT Tavşanlı Zone. The Simav Magmatic Complex, comprising the shallow-seated, I-type, calc-alkaline, post-collisional Eğrigöz and Koyunoba granites, and associated subvolcanic-volcanic sequences crosscuts the Menderes Massif, Afyon Zone and tectonic contact between them.

In this paper, the age relation between gneisses, metagranites of the Menderes Massif and the Eğrigöz and Koyunoba granites was evaluated by isotope dating. $^{207}Pb/^{206}Pb$ evaporation ages between 607-501 Ma and U-Pb zircon ages of 543 ± 10 Ma and 30.04 ± 0.56 Ma were obtained for two gneiss samples and a metagranite in the Menderes Massif, respectively. U-Pb zircon analyses yield crystallization ages of 21.7 ± 1.0 Ma for the Koyunoba granite and 19.4 ± 4.4 Ma for the Eğrigöz granite. A cooling age of 18.77 ± 0.19 Ma for the Eğrigöz granite was obtained by Rb-Sr (whole rock, biotite) analyses. Field occurrences, geochemical characteristics and geochronological data obtained from the Eğrigöz and Koyunoba granites show close similarities with other Oligo-Miocene granitoids in northwestern Anatolia indicating that they emplaced along an E-W trending regional magmatic belt and are not individual bodies related to local, north-dipping, low angle detachment faults as suggested in previous papers.

Keywords: Eğrigöz granite · Koyunoba granite · geochronology · Menderes Massif · geochemistry

Introduction

The Cenozoic suture zone formed by the collision of the Tauride-Anatolide Block to the south, and the Sakarya Continent to the north, crops out in the northwest Anatolia. The Anatolide-Tauride Block underwent greenschist to blueschist-facies metamorphism in the Paleocene due to the collision with the Sakarya Zone. During the collision, the Tauride-Anatolide Block was internally sliced and converted into a south to southeast vergent thrust pile (Okay et al., 1996; 2005; Collins and Robertson, 1998; Okay, 2004; Davis and Whitney, 2006; Whitney and Davis, 2006; Candan et al., 2005). In NW Anatolia, the regionally metamorphosed Menderes Massif forms the continental basement. For the timing of metamorphism in the massif, from the south to the north 35 ± 5 Ma (Rb-Sr phengite-biotite), 40 Ma (Bozkurt and Satır, 2000 and references therein) and ~ 29-28 Ma (Catlos and Çemen, 2005) ages have been previously obtained. In the overlying thrust pile, from south to north, two different tectonic belts are distinguished: (1) a relatively high pressure and low temperature metamorphic zone, overlying the Menderes Massif, the Afyon Zone (Okay et al., 1996; Okay, 2004; Candan et al., 2005) which was probably metamorphosed during the Paleocene (Candan et al., 2005 and references therein) and (2) a high pressure-low temperature metamorphic belt consisting of metaclastics and platform type marbles, the Tavşanlı Zone (Okay, 1980; Okay et al., 1996; Okay, 2004; Davis & Whitney, 2006; Whitney & Davis, 2006). An internally sheared flysch, the Bornova Flysch Zone tectonically overlies the Menderes metamorphic rocks along its northwest margin (Okay et al., 1996) (Fig. 1). From west to east, the Oligo-Miocene Kestanbol, Evciler, Eybek, Kozak, Alaçam, Koyunoba, Eğrigöz and Baklan granites form a NW-SE trending magmatic belt intruded into the Sakarya Continent, the Menderes Massif, and different slices of the thrust pile separating these two continental blocks (Altunkaynak and Yılmaz, 1999; Genç, 1998; Yılmaz et al., 2001; Altunkaynak, 2007; Dilek and Altunkaynak, 2009; Karacık et al., 2007; Aydoğan et al., 2008; Özgenç and İlbeyli, 2008; Akay, 2009; Hasözbek et al., 2010) (Fig. 1).

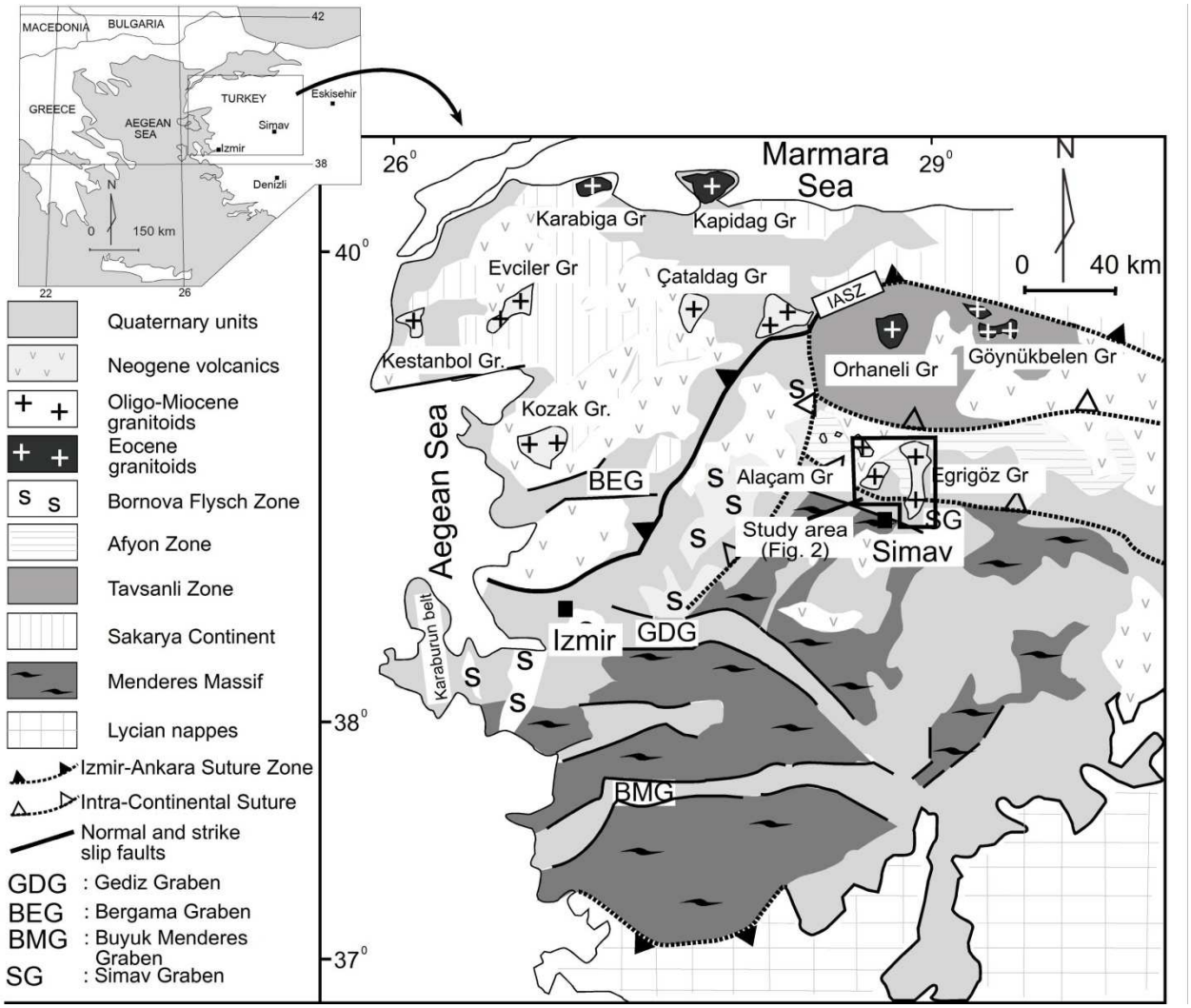

Fig. 1. Simplified geological map of western Anatolia and location of the study area. Modified after Genç, (1998), Okay et al. (1996), Okay and Satır, (2000), Gürer et al. (2009) (Gr: granite).

In the Simav region, the tectonic contact separating the Menderes Massif, in the footwall, and the Afyon Zone succession, in the hanging wall, has recently been defined as a regional detachment fault (Işık and Tekeli, 2001; Işık et al., 2004; Seyitoğlu, et al., 2004; Ring and Collins, 2005). The main evidences presented for this model are: (1) field mapping of a low-angle fault surface, (2) structural data showing ductile deformation with low-angle top-to-NE sense of shear, (3) synkinematic granite intrusions (Eğrigöz and Koyunoba granites) into footwall rocks and (4) $^{40}Ar/^{39}Ar$ and U-Th-Pb (SIMS) data showing close age relationships between metamorphic host rocks and undeformed granites (Işık et al., 2004; Ring and Collins, 2005; Thomson and Ring, 2006). These age data were interpreted as unequivocal evidence for synkinematic granite intrusions along this "so-called" detachment fault. In these studies, radiometric age

determinations, however, were limited and did not comprise certain mylonitic rocks surrounding the undeformed Eğrigöz and Koyunoba granites. On a regional scale, some contradictions between these new and pre-existing age determinations appeared: Similar Miocene granites can be found not only along the tectonic contact between the Menderes Massif and the overlying tectonic slices but also in the Menderes Massif itself, in the Afyon and Tavşanlı Zones and the Sakarya Continent (Fig. 1). Some of these plutons were already investigated previously and suggested to have been formed in a subduction-related setting (Altunkaynak and Yılmaz, 1998, 1999; Genç, 1998; Yılmaz et al., 2001). Akay (2009) presented detailed geological maps and field observations showing the cross-cutting intrusive contact relationship of these granites with the Menderes Massif and the Afyon Zone. Besides, the author presented geological and geochemical data suggesting that these granites are very shallow seated bodies that intruded into different tectonic slices of the collision zone. Based on these observations, Akay (2009) suggested that the Eğrigöz and Koyunoba granites are not genetically related to extensional detachment faulting. So far, radiometric age determinations are lacking which would help to clarify relationships between the undeformed Eğrigöz-Koyunoba granites and the "mylonitic" host rock associations.

Here we present new radiogenic age determinations on the samples taken close to the endocontacts of the Eğrigöz and Koyunoba granites to clarify if these undeformed granites are genetically related to the hosting gneiss and metagranite or not. Following the geological mapping of a large area (~ 24 x 30 km) on 1/25.000 scale including the Egrigöz and Koyunoba granitic bodies, we evaluate the geochemical characteristics of the undeformed granites in comparison with the hosting metagranites. Zircon ages were obtained from a metagranitic body which was considered in earlier studies as the mylonitic upper part of the Egrigöz and Koyunoba granites (Işık and Tekeli, 2001; Işık et al., 2004; Seyitoğlu et al., 2004; Ring and Collins, 2005; Thomson and Ring, 2006) and from the Eğrigöz and Koyunoba granites. Our results show the lack of any petrogenetic and age relation between the metagranitic body of the Menderes Massif and the Eğrigöz and Koyunoba granites.

Geological Framework

In the Simav region, the Menderes Massif forms the structurally lowest association and is tectonically overlain by nappes of the Afyon Zone. An ophiolitic melange nappe, the Dağardı melange, sits tectonically on top of this sequence. These three tectonic zones are intruded by

undeformed granitic bodies and their subvolcanic phases, called the Simav Magmatic Complex (Akay, 2009) and unconformably covered by middle-late Miocene flat-lying fluvial and lacustrine sedimentary and subaerial volcanic rocks (Akdeniz and Konak, 1979a, b; Ercan et al., 1979, 1984).

Menderes Massif

The Menderes Massif dominantly consists of greenschist-lower amphibolite-facies (Konak, 1982) metamorphic rocks of a gneiss-schist-marble association and metagranites (Fig. 2). The gneiss-schist-marble association is characterized by banded-augen gneisses, biotite-rich gneisses with white to bluish K-feldspar and quartz porphyroclasts set in a foliated quartz-feldspar-mica matrix (Fig. 3a, b). With decreasing feldspar and quartz contents, the layered gneisses pass into biotite schists which contain abundant almandine porphyroblasts. The gneiss-rich parts laterally and vertically grade into biotite schists, quartz-mica schists, and muscovite-biotite schists. Sporadic marble lenses are found in the metapelitic sequence. Tourmaline, chlorite, zircon, titanite and apatite form accessory minerals in the schists. The gneiss-schist association which is widely exposed in the southern and central Menderes Massif has been described as a part of the Ediacaran-Cambrian (570-520 Ma) basement (Satır and Friedrichsen, 1986; Kröner and Şengör, 1990; Hetzel and Reischmann, 1996; Loos and Reischmann, 1999; Gessner et al., 2004; Koralay et al., 2004).

The gneiss-schist-marble association is intruded by metagranites in the northern and central parts of the study area (Fig. 2). The metagranites display homogenous foliation with preserved relic igneous texture in some parts. Main mineral association is elongated biotite, K-feldspar, plagioclase, quartz, biotite, rare muscovite and rare hornblende (Fig. 3c, d). There is a significant difference between the gneiss-schist association and the metagranites from banded-augen texture in gneisses to preserved igneous texture in metagranites along a relatively sharp intrusive contact (Fig. 3). Along the contact zones the metagranites in some areas injected into the banded-augen gneisses and biotite schists (Fig. 4). In places, the foliation planes of the metagranites have the same orientation to those in the country rocks, but locally, a cross-cutting intrusive contact relationship is observed (Fig. 4a, b). Close to the contact zone, there are aplitic and pegmatitic dykes emplaced parallel to the foliation planes of the micaschists. Metagranites cutting the high-grade gneisses (dominantly augen gneisses) and schists have already been documented in other parts of the Menderes Massif (Akkök, 1983; Gessner et al., 2001; Candan, 1994; Bozkurt and

Park, 2001). Amphibolite-facies metamorphic conditions have been suggested for the augen gneisses and metapelites (Gessner et al., 1998) and prograde greenschist conditions for the metagranites (Gessner et al., 2001).

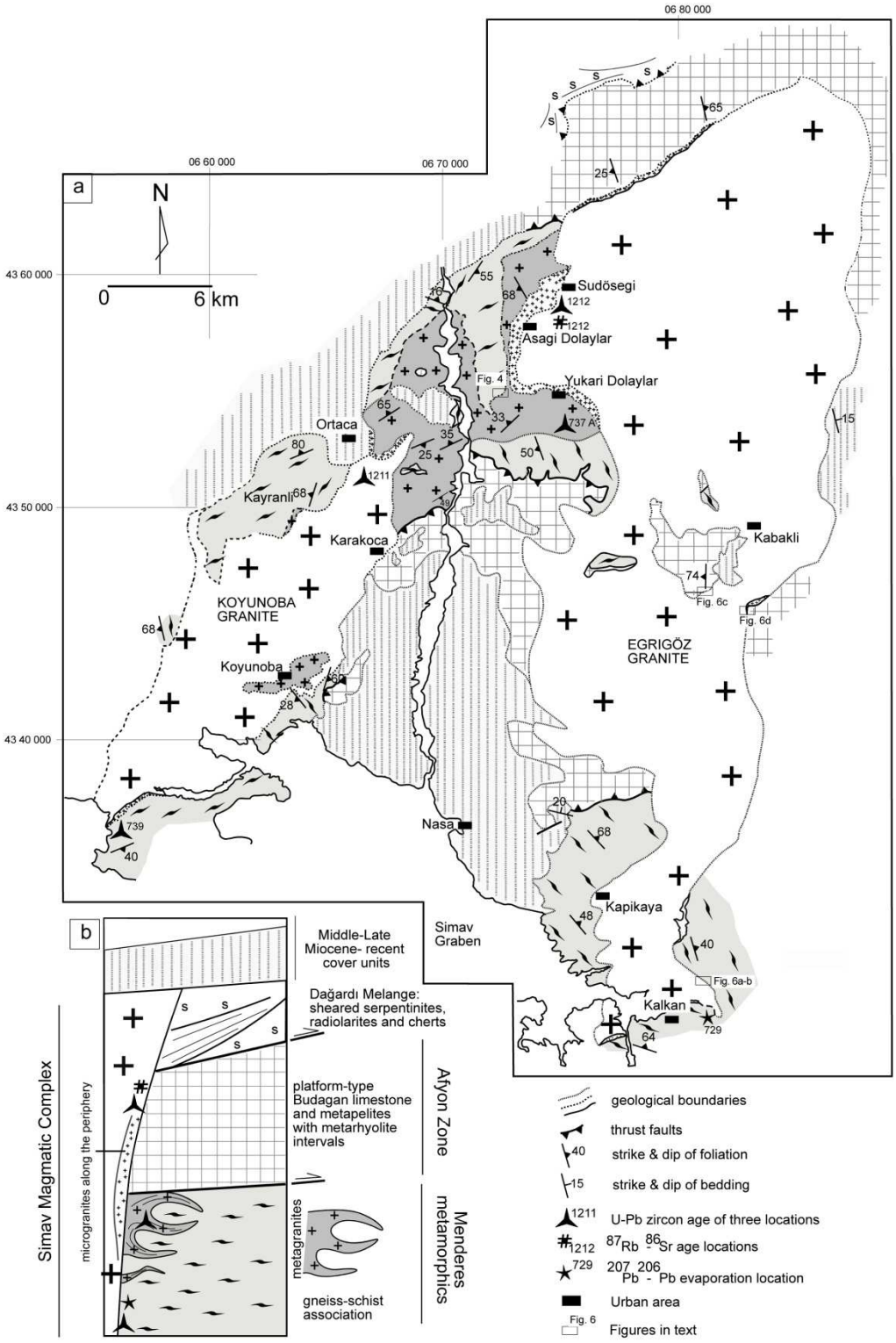

Fig. 2. (a) Geological map and (b) generalized stratigraphic column of the study area (modified after Akay, 2009).

Afyon Zone

A metapelitic association and overlying Mesozoic recrystallized carbonates cropping out along the northern border of the Menderes Massif around Simav was first mapped by Kaya (1972) and Akdeniz and Konak (1979a, b). Kaya (1972) and Kaya et al. (1995) separated the metaclastic lower part of this sequence from the surrounding units and defined it as an “anchimetamorphic zone” situated between the Menderes metamorphic rocks and the Tavşanlı ophiolite. Later, Okay (1984) and Okay et al. (1996) named this sequence “the Afyon Zone” and defined it as a tectonically sliced part of the Tauride-Anatolide Platform which is at present the most commonly accepted definition for the unit. The Afyon Zone in our study area consists of a thick metapelitic sequence at the base and thick platform type marbles in the upper parts.

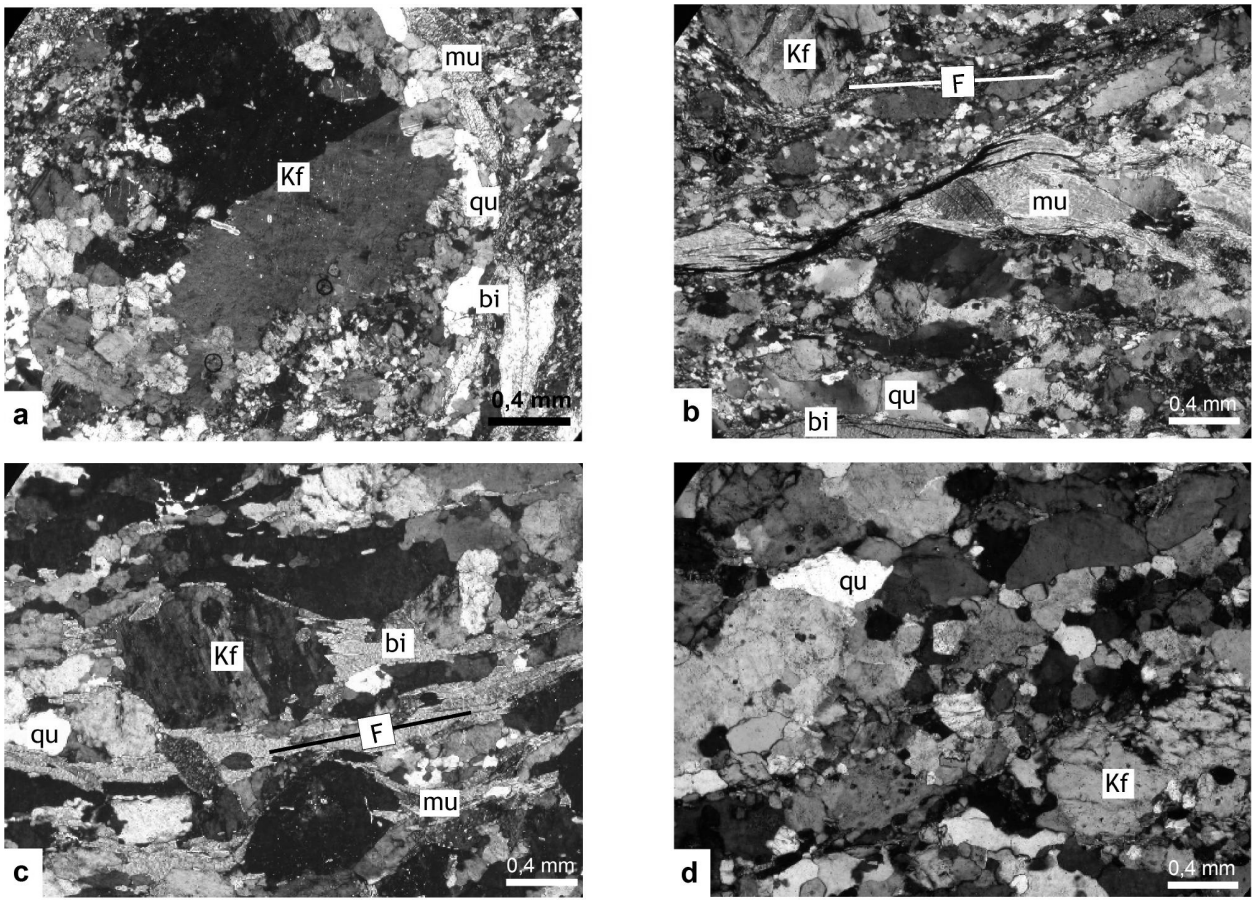

Fig. 3. Photomicrographs showing the textural characteristics of the gneisses and metagranites hosting the undeformed Eğrigöz and Koyunoba granites. (a) augen, (b) porphyroblastic texture in augen gneisses. (c) foliated, (b) primary granitic texture in metagranites (bi: biotite, qu: quartz, mu: muscovite, Kf: K-feldspar, F: foliation).

The metapelitic sequence is dominated by phyllites intercalated with recrystallized limestone lenses. Bimodal metabasic-metarhyolitic lavas and accompanying volcanoclastic lenses interlayer this sequence at different stratigraphic levels. Metarhyolites contain euhedral quartz and feldspar porphyroclasts wrapped by mica. Basaltic lava flows and mafic tuffs accompany the metapelites and metarhyolites mostly in the middle and upper parts of the Afyon sequence. Chlorite, amphiboles and rare olivine are the main mafic, and plagioclase is the felsic minerals. In tuffs, rock fragments accompany the mafic crystals. Akal et al., (2008) reported a 240.8 ± 3.7 Ma (Middle Triassic) $^{207}Pb/^{206}Pb$ zircon evaporation age from a metarhyolite near Eğrigöz village and Late Triassic to Jurassic foraminiferas have been reported from the carbonates by Kaya et al. (1995), Akay et al. (2007) and İşintek et al. (2007).

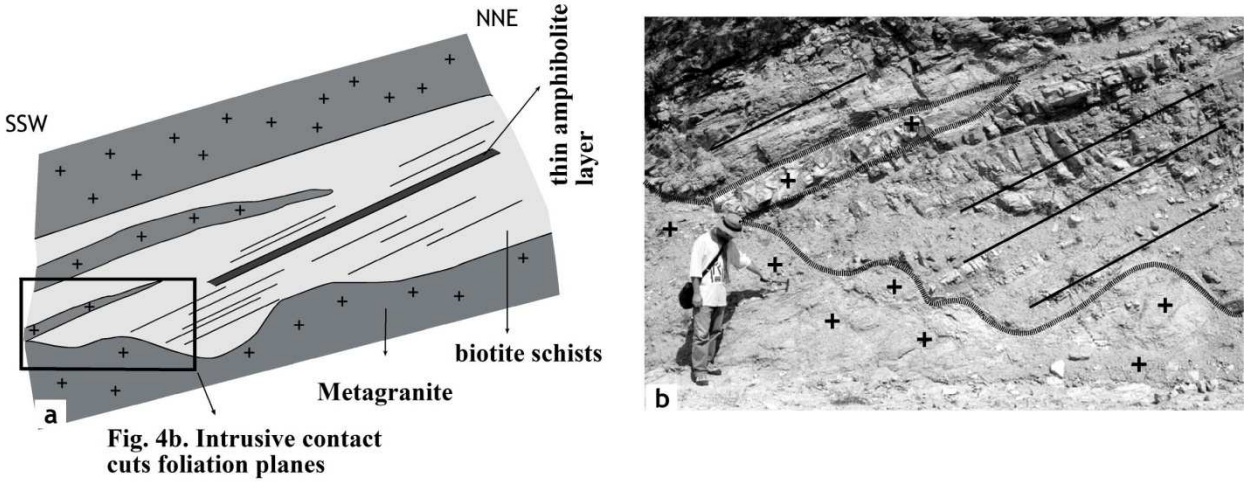

Fig. 4. (a) Cross section and (b) field photograph of the cross-cutting relation between metagranites and high grade metamorphic rocks of the Menderes Massif (UTM 671728; 4354620). The metagranites clearly bisect the foliation planes of the schists. Dotted line shows the intrusive contact and solid lines show the foliation planes of the mica schists in Fig. 4b. For location of photograph see Fig. 2a.

Low temperature-high pressure metapelites and carbonates of the Afyon Zone directly overlay different levels of the high temperature-low to medium pressure metamorphic rocks of the Menderes Massif along a low-angle tectonic contact. Along this contact, Afyon Zone rocks obliquely cut the foliation planes and linear structures of the underlying Menderes metamorphics (Akay, 2009).

Dağardı Melange

In the northernmost part of the study area, an internally sheared ophiolitic melange directly overlays the metarhyolites, metapelites and limestones of the Afyon Zone along a low-angle fault. This unit is called the Dağardı Melange by Akdeniz and Konak (1979a), and represents the southernmost continuation of the Tavşanlı Zone of Okay et al. (1996). Late Cretaceous foraminiferas have been determined from the limestone lenses (Akdeniz and Konak, 1979a, b; Konak, 1982), and late Cretaceous-early Paleocene ages were obtained from the matrix of the ophiolitic melange in the westernmost part of Anatolia (Özer and İrtem, 1982).

Simav Magmatic Complex

The Simav Magmatic Complex consists of two large granitic plutons which intruded into the stacked nappe packages of the Menderes Massif and Afyon Zone. The complex is composed of two petrographically and geochemically similar NNE-trending granitic bodies (Eğrigöz and Koyunoba) and a small volume of subvolcanic rocks (Akay, 2009). The Eğrigöz and Koyunoba granites are two of the largest granites in western Anatolia (Figs. 1, 2) and granitic to monzogranitic-granodioritic in composition. Along the periphery, fine microgranitic chilled texture is characteristic which, inward, changes into coarser holocrystalline texture and, in places, into coarse porphyritic texture with K-feldspar phenocrystals up to 3 cm in length (Fig. 5). No deformation is observed along the intrusive contact. Undeformed aplites, 2 to 30 cm thick, cut both the granites and metamorphic host rocks. Euhedral to subhedral orthoclase (20-25 %), plagioclase (30-35 %), quartz (20-25 %), biotite (5-10 %), and hornblende form the main mineral association; zircon and tourmaline are found as accessory phases.

The Eğrigöz and Koyunoba granites cut various units of the Menderes Massif and the Afyon Zone (Figs. 2, 6). Around the granites, a 10 to 200 m wide contact metamorphic aureole is locally observed. In different aureoles of this zone, Albayrak (2003) documented a mineral association consisting of pyroxene, plagioclase, garnet, rare sillimanite and staurolite, orthoclase, biotite, phlogopite, sphene, apatite, chlorite and quartz. Based on this mineral association and limited extension of this contact metamorphic zone, Albayrak (2003) concluded that the contact metamorphism occurred in a relatively shallow crustal environment.

At those places where the Koyunoba and Eğrigöz granites cut the foliated metagranites and gneissic granites of the Menderes metamorphics, undeformed microgranitic textures at the periphery and a steeply dipping boundary cutting the foliation planes of the foliated metagranites (Fig. 6a, b) are developed. An approximately 5 km-long and 2 km-wide body of metapelite was intruded and swallowed by the Eğrigöz granite (Fig. 6c, d). Along the intrusive contact aplitic dykes cut the chloritized and silicified metapelites. The map view (Fig. 2) and intrusive contact relation indicate that during granite emplacement the metapelite collapsed and settled into the granite as a roof pendant. Field characteristics of this contact relationship were documented by Akay (2009). Summarizing, the geological evidence presented here show that the Eğrigöz and Koyunoba granites are shallow-seated plutons with abundant aplitic dykes and angular enclaves from the country rocks and a large roof pendant in their center.

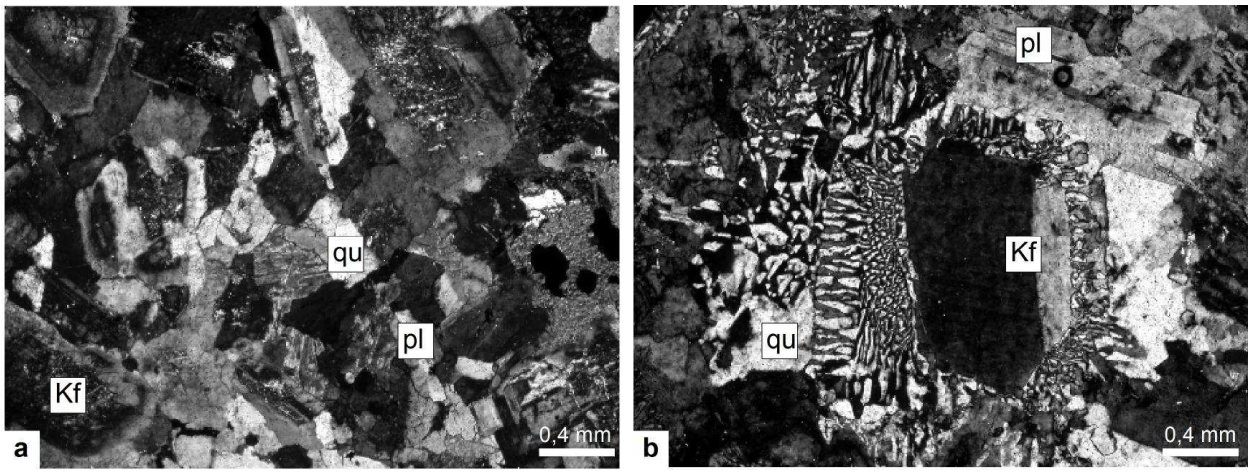

Fig. 5. Photomicrographs of the Eğrigöz and Koyunoba granites. (a) Both granites show undeformed microgranitic texture along the periphery. (b) Inward, texture becomes coarser with 3-4 mm to 3 cm-long crystals (bi: biotite, qu: quartz, Kf: K-feldspar, pl: plagioclase).

Cover units

Neogene continental sedimentary and volcano-sedimentary cover units overlie the strongly eroded surface of the underlying successions (Fig. 2). In the study area, they are composed of coarse-grained conglomerates, sandstones and shales, andesitic-rhyodacitic to rhyolitic tuffs or lavas of Middle-Late Miocene age (Akdeniz and Konak, 1979a, b; Ercan et al., 1979, 1984). Miocene conglomerates also overlay central parts of the Eğrigöz granite indicating that, before their deposition, the granite was already exposed to the surface.

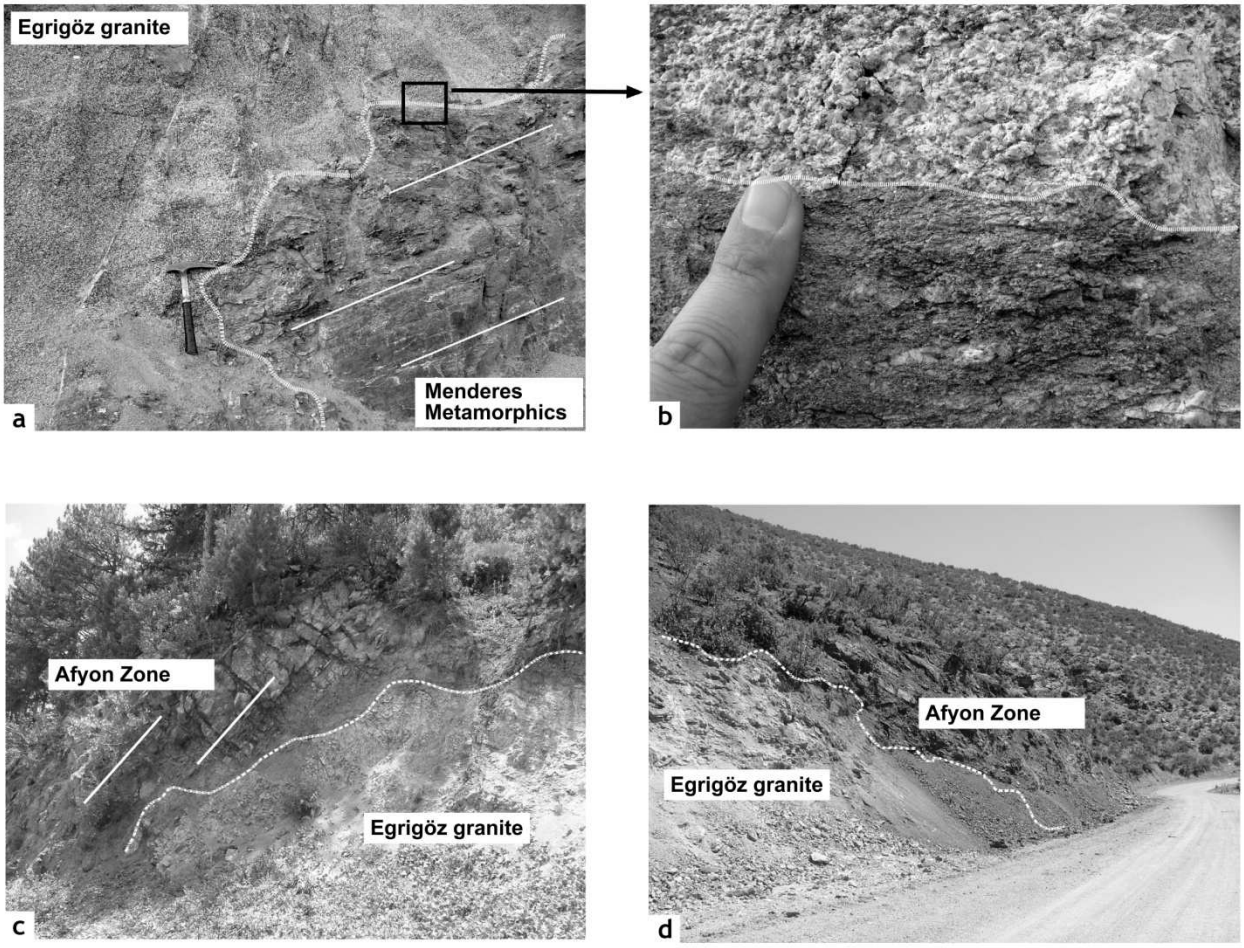

Fig. 6. (a-b)Undeformed Eğrigöz granite crosscutting the foliation planes of the high grade Menderes metamorphic rocks. A significant difference from undeformed to metamorphic texture is seen along the contact. The white squared area in (a) is zoomed in (b) (UTM 680832; 4328816). (c) A large body of the Afyon Zone metapelite swallowed by the Eğrigöz granite (Akay, 2009) (d) intrusive contact with Afyon Zone along the eastern contact of the Eğrigöz granite. Dashed lines show foliation planes and dotted lines show the intrusive contact. For locations of photographs, see Fig.2a.

Previous Work on Geochemistry and Geochronology

Geochemical features of the Oligo-Miocene granitic suites in NW Anatolia including the Eğrigöz and Koyunoba granites were documented in detail Akay (2009). In previous studies, the metagranites of the Menderes Massif were interpreted as the sheared upper part of the Eğrigöz and Koyunoba granites (Işık & Tekeli, 2001; Işık et al., 2004) therefore, a close geochemically relation between the granites and the metagranite should be expected. Prior to this study the following age information from the area was available (Table 1): a) $^{40}Ar/^{39}Ar$ mica ages obtained from the shear zone (22.86 ± 0.47 Ma) and Eğrigöz granite (20.19 ± 0.28 Ma) (Işık et al., 2004), b) U-Th-Pb (SIMS) zircon ages obtained from the Koyunoba granite (21.0 ± 0.2 Ma), Eğrigöz

granite (20.7 ± 0.6 Ma) and a leucogranitic dyke of the Menderes Massif (24.4 ± 0.3 Ma) (Ring and Collins 2005), c) (U-Th)/He apatite and zircon fission track ages (ca. 28-14 Ma) of the post-collisional extension-related intrusions (Thomson and Ring 2006) (Table 1). Recently, Bozkurt et al. (2009) presented a Rb-Sr mica age of 14.5-12 Ma from the postulated Simav detachment fault surface. The age gap (7-8 Ma) between the intrusion age of the Eğrigöz pluton and the activity of the detachment fault casts some doubt on a genetic relation between the extensional regime in western Anatolia and granite intrusion.

Analytical Methods

Major, trace and rare earth element analyses for metagranite samples were carried out in Acme Analytical Laboratories Ltd (Vancouver, Canada) by ICP-AES (Inductively Coupled Plasma Atomic Emission Spectrometry), and ICP-MS (Inductively Coupled Plasma Mass Spectrometry). SO-17/CSB standard was used for major oxide analyses, and SO-17 and DS-4 for trace element analyses. Accuracy in major oxides is < 0.02 and in trace elements < 0.10. Detailed information about analytic methods can be found in Akay (2009).

Four samples, each 20-25 kg in weight, were collected: Two augen gneisses (729-UTM: 0664844; 4342195; 739-UTM: 0654912; 4334479), metagranite of the Menderes Massif (737A-UTM: 0670519; 4353610), Eğrigöz granite (1212-UTM: 0674000; 4359183) and Koyunoba granite (1211-UTM: 0666189; 4352350) (Fig. 2a).

Zircon separation by sieving, wet shaking table, magnetic separator, and heavy liquids was performed at the Dokuz Eylül University, Engineering Faculty, Department of Geological Engineering (Izmir, Turkey). Zircons were hand-picked and classified under a binocular microscope based on their morphology and prepared for cathodoluminescence images in the SEM laboratory of the Tübingen University. Geochronological analyses were carried out at Tübingen University. Chemically abraded zircons (Mattinson, 2005) of metagranite and unabraded zircons of the Eğrigöz and Koyunoba granites were washed in 6N HCl and ultra clean water before isotope dilution. All zircons were spiked with a ^{205}Pb-^{235}U tracer solution. The details for wet-chemical analytical procedures are described in Chen and Siebel (2004). U-Pb analyses were performed on a Finnigan MAT 262 mass spectrometer with NBS 981 as standard material. The PBDAT programme was used for evaluating U-Pb analytical data (Ludwig, 1988) and the Isoplot programme for calculating the discordia lines (Ludwig, 2001). For more details

about analytical methods and chemical procedures of U-Pb isotope analyses, the reader is referred to Chen et al. (2000, 2002).

Table 1. Geochronological data from the Simav region including the results of this study.

Rock Type	Mineral	Method	Age result	Reference
Granite (Eğrigöz)	apatite	(U-Th)/He and Fission track	15.04 ± 0.1 to 14.57 ± 0.11 Ma	Thomson and Ring, (2006)
	zircon		22.9 ± 1.6 to 20.5 ± 1.5 Ma	
Granite (Koyunoba)	apatite		14.91 ± 0.24 to 14.69 ± 0.11 Ma	
	zircon		28.8 ± 2.0 to 23.7 ± 1.9 Ma	
Granite (Eğrigöz)	zircon	U-Th-Pb (SIMS)	20.7 ± 0.6 Ma	Ring and Collins, (2005)
Granite (Koyunoba)	zircon		21.0 ± 0.2 Ma	
Leucogranite dyke	zircon		24.4 ± 0.3 Ma	
Granite (Eğrigöz)	biotite	$^{40}Ar/^{39}Ar$	20.19 ± 0.28 Ma	Işık et al., (2004)
Mylonitic gneiss (Eğrigöz)	muscovite		22.86 ± 0.47 Ma	
Granite (Eğrigöz)	zircon	U-Pb isotopic dilution	19.4 ± 4.4 Ma	this study
Granite (Koyunoba)	zircon		21.7 ± 1.0 Ma	
Metagranite (Menderes Massif)	zircon		30.04 ± 0.56 Ma	
Granite (Eğrigöz)	biotite, whole rock	$^{87}Rb/^{86}Sr$	18.77 ± 0.19 Ma	
Gneiss (Menderes Massif)	zircon	$^{207}Pb/^{206}Pb$ evaporation	~ 607-551 Ma	
Gneiss (Menderes Massif)	zircon	U-Pb isotopic dilution	543 ± 10 Ma	

Table 2. Major, trace and rare earth element composition from the metagranite body of the Menderes Massif

Sample	**1271b**	**1285**	**1299**	**1313b**	**1340**	**1267**	**1312a**	**220**	**1433b**	**222**	**1416**
SiO2	66,16	65,34	65,47	66,2	68,33	66,56	73,14	72,39	69,07	69,31	72,14
Al2O3	16,21	15,34	16,19	16,38	16	16,09	14,17	14,78	16,04	15,54	14,82
Fe2O3	4,02	5,8	4,31	3,8	3,54	3,94	1,26	2,13	2,91	3,05	2,16
MgO	1,48	2,88	1,57	1,32	1,12	1,5	0,35	0,53	0,8	0,92	0,51
CaO	3,79	1,5	3,73	3,73	3,68	3,65	1,51	1,83	2,82	2,19	1,94
Na2O	3,16	3,21	3,06	3,28	3,33	3,14	2,74	3,32	4,07	3,1	3,45
K2O	3,18	3,14	3,4	3,22	3,06	3,18	5,8	3,49	2,81	3,93	3,39
TiO2	0,46	0,95	0,5	0,42	0,37	0,44	0,14	0,27	0,34	0,35	0,27
P2O5	0,27	0,24	0,3	0,24	0,19	0,27	0,24	0,05	0,18	0,32	0,11
MnO	0,07	0,06	0,07	0,07	0,08	0,07	0,02	0,03	0,05	0,06	0,02
Cr2O3	0,003	0,011	0,001	< .001	< .001	< .001	< .001	< .001	0,001	< .001	< .001
LOI	0,9	1,4	1,1	1	0,1	0,9	0,5	1	0,7	1	1
total	99,87	99,94	99,88	99,85	99,92	99,89	99,97	99,95	99,9	99,93	99,95
Ba	1514	585	1585	1681	1090	1417	894	1190	971	1417	1180
Sc	7	14	7	6	5	6	4	3	3	5	3
Co	6,1	12,4	6,6	5,1	5,1	5,6	1,2	2,3	3,1	4,5	2
Cs	5,7	39,5	3,6	3,9	4,9	4,6	4,2	2,7	4	5,7	2,2
Ga	20,5	24,3	20,1	21,3	19,1	20,4	16,6	20,2	19,9	22,9	19,3
Hf	4,6	5,3	4,1	3,4	4,2	4,6	3,6	4,5	2,9	4,4	3,8
Nb	16,2	12,7	15,7	14,6	12,9	19,4	20,7	10,3	8,7	17,1	9,6
Rb	109	147	111	108	100	109	150	93	88	148	88,3
Sn	4	7	3	4	3	4	2	1	2	7	1
Sr	808	149	847	811	569	760	345	432	668	489	451
Ta	1,5	0,9	1,4	1,3	1,3	2,1	6,8	0,8	0,9	2,1	0,8
Th	21,2	8,6	13,3	16,9	16,9	12,6	14,7	15,4	8,4	25,4	16,3
U	7,3	2,4	3,3	2,2	3,8	5,7	6,1	2,1	3,2	4,2	4
V	58	124	62	52	35	55	12	12	28	30	13
Zr	159	203	156	138	150	148	81	151	116	151	143
Y	25,1	31,7	18,5	20,7	22,4	36,3	33,9	10,7	10,1	23,3	14,5
La	61,6	32,5	39,4	63,4	46,9	36,7	19,4	44,3	31,7	61,6	45
Ce	106	65,3	72,2	107	83,9	66,7	38,4	80,7	57,2	106	81,6
Pr	11,55	7,63	7,5	11,04	9,23	7,47	4,19	8,94	6,17	11,04	8,97
Nd	40,9	30,2	27,1	37,8	35	26,3	15,1	33,2	24,5	39,8	32,7
Sm	7,7	6,6	5	6,3	5,9	6,1	4,3	6	4,9	7,8	6,4
Eu	1,47	1,47	1,1	1,21	1,26	1,34	0,81	1	0,78	1,17	0,99
Gd	5,31	5,96	3,63	3,84	4,45	4,63	3,43	3,5	3,27	4,54	3,65
Tb	0,77	0,87	0,55	0,6	0,66	0,92	0,78	0,51	0,39	0,76	0,54
Dy	3,92	4,94	3,13	3,35	3,81	5,03	4,32	2,23	1,9	3,59	2,47
Ho	0,75	0,99	0,57	0,63	0,67	1,06	0,85	0,3	0,33	0,61	0,37
Er	2,27	2,74	1,69	1,82	1,83	2,97	2,61	0,57	0,67	1,72	1,06
Tm	0,31	0,42	0,27	0,29	0,32	0,46	0,41	0,1	0,13	0,28	0,19
Yb	2,35	2,9	1,76	1,99	1,93	3,34	3,35	0,58	0,7	1,68	0,84
Lu	0,37	0,43	0,27	0,27	0,32	0,46	0,47	0,07	0,08	0,24	0,09
Zn	48	69	51	162	43	47	15	33	37	43	33
Ni	2	38,2	2,7	2,2	1,7	2,7	0,6	1,8	1,8	1,9	2,1
(La/Yb)cn	18,8	8,0	16,1	22,9	17,4	7,9	4,2	54,8	32,5	26,3	38,4
(Gd/Yb)cn	1,9	1,7	1,7	1,6	1,9	1,1	0,8	5,0	3,9	2,2	3,6
Eu/Eu*	0,7	0,7	0,8	0,8	0,8	0,8	0,6	0,7	0,6	0,6	0,6
ASI	1,0	1,3	1,0	1,0	1,0	1,1	1,0	1,2	1,1	1,2	1,2

LOI: Loss on Ignition; ASI (Alumina Saturation Index) = molar $[Al_2O_3/(Na_2O+CaO+K_2O)]$; Eu/Eu*= $[Eu_{cn}/(Sm_{cn}*Gd_{cn})^{0,5}]$; oxides are given in weight percentage, trace elements are in ppm.

For Rb-Sr analyses, biotite (200-300 μm) and powdered whole rock were spiked with a ^{85}Rb-^{84}Sr mixed tracer solution and dissolved in HF and $HClO_4$. The ion exchange chromatography procedure was applied for separating Rb and Sr from the sample solutions. Rb and Sr isotope analyses were carried out on a Finnigan MAT 262 mass spectrometer. Sr was measured on a single W filament with a Ta-HF activator and Rb was measured in double filament configuration. The NBS 987 Sr-standard yielded a $^{87}Sr/^{86}Sr$ ratios of 0.710259 ± 10. The input error for age calculations is ±1 % (2σ) for the $^{87}Rb/^{86}Sr$ ratio and ±0.03 % (2σ) for the $^{87}Sr/^{86}Sr$ ratios. Regression lines were calculated by the least squares cubic method of York, (1969) using the ISOPLOT software of Ludwig (1988).

For zircon evaporation (Kober, 1986), single zircon grains were embedded in a 0.7 mm wide Re-filament and measured on double filament configuration on a Finnigan MAT 262 mass spectrometer by dynamic ion counting mode in the mass sequence of 206-207-208-204-206-207. The age error on each temperature step is calculated according to formula given in Siebel et al. (2004) (Table 3). Details for the single zircon evaporation technique can be found in Okay et al. (1996), Chen et al. (2000), Siebel et al. (2003), and Koralay et al. (2004).

Results

Geochemistry

Eleven representative samples from the metagranites were analyzed. Major, trace and rare earth element composition of metagranites are presented in Table 2. The SiO_2 ratios range from 65.34 % to 73.14 %, Al_2O_3 from 14.17 % to 16.38 %, CaO from 1.50 % to 3.79 %, Na_2O from 3.06 % to 4.07 % and K_2O from 2.81 % to 5.80 %. Negative correlation between TiO_2, MgO vs. SiO_2, content are similar in metagranites and undeformed granites (Fig. 7), but the metagranites define different (parallel) trends. Similarly, Ba, Rb and V contents in metagranite samples are remarkably different from the samples from Eğrigöz and Koyunoba granites (Fig. 7). Although, the undeformed granites are clearly I-type in nature (Akay, 2009), ASI values of most of samples from metagranites indicate an S-type affinity (Table 2). Chondrite- and primitive mantle-normalized REE patterns of the metagranite and undeformed granites also indicate differences between these magmatic bodies (Fig. 8). Compared to the REE patterns of the undeformed granites, the metagranites are more enriched in light rare earth elements (LREE) ($[La/Yb]_N$ = 8-

38.4), and less enriched in heavy rare earth elements (HREE) ($[Gd/Yb]_N$ = 0.8-5.0). Besides, negative Eu anomalies observed in the undeformed granites are not seen in the metagranites (0.6 < Eu/Eu* < 0.8 (Fig. 8).

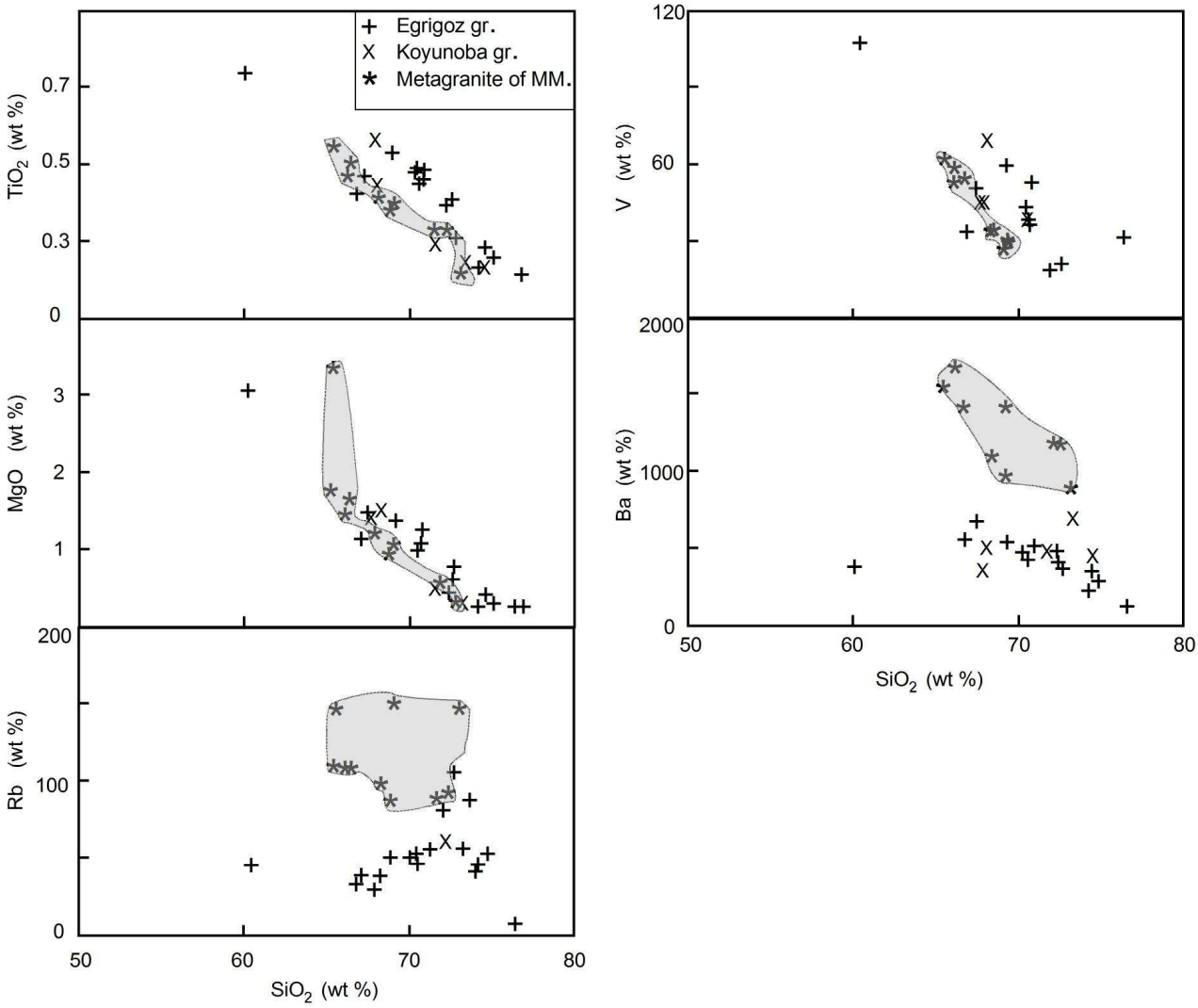

Fig. 7. Harker-type variation diagrams of the samples from the Eğrigöz and Koyunoba granites and metagranites from the Menderes Massif.

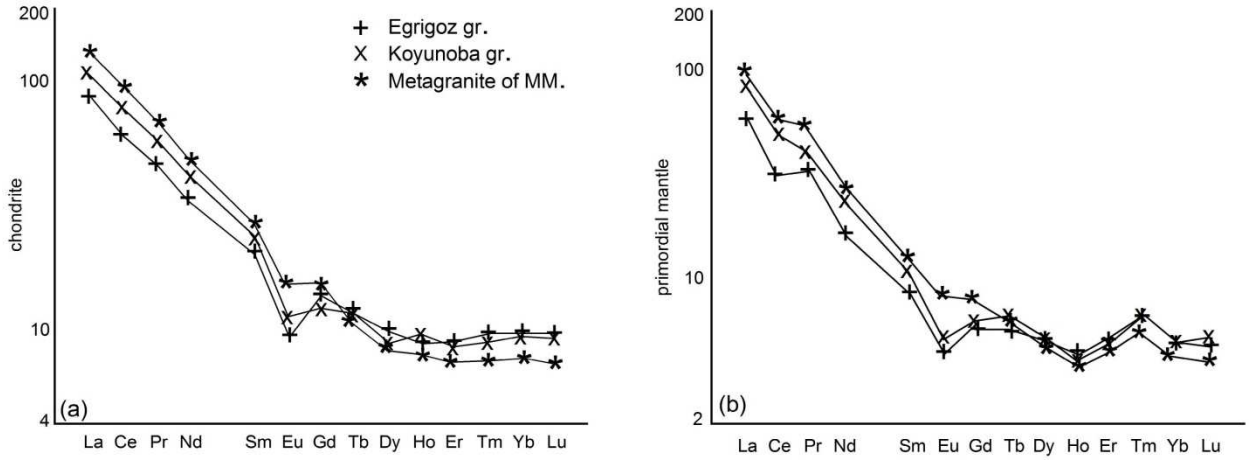

Fig. 8. (a) Chondrite- and (b) primordial mantle-normalized REE patterns of Eğrigöz, Koyunoba granites and metagranites. Normalized values are after Taylor and McLennan (1985).

Geochronology

$^{207}Pb/^{206}Pb$ zircon evaporation age data of a gneiss sample and U-Pb isotopic dilution zircon data from a gneiss and a metagranite from the Menderes Massif, the Eğrigöz and Koyunoba granites are given in Tables 3, 4 and Figs. 9, 10. Transparent zircon grains free of inclusions and cracks were chosen for analyses. Mineral composition of the measured gneiss samples from the Menderes Massif is characterized by the paragenesis quartz, K-feldspar, plagioclase, biotite and muscovite. Biotite is rarely altered to chlorite in this sample. The dated metagranite of the Menderes Massif is mainly made up of quartz, K-feldspar, plagioclase, biotite and ± muscovite. The analyzed Eğrigöz and Koyunoba granites contain orthoclase, plagioclase, quartz, biotite, and hornblende with zircon, titanite as mainly accessory minerals.

Augen gneiss (sample no. 729): Dated colorless zircons present a homogeneous internal microstructure in CL images. Four subhedral, nearly prismatic and semi-rounded zircon grains were selected for $^{207}Pb/^{206}Pb$ evaporation (Fig. 9a, b). The grains give $^{207}Pb/^{206}Pb$ ages of 606.6 ± 3.1 Ma (729-4), 565.3 ± 3.6 Ma (729-1), 552.2 ± 3.0 Ma (729-3), and 551.1 ± 4.6 Ma (729-2) (Table 3).

Table 3. Zircon evaporation data for a gneiss sample (729) of the Menderes Massif

Sample	Grain no & characteristics	Mode of measurement	Evaporation temperature (^{0}C)	No. of scans	Mean value $^{207}Pb/^{206}Pb$ ratios ±2 σ	$^{207}Pb/Pb^{206}$ age (Ma)
Gneiss (729)	1 63-125 µm, medium long, subround, prismatic, yellowish	IC, dynamic	1400	114	0.058950 ± 21	565.3 ± 3.6
	2 63-125 µm, medium long, subround, prismatic, brownish	IC, dynamic	1420	114	0.058568 ± 27	551.1 ± 4.7
	3 63-125 µm, medium long, subround, prismatic, yellowish	IC, dynamic	1420	418	0.058596 ± 17	552.2 ± 3.0
	4 63-125 µm, medium long, subround, prismatic, yellowish	IC, dynamic	1400	304	0.060081 ± 18	606.6 ± 3.1

Error calculation formula is below:

$$\Delta age = \sqrt{\left(\left(\frac{2\sigma}{\sqrt{n}}\right)^2 + \Delta f^2\right)}$$

(n): number of $^{207}Pb/^{206}Pb$ isotope ratio scans; (2σ): the 2sigma standard error of the Gausian distribution function of $^{207}Pb/^{206}Pb$ ratios; (Δf): an assumed error of 0.1% which includes potential bias caused by mass fractionation of Pb isotopes and uncertainty in linearity of the multiplier signal

Augen gneiss (sample no. 739): Prismatic, sub-idiomorphic, long and thick zircon crystals from the augen gneiss show well-defined oscillatory zoning typical of magmatic zircon (Fig. 9c, d). Five zircon fractions define a discordia and regression of these data points, anchored at the origin, yields an upper intercept age of 543 ± 10 Ma (MSWD=2.9) and a lower intercept age of -36 ± 28 Ma which might be attributed to Pb-loss (Fig. 10a). It should be noted that Koralay et al. (2004) obtained zircon evaporation ages between 570-520 Ma from augen gneisses of the central Menderes Massif and Gessner et al. (2004) reported a $^{207}Pb/^{206}Pb$ zircon evaporation age of 547.2 ± 1.0 Ma from metagranites of the southern Menderes Massif.

Metagranite (sample no. 737A): Zircon grains from the metagranite in the Menderes metamorphic rocks show clear prismatic morphology and oscillatory zonation in cathodoluminescence (CL) images and inherited (or pre-magmatic) cores are absent (Figs. 9e, f). Six zircon fractions from this sample were analyzed by the U-Pb isotopic dilution method (Table 3). Three zircon fractions plot close to the concordia curve at 30 Ma, but two of them are slightly discordant. All fractions define a discordia with a lower intercept age of 30.04 ± 0.56 Ma and an upper intercept age of 1.8 Ga (MSWD=2.9). The upper intercept age is mainly defined by one fraction. Excluding the youngest zircon fraction, which is expected to have suffered some lead

loss (Fig. 10b, c), the other four fractions yield an age of 30.28 ± 0.24 Ma which is still identical, within error limits, with the age of the total data set. This age is interpreted as the crystallization age of metagranite (Fig. 10b, c).

Eğrigöz and Koyunoba granites (sample no. 1212, 1211): Dated zircon grains have well-preserved euhedral transparent to translucent crystals of various sizes. CL images exclusively show oscillatory zoning typical for magmatic zircons and no sign of inheritance in CL images (Fig. 9g-j). Nine zircon fractions from the Eğrigöz granite and five from the Koyunoba were selected for U-Pb isotope analyses (Fig. 10e-g; Table 3). All zircon fractions of the Eğrigöz granite (1212) plot along a discordia line with a lower intercept age of 19.3 ± 4.4 Ma and an upper intercept age of 562 ± 72 Ma (Fig. 10f), but with a high MSWD value (ca. 33). However, the lower intercept age is almost identical to the age of the youngest concordant zircon fraction (ca. 19 Ma) and this allows us to assume that this age is close to the crystallization age of the Eğrigöz granite. Similarly, a lower intercept age of 21.7 ± 1.0 Ma and an upper intercept age of 556 ± 93 Ma (MSWD=0.48) were obtained from five zircon fractions of the Koyunoba granite (Fig. 10d, e). The lower intercept age is interpreted as the crystallization age of the Koyunoba granite at about 22 Ma. The upper intercept ages of these granites (562 ± 72 Ma; 556 ± 93 Ma) show close similarity with the U-Pb zircon age (Fig. 10a) and $^{207}Pb/^{206}Pb$ ages of the gneisses of the Menderes Massif (Table 4) suggesting that the magma of the Eğrigöz and Koyunoba granites were derived from similar sources

Rb-Sr data

$^{87}Rb/^{86}Sr$ (biotite-whole rock) data were obtained from the Eğrigöz granite (1212) and the results are given in Table 5. Biotite contains 1113.1 ppm Rb and 5.85 ppm Sr (Table 5). Whole rock and biotite from the Eğrigöz granite define an isochron age of 18.77 ± 0.19 Ma (Table 5). The closure temperature interval for Sr-diffusion in biotite is estimated as 350 - 450^{o}C (Jenkin et al., 2001; Giletti, 1991) and the biotite-whole rock age, determined here, most likely represents the cooling age of the Eğrigöz granite through this temperature interval.

Table 4. U-Pb isotopic data from gneiss (739), metagranite (737A), Eğrigöz granite (1212) and Koyunoba granite (1211).

Sample				Atomic ratios				Mean ages (Ma)		
	$^{206}Pb/^{204}Pb$	U (ppm)	Pb*(ppm)	$^{208}Pb^*/^{206}Pb^*$	$^{206}Pb^*/^{238}U$	$^{207}Pb^*/^{235}U$	$^{207}Pb^*/^{206}Pb^*$	$^{206}Pb^*/^{238}U$	$^{207}Pb^*/^{235}U$	$^{207}Pb^*/^{206}Pb^*$
Gneiss										
739-1Y	5856	1138.2	50.5	0.05	0.04645 ± 26	0.37820 ± 36	0.05904 ± 47	292.7	325.7	568.7
739-2Y	6790	1018.3	42.2	0.07	0.04256 ± 22	0.34612 ± 33	0.05898 ± 46	268.6	301.8	566.5
739-3Y	6896	1062.5	67	0.04	0.06691 ± 35	0.54382 ± 40	0.05897 ± 31	417.5	440.9	565.1
739-5	11620	727.7	39.5	0.03	0.05757 ± 30	0.46524 ± 26	0.05860 ± 12	360.8	387.9	552.6
739-6	4578	456.7	54.7	0.02	0.12934 ± 08	1.03575 ± 06	0.05807 ± 06	784.1	721.8	532.6
Metagranite										
737A-1	220770	2542	12	0.10	0.00472 ± 29	0.03042 ± 44	0.04665 ± 60	30.4	30.4	31.7
737A-2	246360	1523	7.4	0.16	0.00491 ± 45	0.03321 ± 113	0.04903 ± 115	31.5	33.1	149.6
737A-4	78394	1734	8.3	0.10	0.00486 ± 37	0.03301 ± 87	0.04921 ± 12	31.2	32.9	157.9
737A-6	105040	1368	6.2	0.10	0.00460 ± 33	0.02997 ± 77	0.04722 ± 11	29.6	29.9	60.7
737A-8	93907	2098	17.7	0.07	0.00859 ± 65	0.08857 ± 13	0.07477 ± 9	55.1	86.1	1062.3
737A-9	62134	2098	9.7	0.09	0.00469 ± 29	0.03016 ± 67	0.04663 ± 97	30.1	30.1	30.5
Eğrigöz granite										
1212-1	80838	1996	6.4	0.08	0.00324 ± 18	0.02132 ± 22	0.04652 ± 40	21.3	21.4	24.9
1212-2	56176	2998	12.7	0.11	0.00425 ± 32	0.03051 ± 77	0.05207 ± 12	27.3	30.5	288.5
1212-3	62044	3317	13.1	0.11	0.00397 ± 22	0.02549 ± 31	0.04654 ± 49	25.5	25.5	26.1
1212-6	36961	6829	110.2	0.21	0.01473 ± 85	0.11525 ± 86	0.05671 ± 25	94.7	110.9	481.4
1212-7	93409	1996	6.4	0.08	0.03049 ± 32	0.02116 ± 63	0.04645 ± 12	21.2	21.2	21.3
1212-8	43564	2226	10.2	0.08	0.00474 ±30	0.03225 ± 63	0.04933 ± 90	30.4	32.2	163.9
1212-9	63719	1554	6.5	0.11	0.00419 ± 26	0.02937 ± 42	0.05076 ± 65	27	29.4	229.9
1212-10	49535	1854	5.3	0.10	0.00291 ± 18	0.01867 ± 65	0.04641 ± 156	18.7	18.7	19.3
Koyunoba granite										
1211-1	24832	548.5	2.8	0.05	0.00382 ± 45	0.02450 ± 155	0.04652 ± 28	24.5	24.9	64.3
1211-2	40420	1146.3	3.9	0.07	0.00349 ± 20	0.02204 ± 41	0.04648 ± 80	22.1	22.2	34.6
1211-3	27047	812.2	2.6	0.08	0.00336 ± 40	0.02157 ± 138	0.04648 ± 28	21.6	22.5	121.2
1211-4	62252	100.4	1.1	0.05	0.01186 ± 63	0.09540 ± 74	0.05829 ± 31	75.9	88.4	442.6
1211-5	20868	893.2	2.7	0.08	0.00321 ± 25	0.02059 ± 78	0.04642 ± 17	20.5	20.5	22.5
1211-6	6713	214.5	0.79	0.13	0.00366 ± 42	0.02372 ± 25	0.04692 ± 48	23.5	23.6	33

All errors quoted are 2σ absolute uncertainties and refer to the last digit
*radiogenic; grain size varies from 80-180 µm

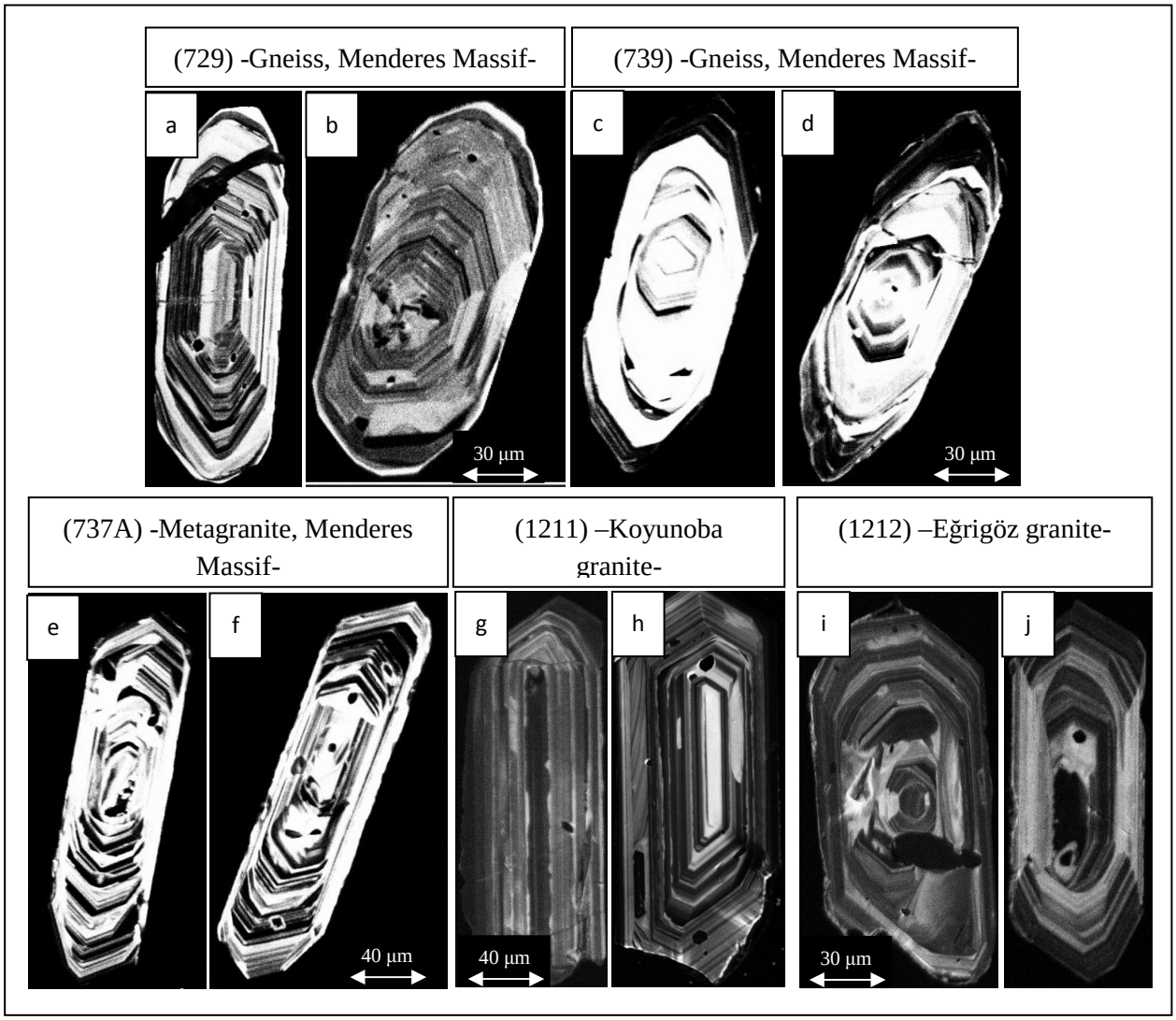

Fig. 9. Cathodoluminescence images of zircon grains from (a-b) augen gneiss (729), (c-d) augen gneiss (739) (e-f) metagranite (737A), (g-h) Koyunoba granite (1211), (i-j) Eğrigöz granite (1212). All zircon grains are prismatic, idiomorphic and show magmatic zonation.

Discussion

Two emplacement models exist for the early Miocene granites of the northern Menderes Massif. One model suggests that the granites were derived from melting of an abnormally thickened crust during a compressional tectonic regime (Genç¸ 1998; Altunkaynak and Yılmaz, 1998; Karacık and Yılmaz, 1998; Yılmaz, 1997; Yılmaz et al., 2001). An alternative model suggests that the granites emplaced syn-kinematically in the footwall of an extensional detachment fault (Işık and Tekeli, 2001; Işık et al., 2004; Seyitoğlu et al., 2004; Ring and Collins, 2005; Thomson and Ring, 2006). Since similar Ar/Ar ages were obtained for the undeformed granites and the surrounding metagranites, the metagranites were suggested to be the mylonitized upper parts of the undeformed granitic plutons and this suggestion has

become one of the strongest evidence for the postulation of a regional detachment fault separating the Menderes metamorphic rocks from the overlying tectono-stratigraphic units in NW Anatolia.

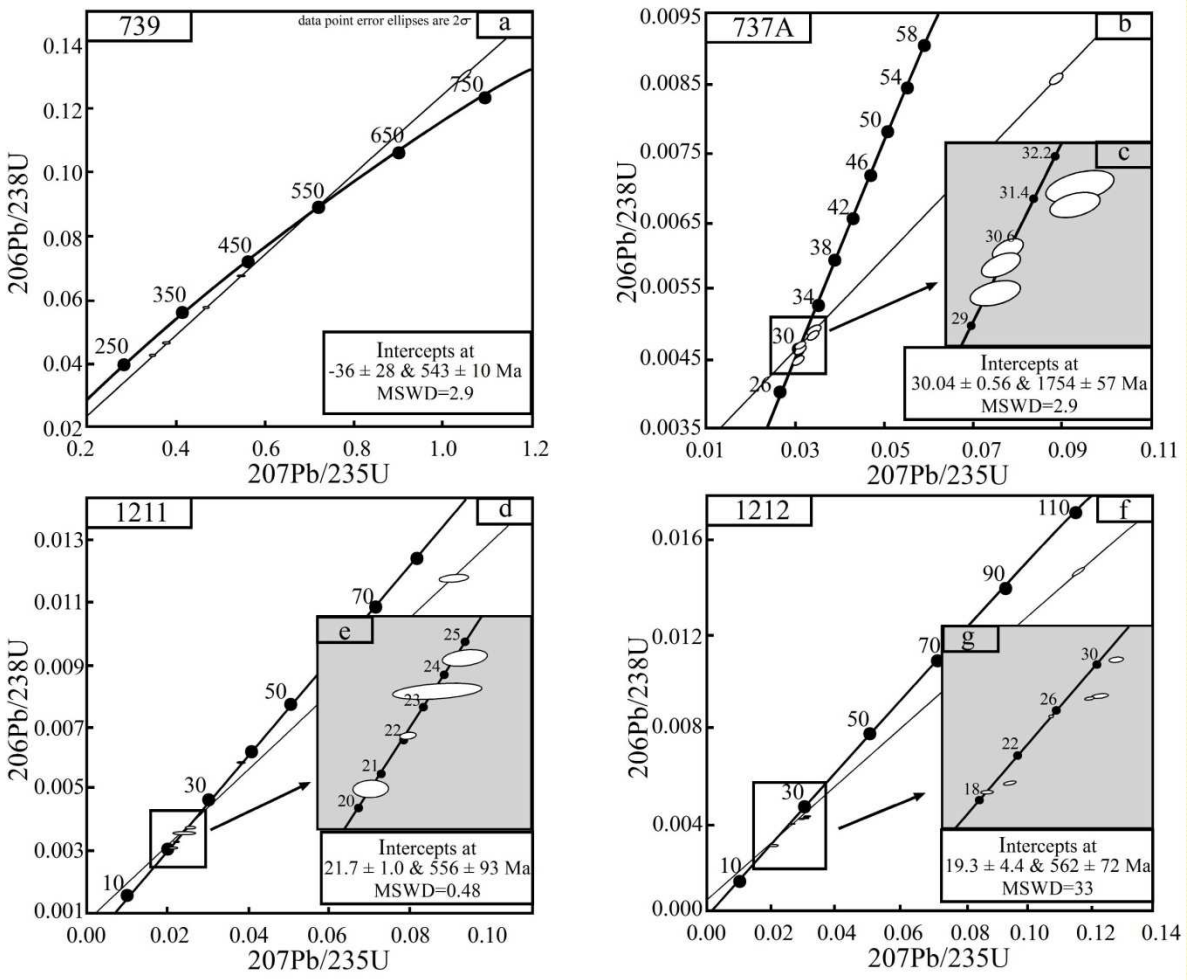

Fig. 10. U-Pb concordia diagram for (a) augen gneiss (739) five zircon fractions define a discordia line with an upper intercept age of 543 ± 10 ma, (b-c) metagranite (737a). Five zircon fractions define a discordia line with a lower intercept age of 30.04 ± 0.56 ma, (d-e) eğrigöz granite (1212). Lower discordia line intercepts at 19.3 ± 4.4 ma, (f-g) koyunoba granite (1211). Four zircon fractions give a well defined lower discordia intercept age of 21.7 ± 1.0 ma. For sample locations, see fig. 2a.

Table 5. $^{87}Rb/^{86}Sr$ data for whole-rock and biotite from a sample of the Eğrigöz granite (1212) (m: measured; i: initial ratio)

Sample	Rb (ppm)	Sr (ppm)	$^{87}Rb/^{86}Sr$	$^{87}Sr/^{86}Sr$ (m)	$^{87}Sr/^{86}Sr$ (i)	Age (Ma)
whole rock	225.7	235.7	2.77	0.710543 ± 10		
biotite	1113.1	5.85	558.24	0.858593 ± 07	0.70980 ± 21	18.77 ± 0.19

The new U-Pb age data, presented in this study, give a ca. 10 Ma age difference between the crystallization age of the undeformed granites (19.3 ± 4.4 Ma; 21.7 ± 1.0 Ma) and the hosting metagranites (30.04 ± 0.56 Ma) (Fig. 10). Besides, Catlos and Çemen (2005) presented monazite ages of ~ 29-28 Ma from gneisses of the Gördes Massif indicating that metamorphism and the intrusion of the metagranite are closely related in time. In addition to the new age data, the metagranites in the Simav region bear geochemical features of S-type granites (Table 2) whereas the Eğrigöz and Koyunoba granites are clearly I-type in nature. The S-type nature is also characteristic for metagranites and gneissic granites in other parts of the Menderes Massif (Bozkurt et al., 1995; Koralay et al., 2004), whereas other undeformed plutons of NW Anatolia (Ezine, Evciler, Kozak, Alaçam, Baklan) (Fig. 1) are exclusively I-type in nature.

Several well-studied early Miocene granites have been suggested to represent shallow-seated intrusions (Genç, 1998; Karacık and Yılmaz, 1998; Altunkaynak and Yılmaz, 1999; Hasözbek et al., 2009). The Eğrigöz and Koyunoba granites show similar geological and mineralogical features and are identical in ages with the other plutons from the Miocene magmatic belt. Our Rb-Sr biotite age (18.77 ± 0.19 Ma) and the U-Pb zircon ages (21-19 Ma) suggest that the metagranites and gneisses were already cold during the emplacement of the Eğrigöz and Koyunoba granites. Change from microgranitic to coarser holocrystalline texture from the periphery to the centre, large amount of xenoliths from the country rocks along the contact, presence of roof structure in the central part of Eğrigöz pluton may indicate a shallow crustal emplacement and rapid cooling (during approximately 2-1 Ma). The contact metamorphic mineral association around the Eğrigöz granite also suggests a shallow crustal emplacement depth (Albayrak, 2003). Al-in-hornblende barometry carried out on the Alaçam granite which is westward continuation of the Eğrigöz and Koyunoba granites (Hasözbek et al., in prep.) indicates 3-6 km depth of emplacement. Ductile behavior related to a detachment fault

causing mylonitic deformation at the periphery of undeformed granites, would not be expected in such a relatively cold shallow environment.

The data, presented above, indicate that the metagranites and the undeformed Eğrigöz and Koyunoba granites are not genetically related to each other. The close correspondence of the Ar-Ar muscovite ages obtained from the metagranites (22.86 ± 0.47 Ma) and undeformed Eğrigöz granite (20.19 ± 0.28 Ma) (Işık et al., 2004), however, does not support this conclusion. If the temperature was above 350 - 450 ^{O}C (Giletti, 1991 and Jenkin et al., 2001) the Miocene granite intrusions might have reset the mica ages of the metagranites. Given the high closure temperature for Pb in zircon, (900- 1000 ^{O}C, Cherniak and Watson, 2001), the U-Pb zircon age (30.04 ± 0.56 Ma) more likely reflects the crystallization age of the metagranite.

Bozkurt et al. (2007) and Bozkurt et al. (in review) have been recently presented Rb-Sr ages for brown and green biotite of 14-12 Ma from the fault surface south of Simav. These authors suggest that the so-called Simav detachment fault was active during late Miocene time. The mica ages would imply that the Eğrigöz and Koyunoba granites predate fault activity and were not synkinematically emplaced along this fault.

Conclusions

In the light of our new data, the following conclusions can be drawn;

Along the northern margin of the Menderes Massif, early Miocene I-type, calc-alkaline granites (Eğrigöz and Koyunoba) and their subvolcanic-volcanic equivalents form a NW-SE-trending magmatic belt that stitches different collision-related tectono-stratigraphic units of the Menderes Massif, the Afyon Zone and the tectonic contact between these units.

A previously suggested genetic relation between the early Miocene granites and the hosting metagranite is inconsistent with our geochemical and geochronological data.

The Eğrigöz and Koyunoba granites crystallized about 22-19 Ma ago and cooled down rapidly (18.77 ± 0.19 Ma) below the Rb-Sr biotite closure temperature.

$^{207}Pb/^{206}Pb$ zircon evaporation ages (607-551 Ma) and a U-Pb zircon age (543 ± 10 Ma) from Menderes gneisses closely agree with U-Pb upper intercept ages (562 ± 72 Ma; 556 ± 93 Ma) of zircons from the Eğrigöz and Koyunoba granites suggesting that the two granites were either derived from, or experienced significant contamination from the Menderes Massif.

Besides, our new $^{207}Pb/^{206}Pb$ evaporation data and U-Pb zircon ages given in this study from Simav region are identical with previous radiogenic age data from the gneissic rocks of the Menderes Massif.

U-Pb zircon ages imply ca. 10 age difference between the undeformed Eğrigöz and Koyunoba granite and the metagranites. Thus, the metagranites are not the sheared equivalents of the undeformed granites. More likely, they represent magmatic bodies metamorphosed during the main Menderes metamorphism.

Granite emplacement (Eğrigöz and Koyunoba) related to a low angle detachment fault is not supported by our new geochronological and geochemical data.

Acknowledgements

This study was financially supported by the Scientific and Technical Research Council of Turkey (TUBITAK) (project no: YDABAG-101Y014) and Dokuz Eylul University, Scientific Research Projects Foundation (project no: 02. KB. FEN. 038). A. Okay, O. Candan, T. Güngör, E. Koralay, C. Akal, and K. Akbayram are thanked for their helps and discussions during field work. N. Önoğlu is thanked for editing the English text. H. Schulz Institute of Geoscience, Tübingen is thanked for CL analyses. C. Shang, G. Bartholomä and E. Reitter, Department of Geochemistry, Tübingen University, are thanked for technical help.

References

Akal, C., Candan, O., Koralay, O.E., Okay, İ.A., Oberhänsli, R., Chen, F., 2008. Afyon Zonu'ndaki erken Devoniyen asidik magmatizmaya ait jeolojik, jeokimyasal ve jeokronolojik ön bulgular. 61th Geol Congr Turk, Abstracts, 204-207

Akay, E., 2009. Geology and petrology of the Simav Magmatic Complex (NW Anatolia) and its comparison with the Oligo-Miocene granitoids in NW Anatolia; implications on Tertiary tectonic evolution of the region. Int J Earth Sci, 98:1655–1675.

Akay, E., Hasözbek, A., Erdoğan, B., 2007. Emet (Kütahya, KB Anadolu) çevresinde Afyon Zonu'nun stratigrafisi ve tektonik konumu. Cukurova University, Geology Symposium, Abstracts, 179-180

Akdeniz, A., Konak, N., 1979a. Geology of Simav-Emet-Tavşanlı-Dursunbey-Demirci area. Report of the Mineral Research and Exploration Institute 108 p (in Turkish with English abstract)

Akdeniz, N., Konak, N., 1979b. Rock units of the MM and setting of the metabasic and metaultramafic rocks around Simav. Geol Soc Turk Bull 22: 175-184

Akkök, R., 1983. Structural and metamorphic evolution of the northern part of the Menderes Massif: new data from the Derbent area and their implication for the tectonics of the massif. J Geol 91: 342-350

Albayrak, O., 2003. Genetic investigation of polymetalic mineralizations along the northern and western border of the Eğrigöz Massif (Tavşanlı, Kütahya). Definition of the geodynamic conditions of Eğrigöz Massif. MSc Thesis, Dokuz Eylul University. 90 p (in Turkish with english abstract)

Altunkaynak, Ş., 2007. Collision-driven slab breakoff magmatism in Northwestern Anatolia, Turkey. J Geol 115: 63-82

Altunkaynak, Ş., Yılmaz, Y., 1998. The Mount Kozak magmatic complex, Western Anatolia. J Volcanol Geotherm Res 85: 211-231

Altunkaynak, Ş., Yılmaz, Y., 1999. The Kozak pluton and its emplacement. Geol J 34: 257-274

Aydoğan, M.S., Çoban, H., Bozcu, M., Akıncı, Ö., 2008. Geochemical and mantle-like isotopic (Nd, Sr) composition of the Baklan Granite from the Muratdağı Region (Banaz, Uşak), western Turkey: Implications for input of juvenile magmas in the source domains of western Anatolia Eocene–Miocene granites. J Asian Earth Sci 33: 155-176

Bozkurt, E., Satır, M., 2000. The southern Menderes Massif (western Turkey): geochronology and exhumation history. Geol. J. 35: 285-296

Bozkurt, E., Park, R.G., 2001. Discussion on the evolution of the southern Menderes Massif in SW Turkey as revealed by zircon dating. Geol Soc, London 158: 393-395

Bozkurt, E., Winchester, J.A., Park, R.G., 1995. Geochemistry and tectonic significance of augen gneisses from the southern Menderes Massif (West Turkey). Geol Mag 132, 287-301.

Bozkurt, E, Satır, M., Crowley, Q.G., 2007. Rb-Sr Mica, "Laser Ablation ICP-MS" and "Pb-Pb evaporation" zircon ages from the Menderes Massif. Colloquium of the Menderes Massif, in honour of O.Özcan Dora, İzmir, Extended Abstracts Book, 32-33

Bozkurt, E., Satır, M., Buğdaycıoğlu, Ç., 2010 (in review). Rb-Sr geochronology of the Simav detachment fault and its tectonic implications for the evolution of the northern Menderes Massif (Western Turkey). Tectonophysics

Candan, O., 1994. Petrography and metamorphism of the metagabbros at the northern part of Alaşehir; Demirci-Gördes submassif of Menderes Massif (in Turkish with English abstract). Geol Soc Turkey Bull 37: 29-40

Candan, O., Çetinkaplan, M., Oberhänsli, R., Rimmele, G., Akal, C., 2005. Alpine high-P/low-T metamorphism of the Afyon Zone and implications for the metamorphic evolution of Western Anatolia, Turkey. Lithos 84: 102-124

Catlos, E.J., Çemen, İ., 2005 Monazite ages and the evolution of the Menderes Massif, western Turkey. Int J Earth Sci 94: 204–217
Chen, F., Hegner, E., Todt, W., 2000. Zircon ages and Nd isotopic and chemical compositions of orthogneisses from the Black Forest, Germany: Evidence for a Cambrian magmatic arc. Int J Earth Sci 88: 791-802
Chen, F., Siebel, W., 2004. Zircon and titanite geochronology of the Fürstenstein granite massif, Bavarian Forest, NW Bohemian Massif: Pulses of the late Variscan magmatic activity. Eur J Miner16: 777-788
Chen, F., Siebel, W., Satir, M., Terzioğlu, N., Saka, K., 2002. Geochronolgy of the Karadere basement (NW Turkey) and implications for the geological evolution of the Istanbul zone. Int J Earth Sci 91: 469-481
Cherniak, D.J., Watson, E.B., 2003. Diffusion in zircon. Reviews in Mineralogy and Geochemistry. V. 53;1; p. 113-143.
Collins, A.S., Robertson, A.H.F., 1998. Processes of Late Cretaceous to Late Miocene episodic thrust-sheet translation in the Lycian Taurides, SW Turkey. J Geol Soc, Lond 155: 759-772.
Davis, P. B., and Whitney, D. L., 2006. Petrogenesis of lawsonite and epidote eclogite and blueschist, Sivrihisar Massif, Turkey. Metamorphic Geol 24, 823-849.
Dilek, Y. & Altunkaynak, S. 2009. Geochemical and temporal evolution of Cenozoic magmatism in western Turkey: mantle response to collision, slab breakoff, and lithospheric tearing in an orogenic belt. Geol Soc London Spec Pub (In: van Hinsbergen, D. J. J., Edwards, M. A. & Govers, R., (Eds)) 311, 213-234.
Ercan, T., Dinçel, A., Günay, E., 1979. Uşak volkanitlerinin petrolojisi ve plaka tektoniği açısından Ege Bölgesi' ndeki yeri. Bull Geol Soc Turkey 22/2: 185-198 (in Turkish with English abstract)
Ercan, T., Günay, E., Savaşçın, M.Y., 1984. Simav ve çevresindeki Senozoyik yaşlı volkanizmanın bölgesel yorumlanması. Min Res and Exp Bull 97/98: 86-101 (in Turkish with English abstract)
Genç, S.C., 1998. Evolution of the Bayramiç magmatic complex, northwestern Anatolia. J Volcanol Geotherm Res 85: 233-249
Gessner, K., Güngör, T., Ring, U., Passchier, C.W., 1998. Structure and crustal thickening of the Menderes Massif, southwest Turkey, and consequences for large-scale correlations between Greece and Turkey. Bull Geol Soc Greece 32: 145-152
Gessner, K., Piazolo, S., Gungor, T., Ring, U., Kröner, A., Passchier, W.C., 2001. Tectonic significance of deformation patterns in granitoid rocks of the Menderes nappes, Anatolide belt, southwest Turkey. Int J Earth Sci 89: 766-780
Gessner, K., Collins, A.S., Ring, U., Gungor, T., 2004. Structural and thermal history of poly-orogenic basement: U-Pb geochronology of granitoid rocks in the southern Menderes Massif, Western Turkey. J Geol Soc, London. 161: 93-101.
Giletti, J.B., 1991. Rb and Sr diffusion in alkali feldspars, with implications for cooling histories of rocks. Geochim Cosmochim Acta 55: 1331-1343
Gürer, F.Ö., Filoreau, S.N., Özburan, M., Sangu, E., Doğan, B., 2009. Progressive development of the Büyük Menderes Graben based on new data, western Turkey. Geol Mag. 146: 652-673

Hasözbek, A., Satir, M., Erdoğan, B., Akay, E., Siebel, W., 2009. Magmatic evolution of the northwestern edge of Tauride-Anatolide Platform: Geochronological and isotopic implications. Geochim Cosmochim Acta 73/13: A499-A499

Hasözbek, A., Satir, M., Erdoğan, B., Akay, E., Siebel, W., 2010. Early Miocene post-collisional magmatism in NW Turkey: geochemical and geochronological constraints. Int Geol Rev. DOI:10.1080/00206810903579302

Hetzel, R., Reischmann, T., 1996. Intrusion age of Pan-African augen gneisses in the southern Menderes Massif and the age of cooling after Alpine ductile extensional deformation. Geol Mag 133: 565-572

Işık, V., Tekeli, V., 2001. Late orogenic crustal extension in the northern Menderes Massif (Western Turkey): evidence for metamorphic core complex formation. Int J Earth Sci 89: 757-765

Işık, V., Tekeli, O., Seyitoğlu, G., 2004. The $^{40}Ar/^{39}Ar$ age of extensional ductile deformation and granitoid intrusion in the northern Menderes core complex: implications for the initiation of extensional tectonics in western Turkey. J Asian Earth Sci 23: 555-566

İşintek, İ., Akay, E., Hasözbek, A., Erdoğan, B., 2007. Afyon Zonu' na ait Geç Triyas-Malm Budagan karbonat istifinin foraminifer ve alg içeriği (Emet, Kütahya, Batı Türkiye). Cukurova University, Geology Symposium. Çukurova. Abstracts, 118-119

Jenkin, G.R.T., Ellam, R.M., Rogers, G., Stuart, F.M., 2001. An investigation of closure temperature of the biotite Rb-Sr system: The importance of cation exchange. Geochim Cosmochim Acta 65: 1141-1160

Karacık, Z., Yılmaz, Y., 1998. Geology of the ignimbrites and the associated volcano-plutonic complex of the Ezine are, northwestern Anatolia. J Volcanol Geotherm Res 85: 251-264

Karacık, Z., Yılmaz, Y., Pearce, A.J., Ece. Ö.I., 2007. Petrochemistry of the south Marmara granitoids, northwest Anatolia, Turkey. Int J Earth Sci. V:97**,** 1181-1200.

Kaya, O., 1972. Tavşanlı yöresi ofiyolit sorununun ana çizgileri. Bull Geol Soc Turk 15/1: 26-108 (in Turkish with English abstract)

Kaya, O., Sadeddin, W., Altiner, D., Meric, E., Tansel, I., Vural, A., 1995. Tavşanlı (Kütahya) güneyindeki ankimetamorfik kayaların stratigrafisi ve yapısal konumu: İzmir-Ankara Zonu ile bağlantısı. Min Res Exp Bull 117: 5-16

Kober, B., 1986. Whole-grain evaporation for $^{207}Pb/^{206}Pb$-age investigations on single zircons using a double-filament thermal ion source. Contrib Mineral Petrol 93: 482-490

Konak, N., 1982. Geology of the Simav region. Istanbul University, Faculty of Earth Sciences, Department of Geological Engineering, PhD thesis (in Turkish with English Abstract, unpublished)

Koralay, O.E., Dora, O., Chen, F., Satir, M., Candan, O., 2004 Geochemistry and age of orthogneisses in the Derbent (Alaşehir) area, Eastern part of the Ödemiş-Kiraz submassif, Menderes Massif: Pan-African magmatic activity. Turkish J Earth Sci 13: 37-61

Kröner, A., Şengör, A.M.C., 1990. Archean and Proterozoic ancestry in late Precambrian to Early Paleozoic crustal elements of southern Turkey as revealed by single-zircon dating. Geology 18: 1186-1190

Loos, S., Reischmann, T., 1999. The evolution of the southern Menderes Massif in SW Turkey as revealed by zircon dating. J Geol Soc Lond 156: 1021-1030

Ludwig, K.R., 1988. Pbdat for MS-Dos- a computer program for IBM-PC compatibles for processing raw Pb-U-Th isotope data. U.S Geol. Surv. Open-file Rep 88-542: 1-37

Ludwig, K.R., 2001. Isoplot/Ex, rev 2.49: A geochronological toolkit for Microsoft Excel. Berkley Geochronology Center Spec. Publ. No: 1a, 1-58

Mattinson, M.J., 2005. Zircon U-Pb chemical abrasion ("CA-TIMS") method: Combined annealing and multi-step partial dissolution analysis for improved precision and accuracy of zircon ages. Chem Geol 220: 47-66

Okay, A. İ., 1980. Lawsonite zone blueschists and a sodic amphibole producing reaction in the Tavsanli region, Northwest Turkey. Contributions to Mineralogy and Petrology 75, 179-186.

Okay, A.İ. 1984. Distribution and characteristics of the northwest Turkey blueschists. In Robertson A.H.F and Dixon J.A (Eds.), The Geological Evolution of the Eastern Mediterranean. Geol. Soc. London, Special Publicatipns, 17, 455-466.

Okay, A.İ., 2004. Tectonics and high-pressure metamorphism in Northwest Turkey. 32th Geological Congress. Field Trip Guide Book, P01, 56 p

Okay, A.İ., Satır, M., 2000. Coeval plutonism and metamorphism in a latest Oligocene metamorphic core complex in northwest Turkey. Geol Mag 137: 495-516.

Okay, A.İ., Tansel, İ., Tüysüz, O., 2005. Obduction, subduction and collision as reflected in the Upper Cretaceous-Lower Tertiary sedimentary record of western Turkey. Geol Mag 138: 117-142

Okay, A.İ., Satır, M., Maluski, H., Siyako, M., Monie, P., Metzger, R., Akyüz, S., 1996. Paleo- and Neo-Tethyan Tethyan events in northwestern Turkey: Geologic and geochronologic constraints. In: A. Yin and M. Harrison (Eds.) The Tectonic Evolution of Asia. Cambridge University Press 420-441

Özer, S., İrtem, O., 1982. Işıklar-Altındağ (Bornova-İzmir) alanı Üst Kretase Kireçtaşlarının Jeolojik Konumu, stratigrafisi ve fasiyes özellikleri. Bull Geol Soc of Turk 25: 41-47 (in Turkish with English abstract)

Özgenç, İ., İlbeyli, N., 2008. Petrogenesis of the late Cenozoic Eğrigöz granite in western Anatolia, Turkey: Implications for magma genesis and crustal processes. Int Geol Rev 50: 375-391

Ring, U., Collins, S.A., 2005. U-Pb SIMS dating of synkinematic granites: timing of core-complex formation in the northern Anatolide belt of western Turkey, J Geol Soc Lond 162: 289-298

Satır, M., Friedrichsen, H., 1986. The origin and evolution of the Menderes Massif, W Turkey: Rb/Sr and oxygen isotope study. Geol Rundsch 75: 703-714

Seyitoğlu, G., Işık, V., Çemen, İ., 2004. Complete Tertiary exhumation history of the Menderes Massif, western Turkey: an alternative working hypothesis. Terra Nova 16: 358-364

Siebel, W., Chen, F., Satir, M., 2003. Late Variscan magmatism revisited: New implications from Pb-evaporation zircon ages on the emplacement of redwitzites and granites in NE Bavaria. Int J Earth Sci 92: 36-53

Siebel, W., Blaha, U., Chen, F., Rohrmüller, J., 2004. Geochronology and geochemistry of a dyke-host rock association and implications for the formation of the Bavarian Pfahl shear zone, Bohemian massif, Int J Earth Sci 94: 8-23

Taylor, S.R., McLennan, S.M., 1985. The continental crust: Its composition and evolution. Blackwell, Oxford.
Thomson, S.N., Ring, U., 2006. Thermochronologic evaluation of postcollision extension in the Anatolide orogen, western Turkey. Tectonics 25: 1-20
Whitney, D. L. & Davis, P. B., 2006. Why is lawsonite eclogite so rare? Metamorphism and preservation of lawsonite eclogite, Sivrihisar, Turkey. Geology 34, 473-476.
Yılmaz, Y., 1997. Geology of western Anatolia active tectonics of northwestern Anatolia-The Marmara poly-project. A multidisciplinary approach by space-geodesy, geology, hydrogeology, geothermics and seismology, Univ. Press Zurich. 31-53
Yılmaz, Y., Altunkaynak, Ş., Karacık, Z., Gündoğdu, N., Temel, A., 1994. Development of neo-tectonic related magmatic activities in western Anatolia. Int Vol Congr, Ankara, Abstract: 13
Yılmaz, Y., Genç, Ş.C., Karacık, Z., Altunkaynak, Ş., 2001. Two contrasting magmatic associations of NW Anatolia and their tectonic significance. J Geod 31: 243-271
York, D., 1969. Least-square fitting with a straight line with correlated errors. Earth Planet Sci Lett 14: 225-280

Chapter 2: Early Miocene post-collisional magmatism in NW Turkey: geochemical and geochronological constraints

Altuğ Hasözbek · Muharrem Satır · Burhan Erdoğan · Erhan Akay · Wolfgang Siebel

Correspondence author: A. Hasözbek
Institut für Geowissenschaften, Universität Tübingen,
Wilhelmstrasse 56, D-72074 Tübingen, Germany
E-mail: altug.hasoezbek@student.uni-tuebingen.de
Tel: +49-7071-2973156
Fax: +49-7071-295713

M. Satır · W. Siebel
Institut für Geowissenschaften, Universität Tübingen,
Wilhelmstrasse 56, D-72074 Tübingen, Germany
E-mail: satir@uni-tuebingen.de
Tel: +49/7071/2978903
Fax: +49/7071/295713
E-mail: wolfgang.siebel@uni-tuebingen.de
Tel: +49/7071/2974991
Fax: +49/7071/295713

B. Erdoğan · E. Akay
Dokuz Eylul University, Engineering Faculty,
Department of Geological Engineering,
Tınaztepe, 35160 Buca, Izmir, Turkey
e-mail: burhan.erdogan@deu.edu.tr
Tel: +90/232/4127306
Fax: +90/232/8531606
E-Mail: erhan.akay@deu.edu.tr
Tel: +90/232/4127326
Fax: +90/232/8531606

Published in International Geology Review

Idea:	60%
Problem:	40%
Production of Data:	70%
Evaluation and Interpretation:	80%
Preparation of the manuscript:	70%

Abstract

The Alaçam region of NW Turkey lies within the Alpine collision zone between the Sakarya continent and the Menderes platform. Four different tectonic zones of these two continents form imbricated nappe packages, intruded by the Alaçam granite. Newly determined U-Pb zircon ages of this granite are 20.0 ± 1.4 Ma and 20.3 ± 3.3 Ma, indicating an early Miocene emplacement. Rb-Sr biotite ages of the granite are 20.01 ± 0.20 Ma and 20.17 ± 0.20 Ma, suggesting fast cooling at a shallow crustal level. Geochemical characteristics show that the Alaçam granite is similar to numerous EW-trending plutons of NW Anatolia.

Gneissic granites of the Afyon tectonic zone were cut by the Miocene Alaçam granite and have been interpreted in earlier studies as the sheared parts of the Alaçam granite which formed along a crustal-scale detachment zone under extensional regime. We determined a U-Pb zircon age of 314.9 ± 2.7 Ma from a gneissic granite sample of the Afyon Zone demonstrating that these rocks have no genetic relation with the Miocene Alaçam granite. The Early Miocene granitic plutons bear post-collisional geochemical features and are interpreted as products of Alpine-type magmatism along the İzmir-Ankara Suture Zone in NW Turkey and seem to have no genetic relation to the detachment zone.

Keywords: Alaçam granite, U-Pb zircon age, Rb-Sr biotite age, rapid cooling, Northwest Anatolia

Introduction

The main post-collisional eastern Mediterranean magmatic belt evolved from the Eocene to the Quaternary and has been addressed in numerous papers (Fytikas *et al*. 1984; Yılmaz 1990; Aldanmaz *et al*. 2000; Pe-Piper and Piper 2006; Akay and Erdoğan 2004; Altunkaynak and Dilek 2006; Dilek and Altunkaynak 2007, 2009; Akay 2009). The general evolution for the generation of this post-collisional magmatism is well documented and most of the authors suggest a large magmatic arc with arc migration to the south to its recent position (Jolievet and Brun 2008 and references therein).

During and after the closure of the Neo-Tethyan Ocean and progressive collision of the Tauride-Anatolide Platform with the Sakarya Continent, widespread post-collisional, alpine-type magmatism formed in the eastern Mediterranean. In NW Anatolia, this magmatism comprises associated subvolcanic and plutonic rocks forming a NW trending belt (Fig. 1) (Bingöl *et al.* 1982; Ercan *et al.* 1984; Harris *et al.* 1994; Seyitoğlu and Scott 1992; Genç and Yılmaz 1997; Genç 1998; Karacık and Yılmaz 1998; Altunkaynak and Yılmaz 1998 1999; Delaloye and Bingöl 2000; Okay and Satır 2000; Aldanmaz *et al.* 2000; Seyitoğlu *et al.* 2004; Yılmaz *et al.* 2001; Okay and Satır 2006; Karacık *et al.* 2008; Altunkaynak 2007; Dilek and Altunkaynak 2007; Özgenç and Ilbeyli 2008; Akay 2009; Dilek and Altunkaynak 2009; Boztuğ *et al.* 2009; Hasozbek *et al.* 2009a).

The exact emplacement mode of the Eocene and Miocene magmatic associations with volcanic suites along the area is still questionable due to complex geodynamic evolution of the belt. Early Eocene continent collision in NW Anatolia and the Marmara region caused a pronounced sub-alkaline, medium to high K magmatism (Altunkaynak 2004; Harris *et al*. 1995; Delaloye and Bingöl 2000; Okay and Satır 2000; Genç and Yılmaz 1997; Karacık *et al*. 2009). This compression was followed by widespread N-S extension with the products of Oligo-Miocene magmatism with extrusive counterparts of the same composition (Altunkaynak and Yılmaz 1998; Yılmaz *et al*. 2000; Altunkaynak and Dilek 2006; Akay 2009 and references therein). Recently, some granitoids of this region (Eğrigöz, Koyunoba, Evciler) have been interpreted as syn-kinematic granitoids emplaced in a north-dipping regional detachment zone (Işık and Tekeli 2001; Işık *et al.* 2004**;** Okay and Satır 2000) and this emplacement model was used as evidence for a thin lithosphere and existence of core complexes in NW Anatolia (Menderes Massif, Kazdağ Massif) (Okay and Satır 2000; Işık *et*

al. 2005; Ring and Collins 2005). In this model, deformed country rocks surrounding the undeformed granites have considered as the mylonitized upper part of the granites (Işık and Tekeli 2001; Işık *et al.* 2004; Okay and Satır 2000). However, geological, petrological and geochronological data of two important early Miocene magmatic bodies (Eğrigöz and Koyunoba granites) contradict this interpretation (Akay 2009; Hasözbek et. al. 2009a). Although numerous geochronological data are available from the undeformed Miocene granites in NW Anatolia (Bingöl *et al.* 1982; Delaloye and Bingöl 2000; Işık *et al.* 2004; Ring and Collins 2005; Thomson and Ring 2006; Okay *et al.* 2008), limited studies focused on the question whether the surrounding mylonitized rocks are co-genetic with the undeformed parts of these granites or not. Our study area is located along the northern Menderes Massif (SE Balıkesir) where the early Miocene magmatic associations show clear contact relations with the basement rocks of the Anatolide-Tauride platform. (Fig 1). Here we present new geochemical and geochronological data from the Alaçam granite, related stocks and associated gneissic granite of the Afyon Zone. Our data imply that the undeformed granite is not genetically related to the surrounding metamorphic rocks of the Menderes Massif and the Afyon Zone.

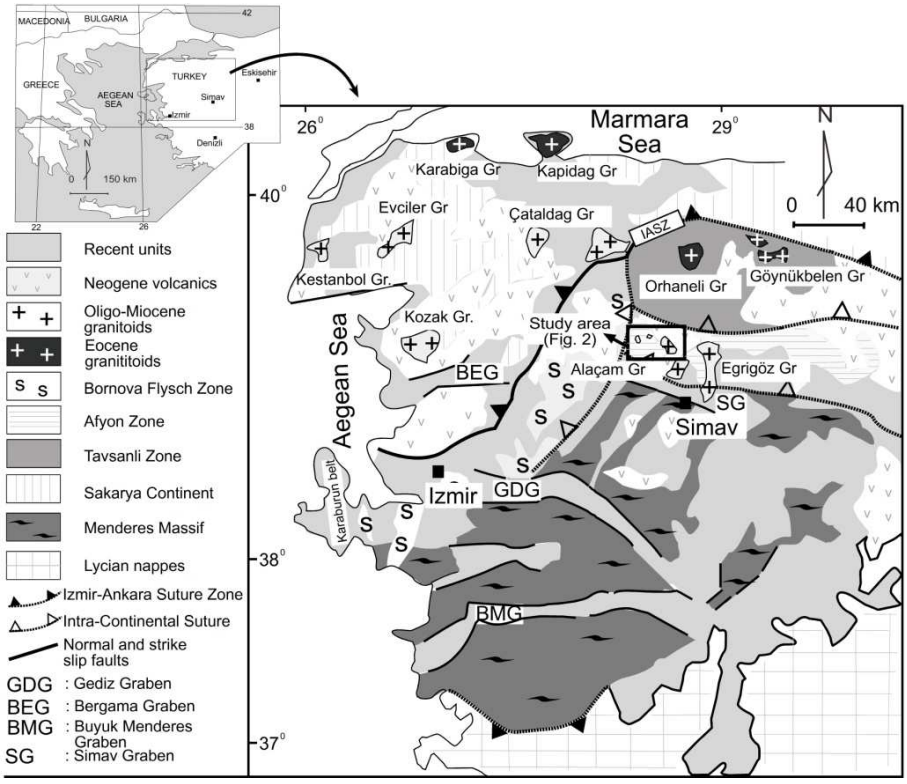

Figure 1. Simplified geological map of western Anatolia and location of the study area. Modified after Genç, (1998), Okay et al., (1996), Okay and Satır, (2000), Gürer et. al (2009) (Gr: granite).

The overall aims of this study are: a) providing geological features and radiometric age relations between the Alaçam granite and basement units of the Menderes Massif and the Afyon Zone, b) discussing the controversial tectono-magmatic evolution models of the region, and c) unveiling the nature of the Early Miocene magmatism during and after the collision of the Sakarya Continent and Anatolide-Tauride Platform.

Geological setting

In the study area, early Miocene Alaçam granite and its related stock intruded into the Menderes Massif, Afyon Zone and Bornova Flysch Zone (Figs 1, 2). The Menderes Massif forms the structurally lowest unit (Fig. 2) and is represented by a high-to-medium grade metapelite association (staurolite-kyanite-sillimanite zone (Konak 1982). Garnet-bearing biotite-muscovite schists and quartz-mica schists dominate the upper parts of the metapelite rocks. A meta-ophiolitic nappe complex, lithologically resembling the late Cretaceous Selçuk Formation of Güngör and Erdoğan (2001; 2002) and consisting of metagabbros and meta-ultramafic rocks, tectonically overlay the Menderes metamorphics. The meta-ophiolitic nappe complex is in turn tectonically overlain by low grade metamorphic rocks of the Afyon Zone in the study area (Okay 1984; Okay *et al.* 1996) which comprises, from bottom to top, gneissic granites, metapelites, metarhyolites and recrystallized limestones. In the study area, the rock associations of the Afyon Zone define a typical green-schist facies assemblage composed of albite, muscovite and chlorite (Konak 1982). However, HP-LT (Fe-Mg carpholite) rocks of this zone are also known around Afyon city (Candan *et al.* 2005). In the study area, well foliated gneissic granites of the Afyon Zone which are characterized by quartz, orthoclase, muscovite and minor amounts of biotite form the lower part of this unit (Fig. 3a, b). A primary granitic texture is well preserved in these rocks (Fig. 3b). The metamagmatic (gneissic granite) and metadetrital lower part of the Afyon Zone is graditionally overlain by a platform type carbonate succession. The Afyon Zone sequence is tectonically overlain by a non-metamorphic ophiolitic melange of the Late Cretaceous- Late Oligocene Bornova Flysch Zone (Okay 1984; Erdoğan 1990; Okay *et al.* 1996). These slices are composed dominantly of slightly deformed and cleaved light brownish mudstones and sandstones. Lenses of serpentinites, blocks of ultramafic rocks and platform limestones are preserved inside the brittly deformed matrix.

The Menderes Massif, meta-ophiolitic nappe complex, Afyon Zone and the ophiolitic melange of the Bornova Flysch Zone are all obliquely cut by the Alaçam granite along steeply dipping contacts (Figs. 2, 5, 6a, b). The Alaçam granite is a NW-SE elongated body, 15 to 4 km in diameter, and crops out in the Alaçam Mountains (Figs. 1, 2). The mineral assemblage of the Alaçam granite and its related stocks is quartz, plagioclase, orthoclase, hornblende, biotite and accessory minerals (zircon, titanite and apatite) (Figs. 4a, b, c). At the margin of the Alaçam granite, the texture is fine grained (0.1 - 0.3 mm) (Fig. 4a) and towards the centre it becomes holocrystalline and coarser grained (0.6 - 0.8 mm) (Figs. 4b, c).

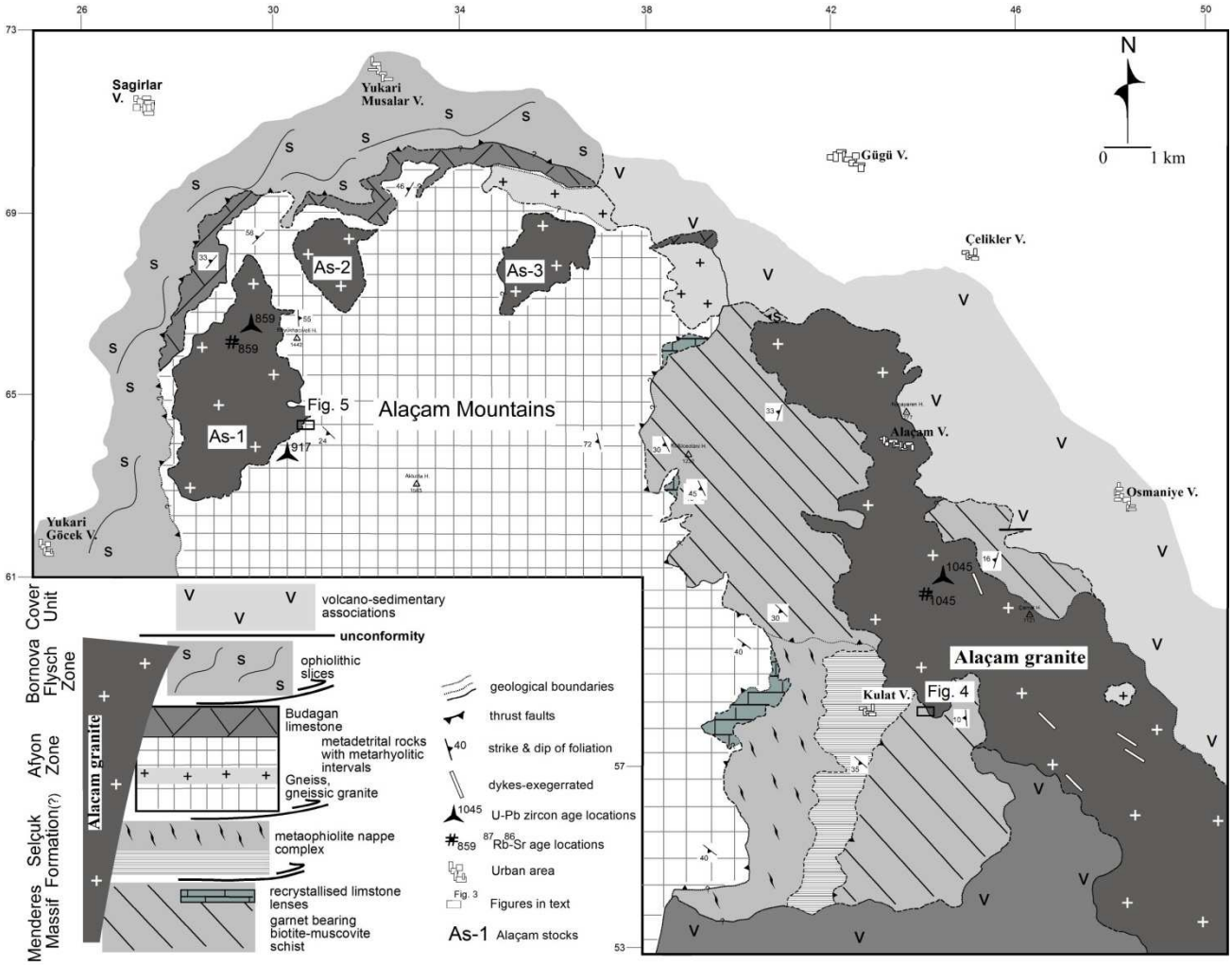

Figure 2. Geological map of the study area

In the east of the Alaçam Mountains around Kulat village, the intrusive relation between the Alaçam granite and the high grade metamorphic rocks of the Menderes Massif are well exposed (Fig. 5). Small individual Alaçam granitic stocks (AS-1, AS-2, AS-3) accompany the main granite body in the northwestern part of the Alaçam Mountains (Fig. 2) and these Alaçam stocks crosscut the foliation planes of the country rocks and contain xenoliths of rocks from the Afyon Zone (Figs. 6a, b). The Alaçam granite also intruded into the uppermost tectonic unit of the nappe package and produced a contact aureole within the ophiolitic rocks of the Bornova Flysch Zone along its northern contact. The Alaçam granite and its host rock association are overlain unconformably by Middle-Upper Miocene continental-lacustrine sedimenantary rocks, and an andesitic volcanic sequence along a peneplained surface (Fig. 2).

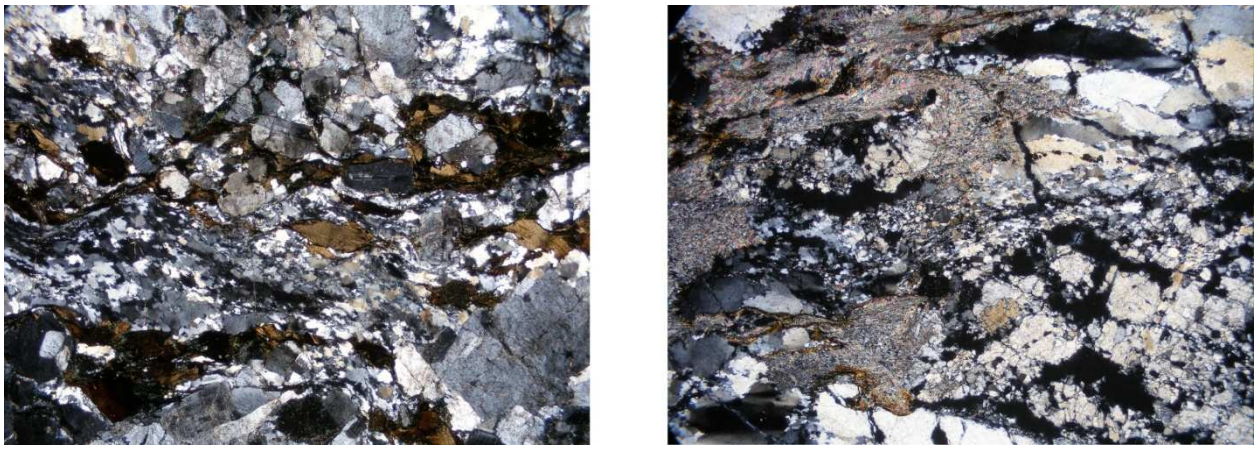

Figure 3. (a-b) Thin section views of the gneissic granite with preserved granitic texture in the Afyon Zone (Kf: K-feldspar, qu: quartz, bi: biotite, mu: muscovite, F: foliation; long side of the photographs are 1.6 cm)

Analytical techniques

Major, trace and rare earth elements of ten samples from the main body of the Alaçam granite and additionally ten samples from the Alaçam granitic stocks (NW of the Alaçam granite) were chosen for geochemical analyses. The analyses were carried out in Acme Analytical Laboratories Ltd (Vancouver-Canada) by ICP-AES (Inductively Coupled Plasma Atomic Emission Spectrometry), and ICP-MS (Inductively Coupled Plasma Mass Spectrometry). Zircon separation by sieving, wet shaking table, magnetic separator, and heavy liquids was performed at the Dokuz Eylül University in İzmir (Turkey). Zircons from the gneissic granite of the Afyon Zone and from the Alaçam granite with its related stock were analyzed by U-Pb

isotope dilution method on a Finnigan MAT 262 mass spectrometer in the University of Tübingen (Table 2).

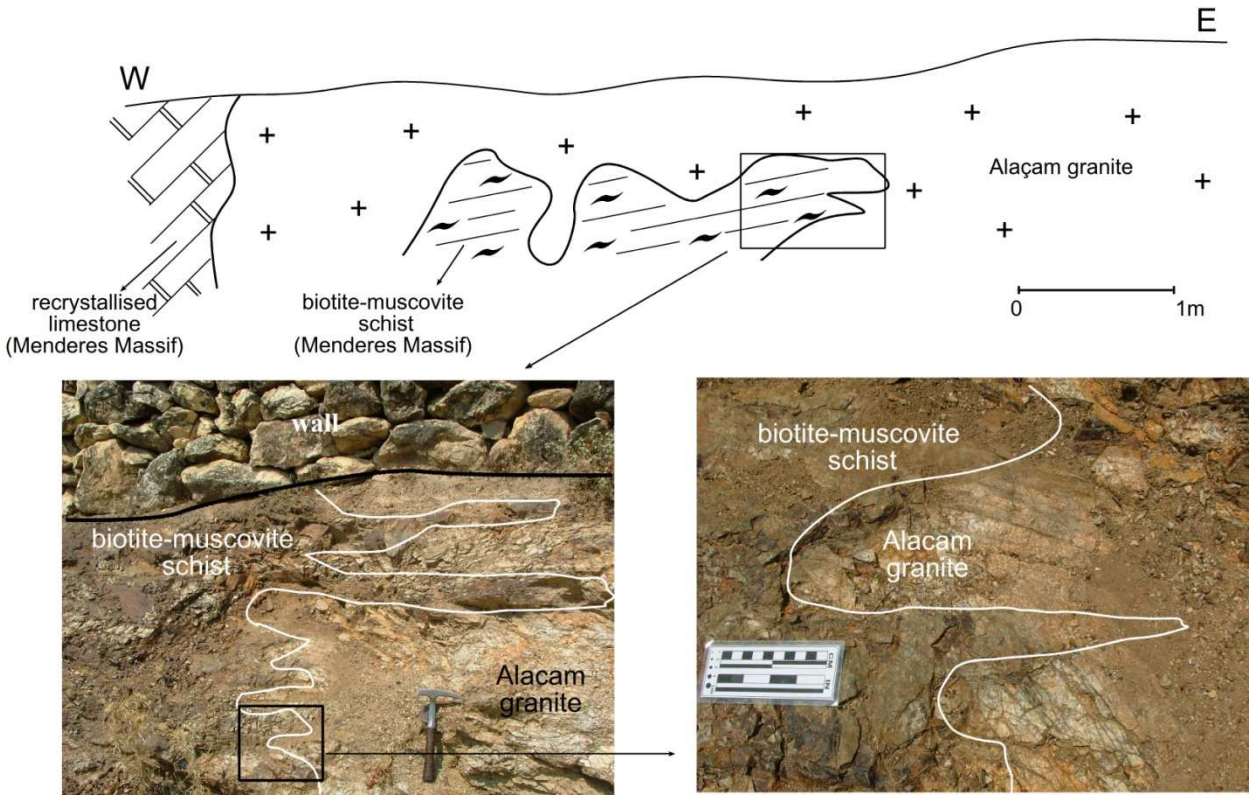

Figure 4. Cross section from the eastern part of the Alaçam granite and field photographs showing the intrusive contact between the Alaçam granite and high-grade metamorphic rocks of the Menderes massif.

Details of the analytical techniques are given in Chen *et al.* (2000; 2002) and Okay and Satır (2006). Zircon grains were prepared for cathodoluminescence images in the SEM laboratory of the Geosciences Faculty, Tübingen. For Rb-Sr analyses, biotite (200-300 μm) and powdered whole rock samples were spiked with a ^{85}Rb-^{84}Sr mixed tracer and dissolved in HF and $HClO_4$. The ion exchange chromatography procedure was applied for separating Rb and Sr from the samples solutions. Rb and Sr isotope analyses were also carried out on a Finnigan MAT 262 mass spectrometer. Details of this method can be found in Okay and Satır (2006). Regression lines were calculated by the least squares cubic method of York (1969) using the ISOPLOT software of Ludwig (2003).

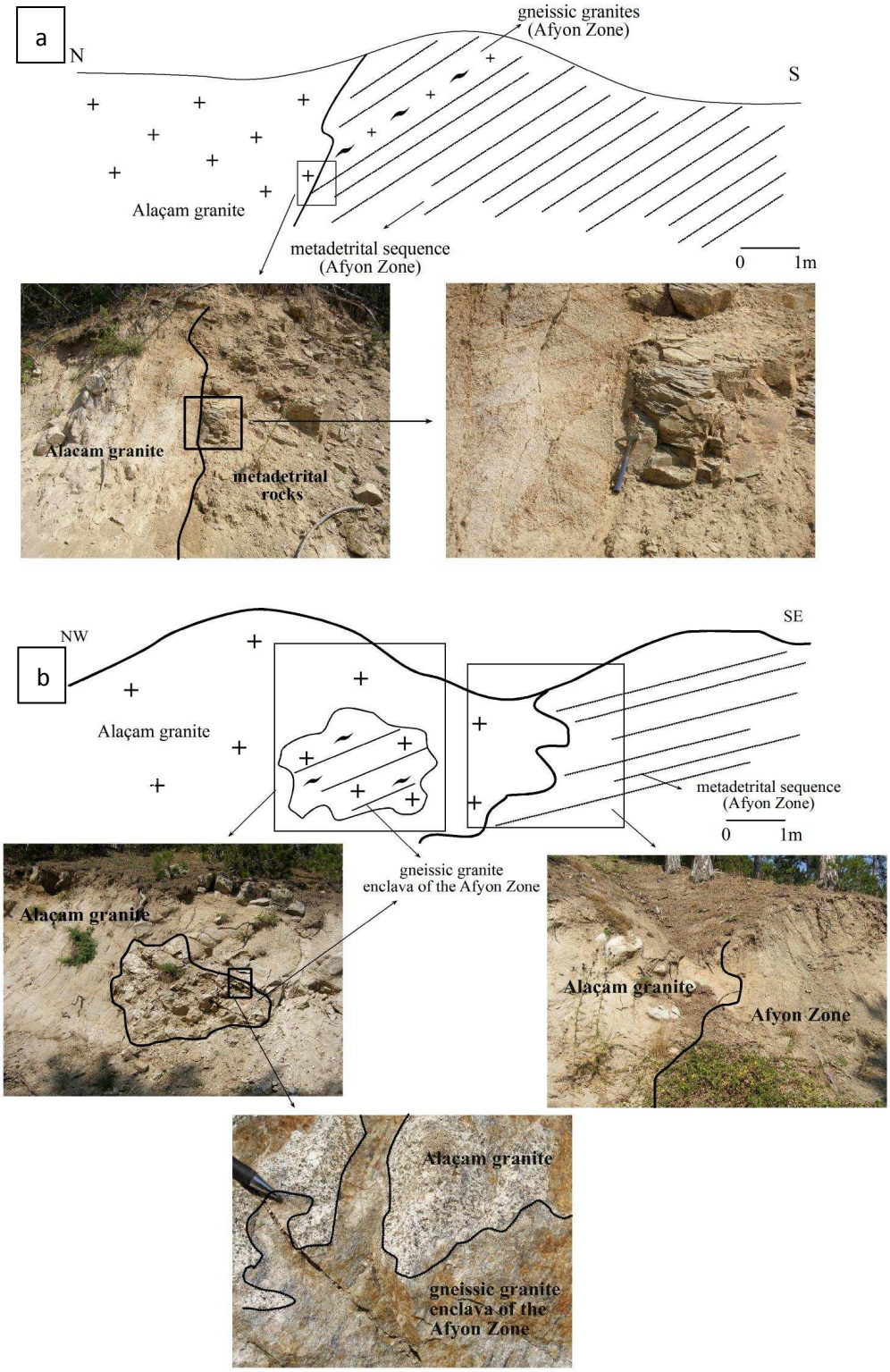

Figure 5. Cross section from the NW Alaçam Mountains and field photographs showing the intrusive contact between the Alaçam granite stocks and low grade metamorphic rocks of the Afyon Zone. (a) Stock of the Alaçam granite cutting the metadetrital sequence of the Afyon Zone, (b) crosscutting relationship between the Alaçam granite stock and metadetrital sequence of the Afyon Zone with gneissic granite xenoliths from the Afyon Zone preserved in the Alaçam granite stock.

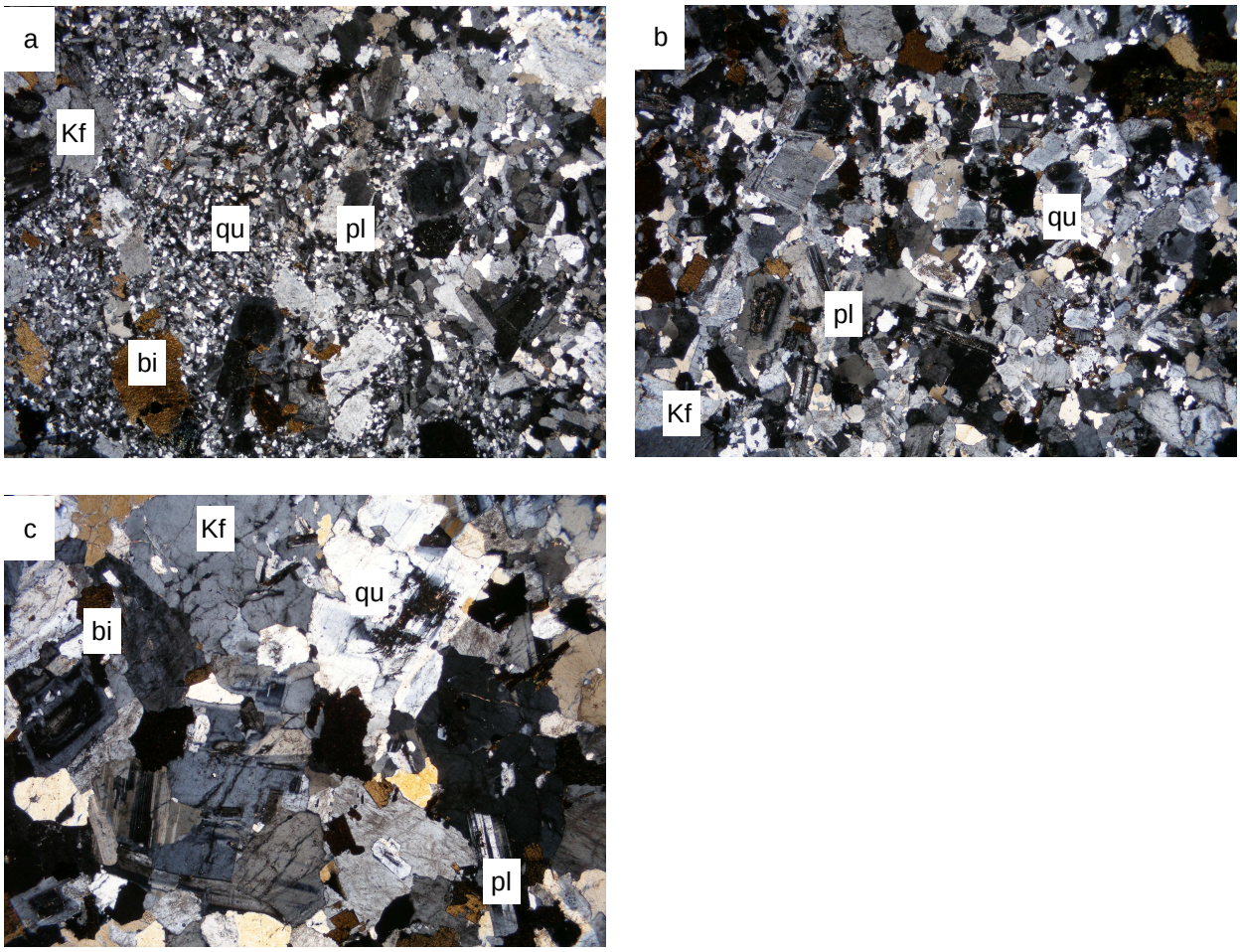

Figure 6. Thin section views and textural differences of the Alaçam granite from edge to center (a) fine-grained holocrystalline texture, (b-c) coarse-grained holocrystalline texture (Kf: K-feldspar, qu: quartz, pl: plagioclase, bi: biotite; long side of the photographs are 1.6 cm)

Geochemistry

Major, trace and rare earth element composition of the samples from the Alaçam granite and accompanying stocks are given in Table 1. In the classification diagram of SiO_2 vs (Na_2O + K_2O) (*Cox et al. 1979),* the majority of the samples plot in granite field and two samples show granodiorite composition (Fig. 7a). Mostly granitic rocks of the Alaçam granite plot in the peraluminous field but only few samples plot on the separation line between the metaluminous and peraluminous fields in A / NK vs A / CNK diagram of Shand (1947) (Fig. 7b). In an AFM diagram, the samples display a calc-alkaline nature (Fig. 8a) and according to their A / CNK < 1.1 values, they are all I-type granites (Fig. 7b) which is common in most of the Oligo-Miocene granitic suites of western Anatolia (Kozak, Evciler, Kestanbol, Eğrigöz and

Table 1. Major, trace and rare earth element composition of the Alaçam granite and related

	ALAÇAM GRANITE										RELATED STOCKS									
Sample	**604**	**583**	**422**	**569**	**505**	**550**	**567**	**589**	**554**	**620**	**175b**	**176**	**179**	**185**	**187**	**189**	**196**	**198**	**209**	**217c5**
SiO2	69.47	69.76	69.54	66.56	69.57	69.99	68.26	67.95	68.30	70.29	76.62	69.1	69.86	67.95	68.16	70.8	66.59	68.72	69.52	75.26
Al2O3	15.06	15.27	14.86	15.95	15.01	14.88	15.52	15.58	15.36	14.79	12.95	15.36	15.16	15.78	15.79	15.01	15.85	15.44	15.21	13.16
Fe2O3	3.01	2.46	3.03	3.48	2.88	3.03	3.36	3.46	3.24	2.97	0.89	2.9	2.68	3.16	3.34	2.47	4.2	3.39	3.38	1.4
MgO	0.90	0.71	0.94	1.07	0.98	1.00	0.99	1.08	1.02	0.86	0.21	1.22	1.02	1.3	1.35	0.89	1.65	1.29	0.96	0.37
CaO	2.31	2.76	2.21	3.16	2.25	2.29	2.72	2.72	2.88	2.24	0.79	2.56	2.58	3.29	3.35	2.47	4.02	3.48	3	1.15
Na2O	3.34	3.67	3.29	3.35	3.23	3.38	3.61	3.73	3.61	3.44	3.04	6.17	3.29	3.43	3.27	3.39	3.23	3.17	3.45	3.4
K2O	4.41	3.84	4.19	3.27	4.49	4.13	4.35	3.88	3.30	4.12	4.77	0.85	3.91	3.41	3.43	4.11	3.08	3.18	3.33	4.78
TiO2	0.43	0.34	0.43	0.50	0.40	0.41	0.40	0.48	0.47	0.41	0.11	0.41	0.35	0.41	0.42	0.35	0.54	0.43	0.37	0.2
P2O5	0.109	0.115	0.148	0.176	0.154	0.131	0.134	0.151	0.156	0.143	0.03	0.14	0.14	0.15	0.15	0.13	0.16	0.13	0.11	0.05
MnO	0.06	0.05	0.06	0.06	0.06	0.06	0.06	0.07	0.06	0.06	0.02	0.06	0.05	0.05	0.07	0.05	0.08	0.07	0.06	0.04
Cr2O3	0.004	<0.002	<0.002	<0.002	<0.002	<0.002	<0.002	<0.002	<0.002	<0.002	0.001	0.001	0.001	0.001	0.001	0.001	0.002	0.001	0.002	0.001
LOI	0.6	0.8	1.1	2.1	0.8	0.5	0.4	0.7	1.5	0.5	0.4	1.1	0.7	0.8	0.4	0.2	0.5	0.6	0.5	0.2
Sum	99.7	99.78	99.8	99.68	99.8	99.81	99.81	99.79	99.87	99.82	99.83	99.87	99.74	99.72	99.73	99.87	99.9	99.89	99.89	100
Ba	1108	844	874	1331	929	767	860	899	800	885	624	844	832	931	954	941	696	723	819	289
Be	2	3	4	4	4	3	4	4	3	4	4	5	4	3	5	4	5	4	5	4
Co	40.9	63.1	100.8	31.2	38.8	78.5	71.4	90.0	91.1	99.1	29.9	29.9	51.1	51.4	45.1	53.7	43.1	34.7	35.9	57.5
Cs	8.2	7.0	6.1	4.4	4.6	6.1	9.1	8.0	4.1	11.6	5.3	1.8	3.9	4.6	4.6	4.5	4.2	3.5	3	6.2
Ga	12.7	16.3	17.1	17.5	15.9	16.9	16.8	16.9	16.2	16.4	12.7	17.6	16.1	17.1	17.6	16.8	17.7	17.3	19.2	15.7
Hf	4.6	4.7	5.2	6.3	5.9	4.7	5.1	5.8	5.6	5.2	3.5	4.8	4.7	4.3	5	5	4.4	4.3	5.7	4.1
Nb	15.8	11.7	14.4	13.3	15.0	13.3	14.5	14.9	13.1	14.8	14.9	15.4	13.3	14.6	12.8	14.3	11.1	11.3	11.9	14.4
Rb	151.1	141.7	160.4	86.3	164.0	163.8	184.5	169.4	109.2	188.9	168.3	43.2	135.4	144.2	133.6	145.3	119.6	114.4	124.1	214.5
Sn	4	2	4	3	2	4	7	3	3	5	1	3	3	3	3	2	3	2	2	2
Sr	298	290	266	391	260	254	276	288	319	261	119	338	317	402	406	344	357	330	310	107
Ta	2.1	1.2	1.4	1.2	1.8	1.4	1.7	1.8	1.0	2.1	2.1	2.3	1.5	1.4	1.3	1.7	1.1	1.3	1.2	2.1
Th	28.0	26.2	27.6	48.6	24.2	22.0	30.6	22.3	27.9	25.3	21.9	16.6	16.8	15	10.7	20.1	9.3	16.4	14.3	31.2
U	6.0	6.2	8.5	11.1	6.4	6.4	7.9	5.9	7.4	8.0	4.9	9.7	8.3	7.3	5.5	7.1	3.4	4.3	3.4	8.3
V	42	33	43	52	41	40	48	49	48	41	6	42	36	43	49	30	60	47	31	15
W	335.6	465.0	809.8	194.0	297.3	610.2	517.2	656.5	729.3	921.8	340	306	505	528	500	598	432	355	392	632
Zr	177.3	151.2	165.4	222.2	198.8	156.5	165.2	184.5	183.5	171.4	65	144	128	145	153	131	128	125	178	105
Y	21.1	21.2	24.5	25.7	24.2	22.1	29.3	33.0	23.5	27.9	25	33	23	23	22	25	25	21	29	26
La	47.1	38.3	35.6	64.4	40.3	34.4	46.5	38.5	34.3	40.1	24	37	32	35	27	46	25	29	45	24
Ce	84.0	71.9	67.3	112.6	75.2	63.5	87.2	71.8	63.1	73.6	45	72	63	69	53	90	52	59	94	49
Pr	9.11	8.01	7.66	11.94	8.36	7.05	9.65	8.21	7.12	8.25	5.3	7.7	6.8	7.1	5.5	8.7	5.6	6.3	10.1	5.3
Nd	29.8	29.6	27.2	41.6	30.3	25.4	35.2	30.3	25.7	29.4	19	28	24	26	20	31	21	23	36	22
Sm	5.24	4.80	5.05	6.33	5.33	4.69	5.95	5.56	4.81	5.48	4	6	5	5	4	5	5	5	6	4
Eu	1.02	0.99	0.94	1.22	0.88	0.89	0.95	1.01	1.00	0.90	0.54	1.06	0.94	1	0.95	0.87	1.05	1	1.11	0.52
Gd	3.52	4.02	4.63	4.98	4.41	4.02	4.92	5.15	4.19	4.52	3.3	4.9	3.8	3.9	3.7	4.2	4.1	3.7	4.9	3.6
Dy	3.20	3.59	4.25	4.51	4.05	3.80	4.90	5.11	3.79	4.58	0.66	0.84	0.68	0.69	0.64	0.66	0.71	0.61	0.82	0.68
Tb	0.66	0.65	0.74	0.79	0.76	0.65	0.82	0.91	0.68	0.78	3.64	5.01	3.9	3.81	3.6	3.67	3.82	3.32	4.56	4
Ho	0.71	0.68	0.82	0.85	0.81	0.71	0.91	1.03	0.71	0.86	0.77	1.01	0.78	0.71	0.73	0.74	0.77	0.69	0.91	0.83
Er	2.05	2.03	2.41	2.47	2.31	2.16	2.75	3.06	2.12	2.66	2.27	2.9	2.07	2.39	2.08	2.19	2.21	2	2.65	2.53
Tm	0.33	0.34	0.39	0.41	0.39	0.34	0.46	0.52	0.35	0.45	0.39	0.44	0.32	0.36	0.31	0.38	0.33	0.31	0.43	0.42
Yb	2.05	2.18	2.54	2.72	2.61	2.24	3.02	3.27	2.15	3.09	2.57	2.91	1.98	2.35	2.07	2.19	2.14	1.9	2.65	2.84
Lu	0.30	0.32	0.38	0.42	0.38	0.35	0.46	0.48	0.33	0.45	0.4	0.45	0.34	0.32	0.32	0.35	0.31	0.32	0.45	0.47
Mo	1.3	5.7	1.2	1.1	0.5	0.2	0.5	1.5	0.6	1.2	0.2	<.1	0.1	0.2	<.1	0.1	0.2	0.2	0.4	0.1
Cu	2.2	2.0	1.1	2.5	1.5	1.8	3.4	1.4	1.5	1.2	1.6	3.1	1.1	71.9	1.2	2.4	2.2	1.3	1.8	1.4
Pb	6.3	15.3	3.9	5.5	4.0	3.1	6.0	15.5	2.9	³ 6	3.8	3.1	3.4	2.9	2.1	2.8	4.1	2.9	5.8	3.7

Table 1 continued

Zn	39	33	39	38	41	39	25	40	37	40	7	22	29	30	40	31	53	41	52	19
Ni	3.1	5.6	3.9	4.7	3.1	5.1	3.5	5.0	4.2	4.4	0.4	1.4	2.7	2.8	2.5	1.5	3	2.5	3.2	1.2
Mg#	31.9	43.1	41.2	35.8	40.8	39.3	38.9	36.9	34.5	12.3	73.1	41.1	49.0	45.9	34.6	57.0	37.8	36.0	17.8	30.9
(La/Yb)N	16.5	12.6	10.1	17.0	11.1	11.0	11.0	8.4	11.4	9.3	6.6	9.2	11.5	10.7	9.2	15.1	8.3	10.8	12.3	6.0
(La/Sm)N	5.8	5.2	4.6	6.6	4.9	4.7	5.0	4.5	4.6	4.7	3.9	4.0	4.2	4.6	3.9	5.6	3.5	4.0	4.6	3.6
(Gd/Yb)N	1.4	1.5	1.5	1.5	1.4	1.5	1.3	1.3	1.6	1.2	1.1	1.4	1.6	1.4	1.5	1.6	1.6	1.6	1.5	1.0
Eu*	24.2	24.8	27.3	31.7	27.3	24.5	30.5	30.2	25.3	28.1	20.3	30.5	24.4	24.6	22.8	26.7	24.6	23.2	31.5	21.9
Eu/Eu*	0.7	0.7	0.6	0.7	0.6	0.6	0.5	0.6	0.7	0.6	0.5	0.6	0.7	0.7	0.7	0.6	0.7	0.7	0.6	0.4

Mg# = [Mg^{2+} /(Mg^{2+} + Fe_{Total}) X 100], with Fe_{Total} as Fe^{+2}. Normalisation values are from Taylor & Mc Lennan (1985)

Koyunoba granites) (Yılmaz *et al.* 2001; Dilek and Altunkaynak 2007; Akay 2009; Hasözbek *et al.* 2009 –in review-). In the K_2O vs SiO_2 diagram, the Alaçam granite and accompanying granite stocks mainly plot in the high-K field (Fig 8b).

A relatively high Mg number (Mg# = 31 - 49, Table 1) is characteristic for most samples. Only two SiO_2 rich samples (samples 620 and 209) of the Alaçam granite display lower Mg# of 12.3 and 17.8 (Table 1). In the Rb vs (Y+Nb) and Nb vs Y discrimination diagrams of Pearce *et al.* (1984) and Pearce (1996), samples of the Alaçam granite show a Post Orogenic Granitoids (POG) signature. (Fig. 9a, b).

Chondrite-normalized REE patterns of samples from the Alaçam granite and its stocks are presented in Fig. 9. The samples display enrichment of LREE ($[La/Yb]_N$ = 6-17) over HREE ($[Gd/Yb]_N$ = 1-1.6). Significant negative Eu anomalies (0.41 < Eu/Eu* < 0.73) either imply plagioclase stability in the source or plagioclase fractionation during crystallization (Nagudi *et al.* 2003 and references therein). REE patterns of the Alaçam granite and its related stocks also indicate that the melt of the granite was generated during low pressure conditions (3-5 kbar) (Nagudi *et al.* 2003 and references therein).

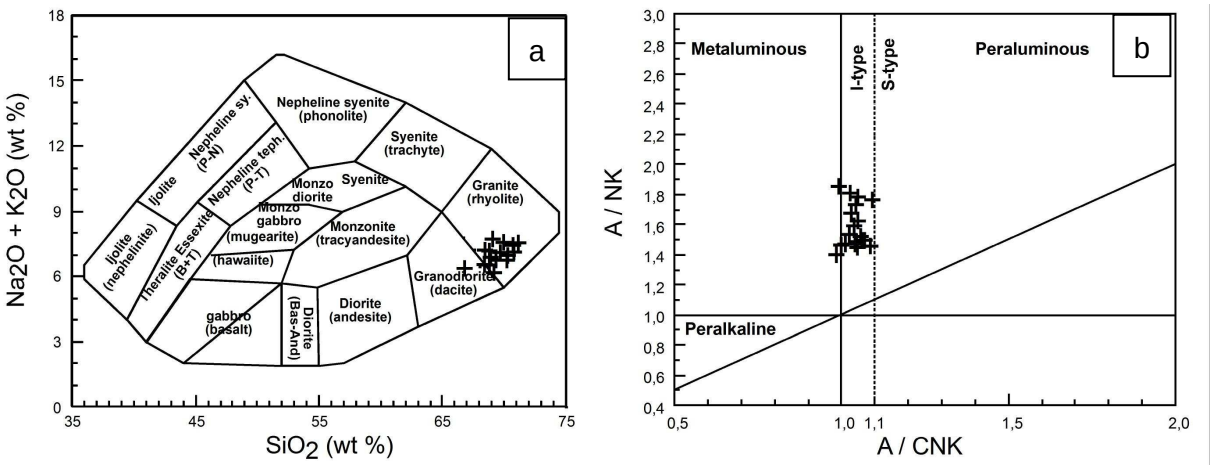

Figure 7 (a) Total alkali (Na_2O + K_2O) vs SiO_2 classification diagram for the Alaçam granite and related granite stocks (Cox et al. 1979). Samples vary in composition from granite to granodiorite. (b) A / NK vs A / CNK diagram of Shand (1947) (A / CNK = [Al_2O_3 / (CaO + Na_2O + K_2O) mol %]).

In comparison with REE compositions of the lower, middle, bulk and upper crust (Rudnick and Gao 2003) the Alaçam granite is similar to that of the upper crust (Fig. 10). In conclusion, geochemical features of the Alaçam granite and its related stocks show remarkably similar geochemical features to other Miocene granites (Kozak, Evciler, Eğrigöz, Koyunoba granites) in the NW Anatolia.

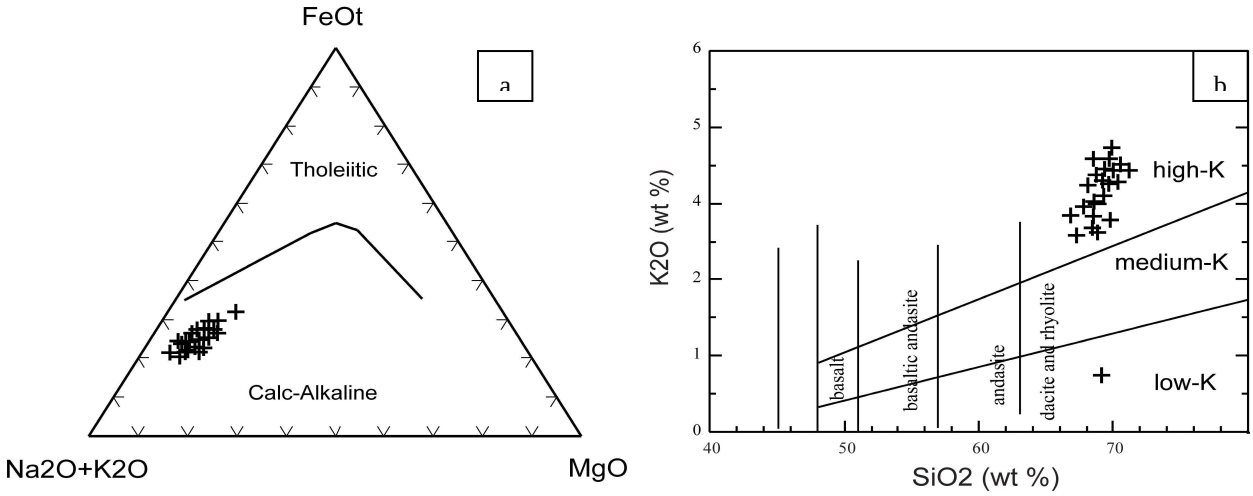

Figure 8. (a) AFM (FeO_t-Na_2O-MgO) triangular diagram of Irvine and Baragar (1971) showing the calc-alkaline nature of the Alaçam granite and its stocks, (b) K_2O vs SiO_2 diagram portraying the high-K character of the samples.

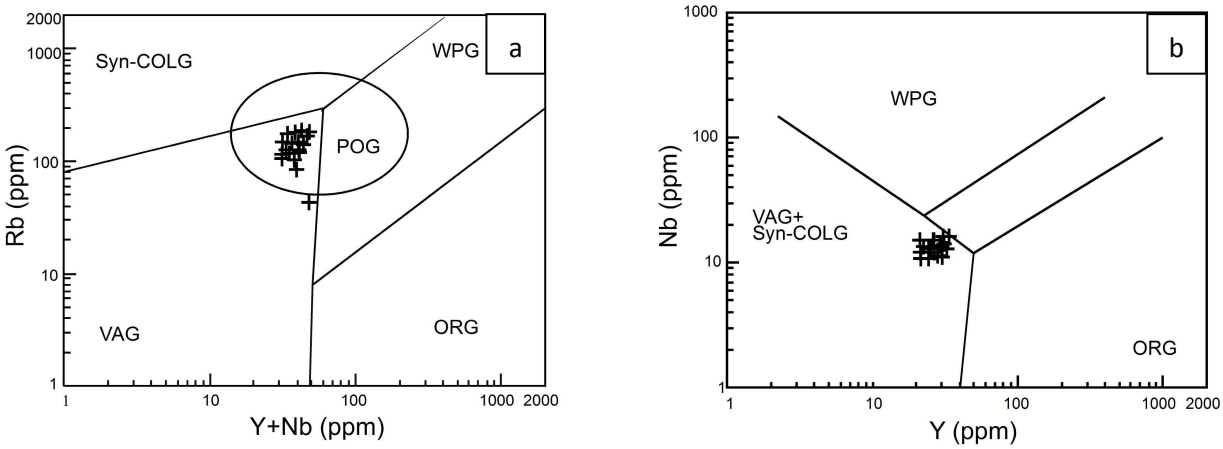

Figure 9. Tectonic discrimination diagrams for the Alaçam granite and its stocks. (a) Rb-(Y+Nb) and (b) Nb-Y diagrams of Pearce et al. (1984) (VAG: volcanic arc granitoids, syn/post-COLG: syn/post-collisional granitoids, WPG: within-plate granitoids, POG: post-orogenic granitoids, and ORG: ocean-ridge granitoids; POG fields are from Pearce (1996)

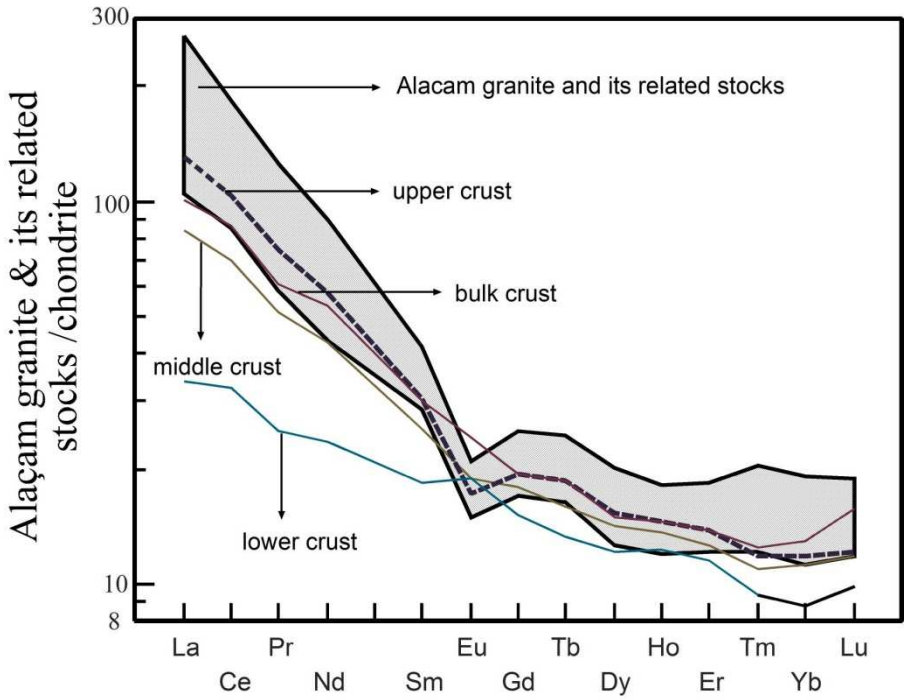

Figure 10. Chondrite-normalized REE patterns of the Alaçam granite and its stocks; chondrite values are from Taylor and Mc Lennan (1985); compositions of average upper, middle, lower and bulk crust are from Rudnick and Gao (2003)

Geochronology

Petrographically well defined relic granitic textures of the gneissic granites from the Afyon Zone (Fig. 3a) consists of idiomorphic crystals exhibiting well-preserved magmatic oscillatory zonation in CL without any visible inherited core (Fig. 11a). The CL images of the zircons from the gneissic granite from the Afyon Zone display similar appearance and internal structure. Five zircon fractions from gneissic granite of the Afyon Zone close to the Alaçam granitic stock were analyzed by the U-Pb dilution method (Table 2). Three of these fractions (917-1Y, 917-3, 917-6) are concordant with $^{206}Pb/^{238}U$, $^{207}Pb/^{235}U$ ages ranging from ~ 315 to 306 Ma (Table 2). All fractions plot along a discordia line which yields an upper intercept age of 314.9 ± 2.7 Ma which is interpreted as a crystallization age of the gneissic granite from the Afyon Zone (Table 2; Fig. 12). A lower intercept age of these fractions define a negative age (-377 ± 820 Ma) which is geologically meaningless.

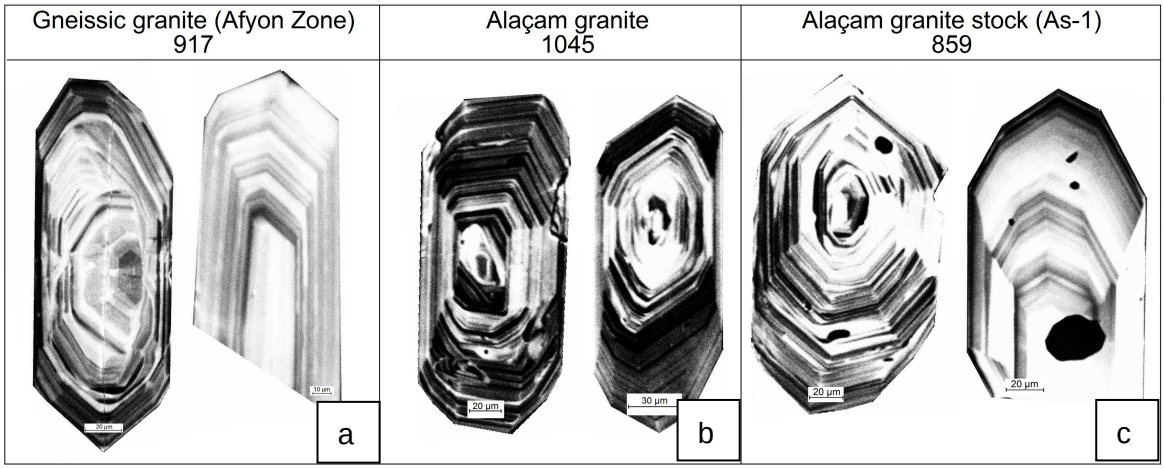

Figure 11 Cathodoluminescence views of zircon grains from (a) gneissic granite of the Afyon Zone, (b) Alaçam granite, (c) stock of the Alaçam granite

Zircons from the main body of the Alaçam granite and a small stock are mostly idiomorphic, long and thick. Their CL images show well defined magmatic zonation with prismatic crystal shape (Figs. 11b, c). From the Alaçam granite, most of the zircon fractions (1045-1, 1045-2, 1045-3, 1045-4) are concordant and yield U-Pb ages ranging from 20 to 21 Ma (Table 2). Whereas, one zircon fraction yields older discordant U-Pb ages due to the pressure of pre-magmatic zircon material (Fig 13a). Seven zircon fractions from the Alaçam granite yield a lower discordia intercept age of 20.0 ± 1.4 Ma which is interpreted as the intrusion age of the Alaçam granite. The upper intercept age of this sample define an age of 462 ± 120 Ma (Fig. 13a) indicating a Pan-African inheritance from the basement material. From the Alaçam granitic stock (As-1) (Fig.2), five zircon fractions were analyzed (Table 2). U-Pb ages ranging from 20 to 21 Ma are seen in three fractions of this granitic stock (859-1, 859-3, 859-1Y) (Table 2). All fractions of this sample define a lower discordia intercept age of 20.3 ± 3.3 Ma (Fig. 13b) interpreted as the crystallization age of the Alaçam stock and an upper intercept age of 389 ± 120 Ma also implies an older inheritance which is probably related to the basement units of the study area.

Rb-Sr whole rock-biotite ages from the Alaçam granite and its stock are given in Table 3. The obtained ages of 20.01 ± 0.20 Ma and 20.17 ± 0.20 Ma are indistinguishable, within analytical uncertainty, from the U-Pb zircon crystallization ages of these granites. Rb-Sr biotite ages of the Alaçam granite and its stock are interpreted as cooling ages implying a fast cooling after

emplacement, considering that the closure temperature interval of biotite with respect to Sr-diffusion is 350 - 450^{o}C (Jenkin *et al.* 2001; Giletti 1991).

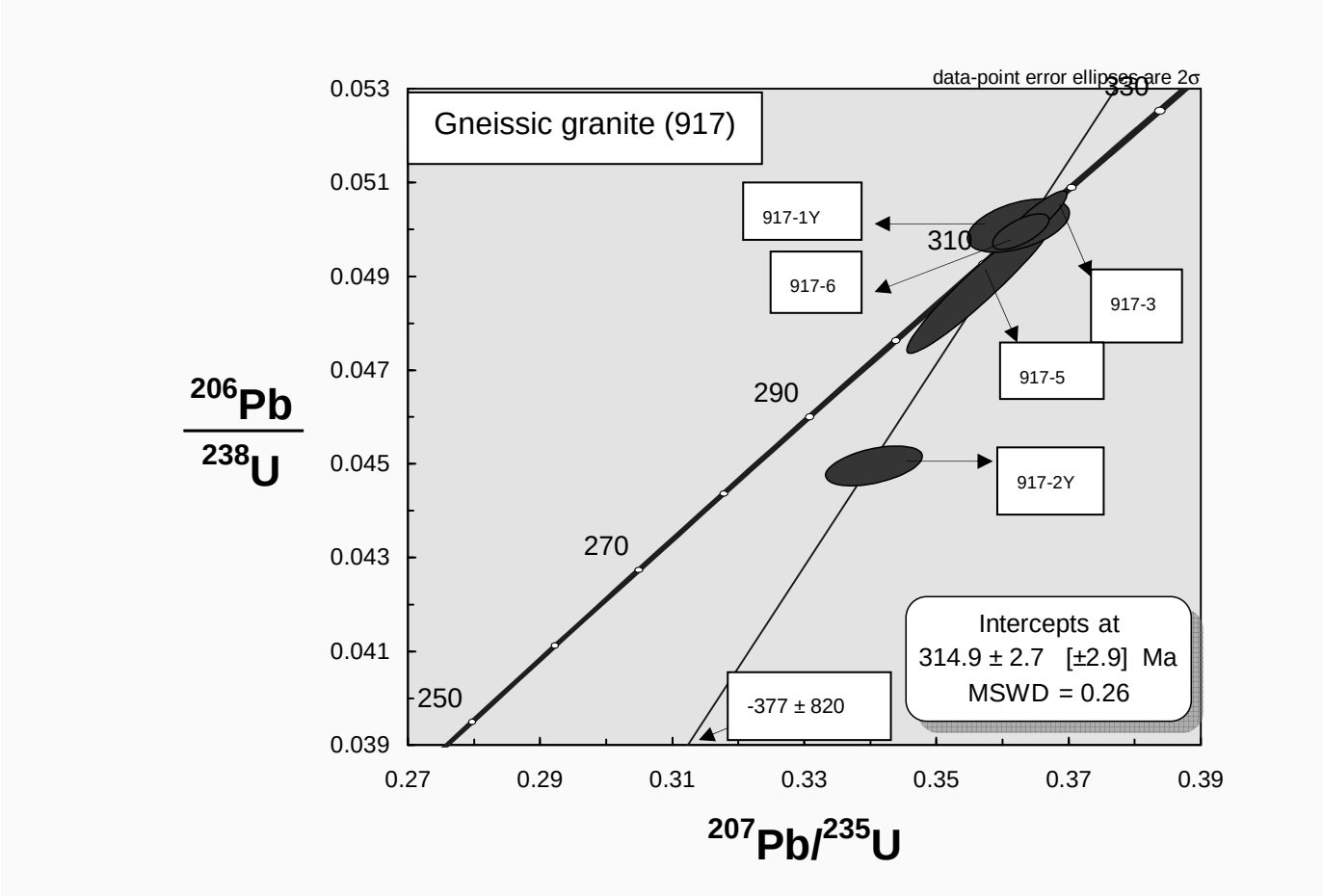

Figure 12 U-Pb Concordia diagram for zircons from the basement gneissic granite of the Afyon Zone (sample no: 917; UTM: 0630768; 4363560). Five zircon fractions define a discordia line with an upper intercept age of 314.9 ± 2.7 Ma.

Table 2. U-Pb analytical data from gneissic granites of the Afyon Zone (sample no: 917), Alacam granite (sample no: 1045), and its stock (sample no: 859)

Sample	$^{206}Pb/^{204}Pb$	U (ppm)	Pb*(ppm)	Atomic ratios				Apparent ages (Ma)		
				$^{208}Pb^*/^{206}Pb^*$	$^{206}Pb^*/^{238}U$	$^{207}Pb^*/^{235}U$	$^{207}Pb^*/^{206}Pb^*$	$^{206}Pb/^{238}U$	$^{207}Pb/^{235}U$	$^{207}Pb/^{206}Pb$
Gneissic granite (Afyon Zone)										
917-1Y	90672	1257	61.1	0.07	0.05008 ± 46	0.36240 ± 63	0.05248 ± 81	315.0	314.0	306.5
917-2Y	177880	664	29	0.07	0.04497 ± 33	0.34046 ± 60	0.05490 ± 86	283.6	297.5	408.2
917-3	13930	535	26.3	0.09	0.04994 ± 30	0.36284 ± 35	0.05268 ± 38	314.2	314.3	315.4
917-5	19881	373	17.6	0.07	0.04883 ± 120	0.35678 ± 92	0.05299 ± 41	307.3	309.8	328.3
917-6	20298	440	22	0.01	0.05022 ± 48	0.36489 ± 39	0.05268 ± 27	315.9	315.8	315.4
Alacam granite										
1045-1	260300	1605	5.3	0.12	0.00333 ± 51	0.02137 ± 127	0.04651 ± 258	21.4	21.4	24.1
1045-2	88101	994	3.3	0.10	0.00337 ± 31	0.02173 ± 74	0.04673 ± 151	21.7	21.8	35.7
1045-3	69917	938	3	0.17	0.00310 ± 44	0.02007 ± 124	0.04696 ± 273	19.9	20.1	47.3
1045-2Y	171980	1664	5.5	0.14	0.00322 ± 30	0.02074 ± 70	0.04669 ± 145	20.7	20.8	33.9
1045-3Y	71603	1068	5.5	0.10	0.00523 ± 39	0.03658 ± 92	0.05067 ± 118	33.6	36.4	225.9
1045-4Y	49016	1302	4.1	0.12	0.00314 ± 32	0.02016 ± 59	0.04645 ± 120	20.2	20.2	21.06
1045-5Y	59361	1298	4.3	0.17	0.00318 ± 25	0.20809 ± 68	0.04710 ± 144	20.4	20.9	69.9
Stock of the Alacam granite										
859-1	37428	1097	3.6	0.08	0.00379 ± 15	0.02165 ± 152	0.04645 ± 32	21.7	21.7	21.4
859-2	38109	1102	6.6	0.08	0.00612 ± 47	0.04267 ± 109	0.05050 ± 119	39.3	42.4	218.2
859-3	63308	1222	4.5	0.32	0.00317 ± 31	0.02033 ± 86	0.04648 ± 185	20.4	20.4	22.9
859-5	65316	1299	4.6	0.09	0.00362 ± 30	0.02403 ± 223	0.04807 ± 189	23.3	24.1	102.9
859-1Y	10116	948	3.1	0.10	0.00333 ± 25	0.02134 ± 136	0.04645 ± 288	21.4	21.4	21.5

All errors quoted are 2σ absolute uncertanities and refer to the last digit

*=radiogenic; grain size varies from 80-180 µm

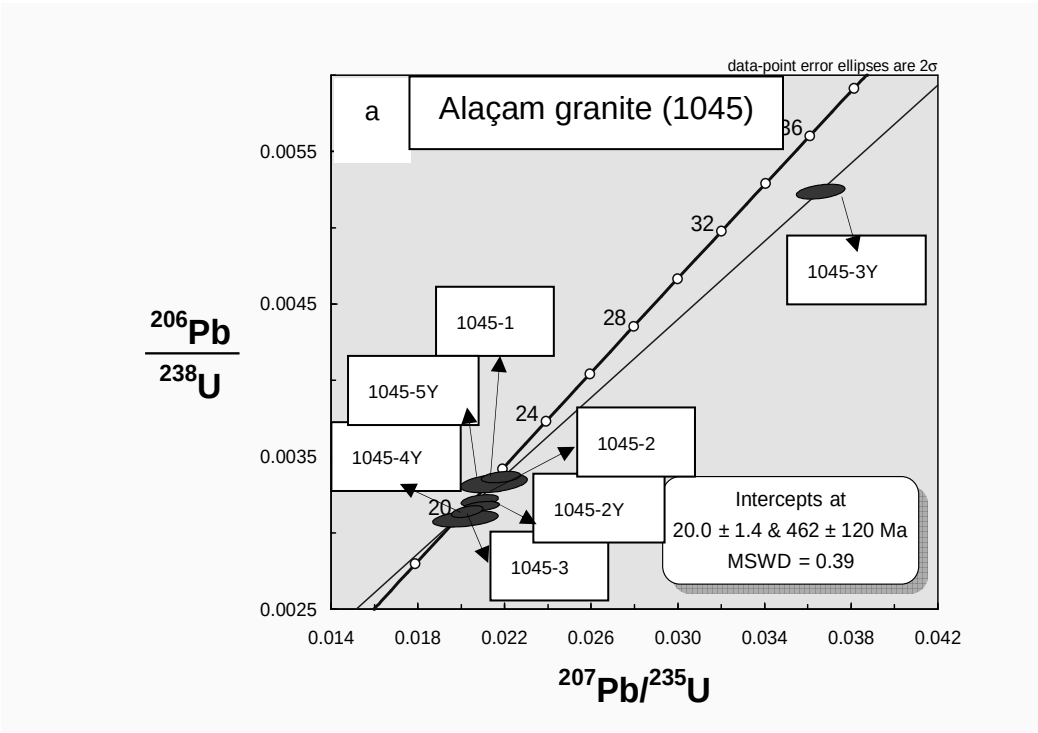

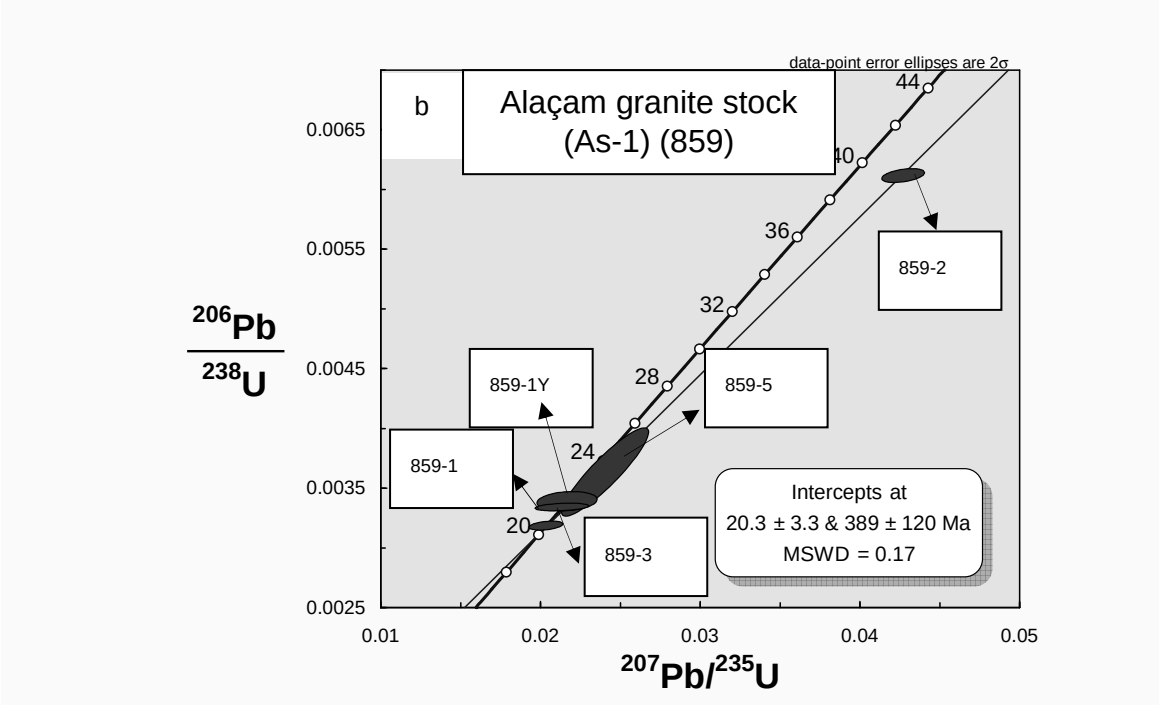

Figure 13 (a) U-Pb Concordia diagram for zircons from the Alaçam granite (sample no: 1045- UTM: 0644798; 4360915). Seven zircon fractions define a discordia line with a lower intercept age of 20.0 ± 1.4 Ma, (b) U-Pb Concordia diagram for related stock (sample no: 859- UTM: 0628932; 4366465). Five zircon fractions define a discordia line with a lower intercept age of 20.3 ± 3.3 Ma

Table 3. Rb-Sr data for whole-rock and biotite from a sample of the Alaçam granite (sample no: 1045) and related Alaçam stock (sample no: 859) (m: measured; i: initial)

Sample	Fraction	Rb (ppm)	Sr (ppm)	$^{87}Rb/^{86}Sr$	$^{87}Sr/^{86}Sr$ (m)	$^{87}Sr/^{86}Sr$ (i)	Age (Ma)
Alaçam granite 1045	whole rock	177	409.5	1.25	0.70933 ± 07		
	biotite	805.7	6.93	339.1	0.80534 ± 12	0.70898 ± 22	20.01 ± 0.20
Alaçam stock 859	whole rock	420	164.8	1.13	0.70934 ± 07		
	biotite	544	4.58	346.6	0.80832 ± 10	0.70902 ± 21	20.17 ± 0.21

Discussion

The emplacement mode of the Oligo-Miocene granites in NW Anatolia was discussed in recent studies (Yılmaz 1997; Altunkaynak and Yılmaz 1998; 1999; Genç 1998; Yılmaz *et al.* 1994; 2001; Işık and Tekeli 2001; Işık *et al.* 2004; Seyitoğlu *et al.* 2004; Ring and Collins 2005; Thomson and Ring 2006; Altunkaynak 2007; Dilek and Altunkaynak 2007; Karacık *et al.* 2008; Özgenç and İlbeyli 2008; Akay 2009; Dilek and Altunkaynak 2009; Boztuğ *et al.* 2009; Hasözbek *et al.* 2009a). Two different models are advocated: 1) One model invokes a syn-kinematic emplacement in an extensional low-angle detachment system. Accordingly, the plutons intruded into the footwall part of detachment faults and attained strong ductile to brittle deformation close to the fault surface (Işık and Tekeli 2001; Işık *et al.* 2004; Seyitoğlu *et al.* 2004; Ring and Collins 2005; Thomson and Ring 2006). 2) The other model advocates a post-collisional setting for the plutons. This model suggests that granitic magma was formed by melting of lower parts of an abnormally thickened crust (Yılmaz 1997; Yılmaz *et al.* 1994; Yılmaz *et al.* 2001). Recently, Dilek and Altunkaynak (2009) and Boztuğ *et al.* (2009) reviewed the post-collisional magmatic response in western Anatolia. They suggest a break-off of the subducting oceanic slab following continent-continent collision. This caused the mantle rose and heat transfer into the overlying lithosphere that resulted in partial melting and magma generation in the crust. However, the plutons are not only found in the overriding Sakarya Continent, as would be expected in the slab break-off model, but are spatially scattered to form an E-W trending belt cutting the Sakarya Continent to the north and the Menderes Massif south of the collision zone. Akay (2008) and Hasözbek *et al.* (2009a) have

shown that the young granites from the NW Anatolia intruded into various nappe packages of the tectonic zones and associated volcanic-subvolcanic rocks (Fig. 14).

In NW Anatolia, the extension-related model for the emplacement of the Miocene granites was first suggested for the Evciler granite (Okay and Satır 2000) and the Egrigöz and Koyunoba granites (Okay and Satır 2000; Işık and Tekeli 2001; Işık *et al.* 2004; Seyitoğlu *et al.* 2004; Ring and Collins 2005; Thomson and Ring 2006). Recently, in the general geological maps of NW Anatolia, a regional-scale low angle fault was also drawn along the northern border of the Alaçam granite (Seyitoğlu *et al.* 2004; Ring and Collins 2005; Thomson and Ring 2006; Seyitoğlu and Işık 2009). Erkül *et al.* (2009a, b) suggested that the Alaçam granite emplaced along a north-dipping detachment fault. These authors interpreted the gneissic granite of the Afyon Zone as the syn-kinematically deformed outer zone of the Alaçam granite. Our U-Pb zircon dating of the Alaçam granite clearly indicates that the granite and accompanying Alaçam granitic stocks are Early Miocene (20.0 ± 1.4 Ma; 20.0 ± 3.7 Ma) in age (Figs. 13a, b). The gneissic granites and metarhyolitic intercalations of the Afyon Zone found in contact with the Early Miocene Alaçam granite yield an upper U-Pb discordia intercept age of 314.9 ± 2.7 Ma (Fig. 12) indicating their Late Carboniferous crystallization age. In the southeastern part of the Afyon Zone, Permo-Carboniferous ages were previously determined from basement associations of the Afyon Zone by foraminifera (Erişen 1982). A Permo-Carboniferous basement age of the Afyon Zone was also determined by Özcan *et al.* (1988) in Kütahya-Bolkardağ and by Akal *et al.* (2008) around Meyvalı village (Balıkesir). The Alaçam granite intruded the gneissic granites of the Afyon Zone obliquely cutting their foliations (Figs. 6a, b). Given the pronounced age difference between the Alaçam granite (20.0 ± 1.4 Ma; 20.0 ± 3.7 Ma) and the gneissic granite of the Afyon Zone (314.9 ± 2.7 Ma) (Figs. 12, 13a, b). It seems highly unlikely that these two granitic bodies are genetically related with each other. Thus, the gneissic granites of the Afyon Zone cannot be interpreted as mylonitic deformed zones of the detachment related parts of the Alaçam granite. Rb-Sr biotite ages of the Alaçam granite indicate that the country rocks were cold during the intrusion causing rapid cooling of the Alaçam granite. Besides, Erkül *et al.* (2009a, b) present ~ 19.2 Ma ^{40}Ar-^{39}Ar biotite ages of volcanic rocks from the cover units of the study area. All this evidence indicates a shallow emplacement of the Alaçam granitic bodies in the study area.

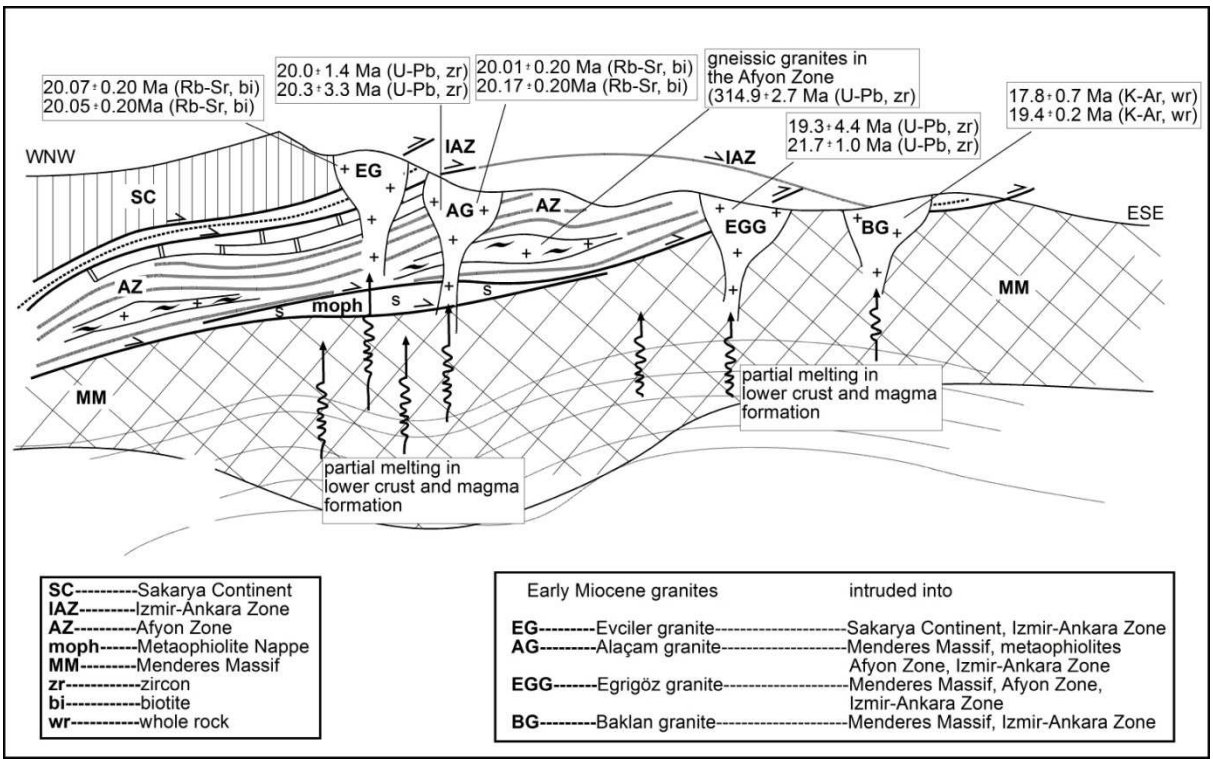

Figure 14. Simplified geological section of the NW Anatolia showing major tectonic zones and Early Miocene granites. Radiometric ages shown on the section are from Okay and Satır (2000) for the Evciler granite, Hasözbek et al. (2009a) for the Eğrigöz granite and Aydoğan et al. (2008) for the Baklan granite. Data for the Alaçam granite and gneissic granites from the Afyon Zone are from this study.

In addition to the geochronological data based on the comparison between the Alaçam granite and gneissic granites of the Afyon Zone presented in this study, Hasözbek *et al.* (2009a, b) presented new U-Pb zircon ages from the Egrigöz and Koyunoba granites (19.3 ± 4.4 Ma; 21.7 ± 1.0 Ma). A metagranitic body of the Menderes Massif which was previously called "mylonitic shear zone" gives an U-Pb zircon lower intercept age of 30.04 ± 0.56 Ma (Hasozbek *et al*. 2009a). The age difference of 10-11 Ma between deformed metagranite of the Menderes Massif and undeformed granitoids of coeval Eğrigöz and Koyunoba granites is an additional proof that the deformed metagranites of the Menderes Massif are not mylonitic equivalent of the undeformed granites that crop out along the northern Menderes Massif. Geographical proximity of these Early Miocene granites (Alaçam, Eğrigöz, and Koyunoba) and their radiometric age evidences put important constraints to understand the emplacement history of these granites along NW Anatolia.

Conclusions

The Alaçam granite and accompanying granitic stocks in NW Anatolia cut a nappe package consisting of four tectonic zones. These are from south to north in ascending structural order: Menderes Massif, a metaophiolite nappe complex resembling the Selçuk Formation, the Afyon Zone and the ophiolitic melange of Bornova Flysch Zone. The age of the shallow-seated and crosscutting Alaçam granite and its related stocks as determined by U-Pb zircon method are 20.0 ± 1.4 Ma and 20.0 ± 3.7 Ma, respectively indicating an Early Miocene emplacement age. Rb-Sr biotite ages of 20.01 ± 0.20 Ma and 20.17 ± 0.20 Ma suggest rapid cooling below the biotite closure temperature (300-400 ^{0}C).

Major, trace and rare earth element patterns of the Alaçam granite and its related stocks display close similarities to subduction related or arc-derived magmatic rock associations and to other adjacent Early Miocene granitic bodies (Evciler, Kestanbol, Kozak, Eğrigöz and Koyunoba granites). Their I-type, calc-alkaline nature and upper crustal REE signature is in accordance with their emplacement along the suture zone between the Sakarya Continent and the Menderes Platform.

The Alaçam granite obliquely cuts gneissic granites of the Afyon Zone and metapelites of the Menderes Massif. The gneissic granites have been previously interpreted as slivers of the Alaçam granite located between the Menderes Massif and the İzmir-Ankara Zone that were deformed along a detachment fault system under an extensional tectonic regime. The 314.9 ± 2.7 Ma U-Pb upper discordia zircon age from a gneissic granite sample from the Afyon Zone does not support a genetic relation with the Early Miocene Alaçam granite. We conclude that the deformed gneissic granites belong to the lower part of the Afyon Zone. The Alaçam granite and related small granitic stocks formed post tectonically by melting of a crustal package which was thickened during Cretaceous to Late Oligocene subduction and collision between the Anatolide-Tauride Platform and Sakarya Continent along the northern border of the Menderes Massif.

Acknowledgements

Part of this study was financially supported by the Scientific and Technical Research Council of Turkey (TUBITAK 104Y036), Scientific Research Projects Foundation of Dokuz Eylül

University (project no: 04. KB. FEN. 038), and Deutscher Akademischer Austausch Dienst (DAAD). . A. Okay and P. Bons are thanked for editing the English text and their pre-scientific review. A. Okay, O. Candan, T. Güngör, E. Koralay, C. Akal, and K. Akbayram are thanked for their helpful discussions during the field work. H. Schulz, Institute of Geoscience, University of Tübingen is thanked for help during CL analyses. G. Bartholomä, E. Reitter and C. Shang, are thanked for technical help in laboratory studies.

References

Akal, C., Candan, O., Koralay, O.E., Okay, İ.A., Oberhänsli, R., Chen, F., 2008, Afyon Zonu'ndaki erken Devoniyen asidik magmatizmaya ait jeolojik, jeokimyasal ve jeokronolojik ön bulgular. 61th Geol Congr Turk, (in Turkish with English Abstracts), 204-207

Akay, E. and Erdogan, B., 2004, Evolution of Neogene calc-alkaline to alkaline volcanism in the Aliaga-Foca region (Western Anatolia, Turkey). Journal of Asian Earth Science, 24: 367–387

Akay, E., 2009, Geology and petrology of the Simav Magmatic Complex (NW Anatolia) and its comparison with the Oligo-Miocene granitoids in NW Anatolia; implications on Tertiary tectonic evolution of the region. International Journal of Earth Sciences, 98:1655–1675.

Akay, E., Erdoğan, B., İşintek, İ., Hasözbek, A., 2009 (in review), Stratigraphy of the Afyon Zone around Emet (Kütahya, NW Anatolia) and geochemical characteristics of the Triassic rhyolitic volcanism. International Journal of Earth Sciences.

Aldanmaz, E., Pearce, J., Thriwall, M.F., Mitchell,J., 2000, Petrogenetic evolution of late Cenozoic, post-collision volcanism in western Anatolia, Turkey. Journal of Volcanology and Geothermal Research, 102: 67-95.

Altunkaynak, Ş., 2007, Collision-driven slab breakoff magmatism in Northwestern Anatolia, Turkey, J Geol 115: 63-82.

Altunkaynak, Ş., Yılmaz, Y. 1999, The Kozak Pluton and its emplacement. Geological Journal, 34: 257-274.

Altunkaynak, Ş., Yılmaz, Y., 1998, The Mount Kozak magmatic complex, Western Anatolia. Journal of Volcanology and Geothermal Research, 85: 211-231.

Aydoğan, M.S., Çoban, H., Bozcu, M., Akıncı, Ö., 2008, Geochemical and mantle-like isotopic (Nd, Sr) composition of the Baklan Granite from the Muratdağı Region (Banaz, Uşak), western Turkey: Implications for input of juvenile magmas in the source domains of western Anatolia Eocene–Miocene granites, Journal of Asian Earth Sciences 33: 155-176.

Bingöl, E., Delaloye, M., Ataman, G., 1982, Granitic intrusions in Western Anatolia: a contribution to the geodynamic study of this area. Eclogae Geolisch Helvetica, 75/2, 437-446.

Boztuğ, D., Harlavan, Y., Jonckheere, R., Can, İ., Sarı, R., 2009, Geochemistry and K-Ar cooling ages of the Ilıca, Çataldağ (Balıkesir) and Kozak (İzmir) granitoids, west Anatolia, Turkey. Journal of Geology, 44**,** 79-103. DOI: 10.1002/gj.1132.

Candan, O., Çetinkaplan, M., Oberhänsli, R., Rimmele, G., Akal, C., 2005, Alpine high-P/low-T metamorphism of the Afyon Zone and implications for the metamorphic evolution of Western Anatolia, Turkey. Lithos, 84: 102-124.

Chen, F., Hegner, E., Todt, W., 2000, Zircon ages and Nd isotopic and chemical compositions of orthogneisses from the Black Forest, Germany: Evidence for a Cambrian magmatic arc. International Journal of Earth Sciences, 88: 791-802.

Chen, F., Siebel, W., Satir, M., Terzioğlu, N., Saka, K., 2002, Geochronolgy of the Karadere basement (NW Turkey) and implications for the geological evolution of the Istanbul zone. International Journal of Earth Sciences, 91: 469-481.

Cox K.G, Bell J.D, Pankhurst R.J., 1979, The interpretation of igneous rocks. George Allen and Unwin Ltd, London.

Delaloye, M., Bingöl, E., 2000, Granitoids from Western and Northwestern Anatolia: Geochemistry and modeling of geodynamic evolution. International Geology Review, 42, 241-268.

Dilek, Y. and Altunkaynak, S. 2009, Geochemical and temporal evolution of Cenozoic magmatism in western Turkey. Mantle response to collision, slab breakoff, and lithospheric tearing in an orogenic belt. In:VAN HINSBERG, D. J. J., EDWARDS, M. A and GOVERS, R. (eds) Geodynamics of collision and collapse at the Africa-Arabia-Eurasia Subduction zone. Geological Society, London, Special Publications, 311, 213-233.

Dilek, Y., Altunkaynak, Ş. 2007, Cenozoic crustal evolution and mantle dynamics of post-collisional magmatism in Western Anatolia. International Geology Review, 49: 431-453.

Ercan, T., Günay, E., Savaşçın, M, Y. 1984, Simav ve çevresindeki Senozoyik yaşlı volkanizmanın bölgesel yorumlanması. Maden Tetkik ve Arama Enstitüsü Dergisi. (in Turkish with English abstract), No.97/98, 86-101.

Erdoğan, B., 1990, İzmir-Ankara Zonu'nun, İzmir ile Seferihisar Arasındaki Bölgede Stratigrafik Özellikleri ve Tektonik Evrimi. Türkiye Petrol Jeologları Derneği Bülteni (TPJD), C.2/1., s. 1-20.

Erişen, B., 1982, Afyon bölgesinin güneydoğusundaki Permo-Karbonifer buluntu hakkında not. Maden Tetkik ve Arama Enstitüsü Dergisi (in Turkish with English abstract), No. 82**,** 148-151.

Erkül, F., Tatar, S., Bozkurt, E, Sözbilir, H, and Helvacı, C. 2009b, Tectonic significance of ductile shear zones within the syn-extensional Alaçamdağ granite, Northwestern Turkey. 62. Geological Kurultai of Turkey, Abstract, 178-179.

Erkül, T, S., Erkül, F., Bozkurt, E, Sözbilir, H, and Helvacı, C. 2009a, Geodynamic setting of the early Miocene Alaçamdağ Volcano-plutonic complex based on petrologic, isotopic and geochronological data: Northwestern Turkey. 62. Geological Kurultai of Turkey, Abstract, 180-181.

Fytikas M, Innocenti F, Manetti P, Mazzuoli R, Peccerillo A, Villari L., 1984, Tertiary to Quaternary evolution of volcanism in the Aegean region. In: Dixon EJ, Robertson AHF (eds) The geological evolution of the Eastern Mediterranean. Geological Society of London. Special Publication, V. 17: 687–699.

Genç, S.C., 1998, Evolution of the Bayramiç magmatic complex, northwestern Anatolia. . Journal of Volcanology and Geothermal Research, 85: 233-249.

Genç, Ş.C., Yılmaz. Y., 1997, An example of the post-collisional magmatism in Northwestern Anatolia: the Kızderbent volcanics (Armutlu Peninsula, Turkey). Turkish Journal of Earth Science (TUBITAK) 6, 33-42.

Giletti, J.B., 1991, Rb and Sr diffusion in alkali feldspars, with implications for cooling histories of rocks. Geochima Cosmochima Acta, 55: 1331-1343.

Güngör, T., Erdoğan , B., 2001, Emplacement age and direction of the Lycian nappes in the Söke-Selçuk region, western Turkey, International Journal of Earth Sciences, 89: 874-882.

Güngör, T., Erdoğan ,B., 2002, Tectonic significance of mafic volcanic rocks in a Mesozoic sequence of the Menderes Massif, West Turkey, International Journal of Earth Sciences, 91. 386-397.

Gürer, F.Ö., Filoreau, S.N., Özburan, M., Sangu, E., Doğan, B., 2009. Progressive development of the Büyük Menderes Graben based on new data, western Turkey. Geological Magazine, 146: 652-673.

Harris, N. B. W., Kelley, S., Okay, A. I., 1994, Post-collison magmatism and tectonics in northwest Anatolia. Contributions to Mineralogy and Petrology. 117, 241-252.

Hasozbek, A., Akay, E., Erdogan, B., Satir, M., Siebel, W., 2009a (in review), Geological and geochronological implications for the magmatic and tectonic evolution of the northern Menderes Massif (Western Turkey). Journal of Geodynamics.

Hasozbek, A., Satir, M., Erdogan, B., Akay, E., Siebel, W., 2009b, Magmatic evolution of the northwestern edge of Tauride-Anatolide Platform: Geochronological and isotopic implications. Goldschmidt Conference Abstracts 2009, Davos, A499.

Irvine, T. N., Baragar, W. R. A., 1971, A guide to the chemical Classification of the common volcanic rocks. Journal of Earth Sciences, 8, 523-548.

Işık, V., Tekeli, O., Seyitoğlu, G., 2004, The $^{40}Ar/^{39}Ar$ age of extensional ductile deformation and granitoid intrusion in the northern Menderes core complex: implications for the initiation of extensional tectonics in western Turkey. Journal of Asian Earth Sciences. 23/4: 555-566.

Işık, V., Tekeli, V. 2001, Late orogenic crustal extension in the northern Menderes Massif (Western Turkey): evidence for metamorphic core complex formation. International Journal of Earth Sciences, 89, 757-765.

İşintek, İ., Akay, E., Hasözbek, A., Erdoğan, B., 2007, Afyon Zonu' na ait Geç Triyas-Malm Budagan karbonat istifinin foraminifer ve alg içeriği (Emet, Kütahya, Batı Türkiye). Cukurova University, Geology Symposium, Abstracts, 118-119.

Jenkin, G.R.T., Ellam, R.M., Rogers, G., Stuart, F.M., 2001, An investigation of closure temperature of the biotite Rb-Sr system: The importance of cation exchange. Geochima Cosmochima Acta, 65/7: 1141-1160.

Jolivet, L., & Brun, J. P. 2010. Cenozoic geodynamic evolution of the Aegean. International Journal of Earth Sciences, 99, 109-138.

Karacık, Z., Yılmaz, Y., 1998, Geology of the ignimbrites and the associated volcano-plutonic complex of the Ezine are, northwestern Anatolia. Journal of Volcanology and Geothermal Research 85, 251-264.

Karacık, Z., Yılmaz, Y., Pearce, A.J., Ece. Ö.I., 2008. Petrochemistry of the south Marmara granitoids, northwest Anatolia, Turkey, International Journal of Earth Sciences, V:97**,** 1181-1200.

Kaya, O., 1972, Tavşanlı yöresi ofiyolit sorununun ana çizgileri. Bulletin Geological Society of Turkey 15/1, 26-108 (in Turkish with English abstract).

Kaya, O., Sadeddin, W., Altiner, D., Meric, E., Tansel, I., Vural, A., 1995, Tavşanlı (Kütahya) güneyindeki ankimetamorfik kayaların stratigrafisi ve yapısal konumu: İzmir-Ankara Zonu ile bağlantısı. Min Res Exp Bull, 117: 5-16.

Konak, N., 1982, Geology of the Simav region. Istanbul University, Faculty of Earth Sciences, Department of Geological Engineering, PhD thesis (in Turkish with English Abstract, unpublished).

Ludwig, K.R., 2003, Pbdat for MS-Dos- a computer program for IBM-PC compatibles for processing raw Pb-U-Th isotope data. U.S Geological. Survey. Open-file Rep 88-542: 1-37.

Nagudi, B., Koeberl, C., Kurat, G., 2003, Petrography and geochemistry of the Singo granite, Uganda and implications for its origin. Journal of African Earth Sciences, 36:73–87.

Okay, A. I., Satır, M., 2000, Coeval plutonism and metamorphism in latest Oligocene metamorphic core complex in northwest Turkey. Geological Magazine, 137, 495-516.

Okay, A. I., Satır, M., 2006, Geochronology of Eocene plutonism and metamorphism in northest Turkey: evidence for a possible arc. Geodinamica Acta, 19/5, 251-266.

Okay, A., 1984, Distribution and characteristics of the northwest Turkey blueschists. In: Robertson, A.H.F., Dixon, J.A. (Eds.9, The Geological Evolution of the Eastern Mediterrenean, Geological Society of London, Special Publication, V: 17: 455-466.

Okay, A.İ., Satır, M., Maluski, H., Siyako, M., Monie, P., Metzger, R., Akyüz, S., 1996, Paleo- and Neo-Tethyan events in northwestern Turkey: Geologic and geochronologic constraints. In: A. Yin and M. Harrison (Eds.) The Tectonic Evolution of Asia. Cambridge University Press, 420-441.

Okay, A.İ., Satır, M., Zattin, M., Cavazza, W., Topuz, G., 2008, An Oligocene ductile strike-slip shear zone: The Uludağ Massif, northwest Turkey: Implications for the westward translation of Anatolia, Geological Society of American Bulletin. Doi, 10.1130/B26229.1.

Özcan, A., Göncüoğlu, M. C., Turan, N., Uysal, Ş., Şentürk, K., Işık, I., 1998, Late Paleozoic evolution of the Kütahya-Bolkardağ belt. METU J. Pure App. Sci., V:21**,** No:1-3, 211-220.

Özgenç, İ., İlbeyli, N., 2008, Petrogenesis of the late Cenozoic Eğrigöz granite in western Anatolia, Turkey: Implications for magma genesis and crustal processes. International Geology Review, 50, 375-391.

Pearce, J.A., 1996, Sources and settings of granitic rocks. Episodes, 19, 120–125.

Pearce, J.A., Harris, N.B.W., Tindle, A.G., 1984, Trace element discrimination diagrams for the tectonic interpretation of granitic rocks. Journal of Petrology, 25: 956–98.

Pe-Piper, G. and Piper, D. J. W. 2006. Unique features of the Cenozoic igneous rocks of Greece. In: DILEK, Y. & PAVLIDES, S. (eds) Postcollisional tectonics and magmatism in the Mediterranean region and Asia.Geological Society of America Special Paper, 409, 259–282.

Ring, U., Collins, S.A., 2005, U-Pb SIMS dating of synkinematic granites: timing of core-complex formation in the northern Anatolide belt of western Turkey, Journal of Geological Society, London, 162, 289-298.

Rudnick, R.L., Gao, S., 2003, Composition of the continental crust. V **3**. Treatise on Geochemistry, V: 3, pp: 1-63.

Seyitoğlu, G., Işık, V., 2009, Meaning of the Küçük Menderes graben in the tectonic framework of the central Menderes metamorphic core complex (western Turkey) Geologica Acta, Vol.**7**, No: 3, 323-331.

Seyitoğlu, G., Işık, V., Çemen, İ., 2004, Complete Tertiary exhumation history of the Menderes Massif, western Turkey: an alternative working hypothesis. Terra Nova, 16/6: 358-364.

Seyitoğlu, G., Scott, B.C., 1992, Late Cenozoic volcanic evolution of the northeastern Aegean region. Journal of Volcanology and Geothermal Research, 54, 157-176.

Shand, S.I., 1947, Eruptive rocks. Thomas Murby and Co, London.

Taylor, S.R., McLennan, S.M., 1985, The continental crust: Its composition and evolution. Blackwell, Oxford.

Thomson, S.N., Ring, U., 2006, Thermochronologic evaluation of postcollision extension in the Anatolide orogen, western Turkey. Tectonics, 25, 1-20.

Yılmaz, Y., 1997, Geology of western Anatolia active tectonics of northwestern Anatolia-The Marmara poly-project. A multidisciplinary approach by space-geodesy, geology, hydrogeology, geothermics and seismology, E.T.H Univ. Press, Zürich. In: Schindler, C., Fister, M.P. (Eds.), 31-53.

Yılmaz, Y., Altunkaynak, Ş., Karacık, Z., Gündoğdu, N., Temel, A., 1994, Development of neo-tectonic related magmatic activities in western Anatolia. Internationa Volcanology Congress, Ankara, Abstracts: 13.

Yılmaz, Y., Genç, Ş.C., K., Karacık, Z., Altunkaynak, Ş., 2001, Two contrasting magmatic associations of NW Anatolia and their tectonic significance. Journal of Geodynamics, 31, 243-271.

York, D., 1969, Least-square fitting with a straight line with correlated errors. Earth Planet Science Letters, 14, 225-280.

Chapter 3: Al- in-hornblende thermobarometry and petrogenesis of the Alaçam granite in NW Anatolia (Turkey)

ALTUĞ HASÖZBEK [1,2], BURHAN ERDOĞAN [3], MUHARREM SATIR [2], , WOLFGANG SIEBEL [2], ERHAN AKAY [3] GÜLLÜ DENİZ DOĞAN [4,5] & HEINRICH TAUBALD [2]

[1] Dokuz Eylül University, Technical Vocational School of Higher Education, 35860, Torbalı, İzmir, Turkey
altug.hasozbek@deu.edu.tr

[2] Institut für Geowissenschaften, Universität Tübingen,Wilhelmstrasse 56, D-72074 Tübingen, Germany

[3] Dokuz Eylül University, Engineering Faculty, Department of Geological Engineering, 35160, Buca, Izmir, Turkey

[4] Hacettepe University, Department of Geological Engineering, 06800, Beytepe-Ankara, Turkey

[5] University Blaise Pascal, OPGC, Lab. Magmas et Volcans, UMR-6524 CNRS, 5 rue Kessler, 63038, Clermont-Ferrand Cedex, France

Submitted in Turkish Journal of Earth Science

Idea:	60%
Problem:	50%
Production of Data:	70%
Evaluation and Interpretation:	80%
Preparation of the manuscript:	70%

Abstract

During and after the closure of the Neo-Tethyan Ocean and progressive collision of the Tauride-Anatolide Platform with the Sakarya Continent, widespread magmatism occurred in NW Anatolia. These magmatic associations form a NW trending belt. The Miocene Alaçam granite with its related stocks is exposed along the suture zone. The granites intruded into the basement rocks of the region which consist of, from bottom to top, the Menderes Massif, a meta-ophiolitic nappe complex, the Afyon Zone and the Bornova Flysch Zone.

Due to the complex geodynamic evolution, the exact emplacement depth and the petrogenesis of the Miocene granitoids in the northern border of the Menderes Massif is still controversially discussed. New Al-in-hornblende barometry and isotopic compositions of the Alaçam granite give rise to reconsider the general emplacement mode of the Miocene granitoids and address the question if the magmatism was triggered by compression or extensional tectonic processes.

Initial isotopic signatures of the Alaçam granites are $^{87}Sr/^{86}Sr(I) = 0.70865\text{-}0.70915$, $e_{Nd}(I) = -5.8$ to -6.4, $\delta^{18}O = 9.5 - 10.5$, and measured $^{206}Pb/^{204}Pb$ isotope ratios vary between 18.87 and 18.90. These characteristics indicate an assimilation-dominated crustal crystallization and most probably its derivation from an older meta-sedimentary protolith. Al-in-hornblende barometry for the Alaçam granite yields an intrusion depth of ca. 2 - 7 km.

A post-collisional extensional emplacement model as was earlier suggested for the Miocene Alaçam granites is not compatible with the new petrogenetic and Al-in-hornblende barometry results of this study.

Key Words: Alaçam granite, Al-in-hornblende barometry, Sr-Nd-O-Pb isotopes, NW Anatolia, petrogenesis

Özet:

Neo-Tetis okyanusunun kapanması ile meydana gelen Anatolit-Torid Paltformu'nun Sakarya Kıtası ile progresif çarpışması sırasında ve sonrasında, KB Anadolu'da yaygın bir magmatizma meydana gelmiştir. Bu magmatizmanın ürünleri Batı Anadolu'daki KB doğrultulu kuşakları oluşturmaktadır. Miyosen yaşlı Alaçam graniti ve stokları sutur zonu boyunca yüzlek verirler. Alaçam Granitleri, alttan üste doğru temeli oluşturan şu birimlere intruzif olarak sokulmaktadır; Menderes Masifi, Meta-ofiyolitik nap kompleksi, Afyon Zonu ve Bornova Filiş Zonu.

Menderes Masifi'nin kuzey sınırındaki Miyosen granotoidlerinin (Eğrigöz, Koyunoba ve Alaçam granitleri) gerçek yerleşim derinliği ve petrojenezi, bölgenin karmaşık jeodinamik evriminden dolayı halen tartışmalıdır. Alaçam granitinden elde edilen yeni Al-hornblend ve izotop analizleri, Miyosen magmatik aktivitesinin hangi mekanizmaya bağlı olarak gelişip gelişmediği sorularının yeniden incelenmesine yol açmıştır.

Alaçam Graniti'nin ilksel izotopik değerleri; $^{87}Sr/^{86}Sr(I) = 0.70865\text{-}0.70915$, $e_{Nd}(I) = -5.8$ to -6.4, $\delta^{18}O = 9.5\text{-}10.5$, $^{206}Pb/^{204}Pb = 18.87\text{-}18.90$ 'dir. Bu izotop verileri asimilasyonunun baskın olduğu bir kabuksal kristallenmeyi ve olası yaşlı bir meta-kıtasal kabuk köken kayasından türediğini göstermektedir. Al-hornblend barometresi hesaplamaları, Alaçam Graniti için intrüzyon derinliğini 2-7 km olarak vermiştir. Miyosen yaşlı Alaçam Granitleri için önerilen çarpışma sonrası açılmaya bağlı yerleşim modeli, bu calismada sunulan yeni Al-hornblend barometre bulguları ile uyumlu değildir.

Anahtar Sözcükler: Alaçam graniti, Al-hornblend barometrisi, Sr-Nd-O-Pb izotopları, KB Anadolu, petrojenez

Introduction

From Eocene to Quaternary, extensive igneous activity took place in the Aegean-NW Anatolian region (Figure 1). Evolution of this widespread magmatic activity has been subjected to close scrutiny by various researchers (Altherr & Siebel 2002; Altherr *et al.* 2004; Altunkaynak 2007`; Brichau *et al.* 2007; Dilek & Altunkaynak 2007; Aydogan *et al.* 2008; Akay 2009; Ilbeyli & Kibici 2009; Hasözbek *et al.* 2010; Jolivet & Brun 2010,; Stouraiti *et al.* 2010). In the Aegean Sea, S-type (e.g. Ikeria - eastern intrusion -, Tinos - Krokos -, Paros), and I-type granitoids (Tinos - Falatados -, Ikeria - western intrusion -, Naxos) are widely exposed, with extrusive and intrusive products. Miocene I-type granitoids of post-collisional origin (e.g. Kozak, Evciler, Alaçam, Eğrigöz, Baklan granitoids) are also exposed in NW Anatolia along a belt straddling the southern and northern parts of the İzmir-Ankara Suture Zone (Figure 1). Petrogenetic models addressing this magmatic zone generally involve a mantle contribution during magma formation (Aldanmaz *et al.* 2000; Dilek & Altunkaynak 2007; Dilek & Altunkaynak 2009). Recent petrogenetic studies of the eastern Aegean Miocene magmatism, however, (Aegean island magmatism) are in basic agreement that these granitoids are derived from a crustal meta-sedimentary source (Altherr & Siebel 2002; Stouraiti *et al.* 2010). Stouraiti *et al.* (2010) suggest that three end members (metasedimentary biotite-gneiss, marble, and amphibolite) were involved in the generation of the Middle-Late Miocene granitoids of the Aegean Sea.

Various researchers have suggested petrogenetic models supporting this hypothesis with new radiometric and structural data (Stouraiti *et al.* 2010, and references therein). The main purpose of these studies was to specify the geodynamic nature of this magmatism from Eocene to Quaternary time, that is, to answer the question whether the melts were produced by continent-continent collision, subduction of oceanic lithosphere, delamination, slab-break off, or within a detachment zone in a continental lithosphere (Akay 2009; Altherr & Siebel 2002; Altherr *et al.* 2004; Altunkaynak 2007; Aydogan *et al.* 2008; Bozkurt & Oberhansli 2001; Brichau *et al.* 2007; Dilek & Altunkaynak 2007; Hasözbek *et al.* 2010a, b ; Ilbeyli & Kibici 2009; Jolivet & Brun 2010; Stouraiti *et al.* 2010).

The Miocene granitoids in the Aegean Sea have been more intensively studied than similar granitoids in NW Anatolia. This paper focuses on the Early Miocene Alaçam granitic body located along the northern border of the Menderes Massif (NW Anatolia) in the NW Anatolia Magmatic Belt. Previous studies on this granite (geology, geochemistry and geochronology)

were published in Hasözbek *et al.* (2010b). In the following, we present new Al-in-hornblende thermobarometry and new Sr-Nd-O-Pb isotope data to propose a model for the emplacement and the petrogenesis of the Alaçam granite. This paper sheds light on the petrogenetic evolution and the emplacement nature of the Alaçam granite and compares it with the Miocene magmatism of the Aegean islands Miocene magmatism.

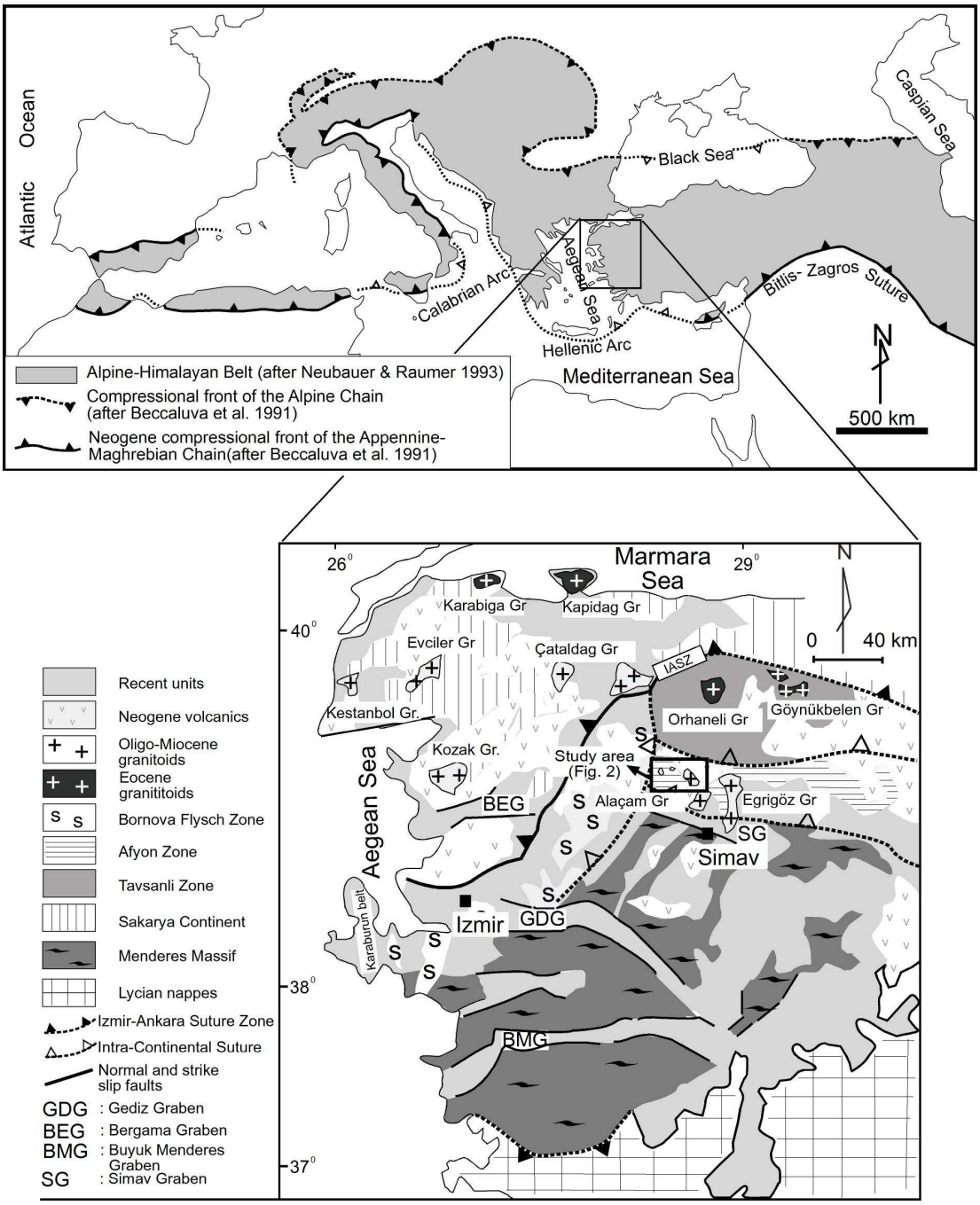

Figure 1. Generalized location of the Alpine-Himalayan Belt (modified after Akal 2003) and location map of the study area (modified after Hasözbek et al. 2010a)

Regional Setting and Geological Framework

Tertiary magmatism in the eastern Mediterranean region, including both the Aegean Sea and NW Anatolia, evolved by a variety of geodynamic processes (Jolivet & Brun 2010, and references therein). Major tectonic events occurring between Eocene and Quaternary time include subduction of the African lithospheric plate beneath the Aegean, collision between Africa and Eurasia, and backarc extension (e. g. Jolivet & Brun 2010; Stouraiti *et al.* 2010) (Figure 1). Both the Aegean islands and NW Anatolia constitute similar geological settings: In both regions, metamorphism resulted in blueschist facies and was almost entirely overprinted by high to medium temperature/low pressure metamorphic conditions (Candan *et al.* 2005; Okay 1980, 1982; Stouraiti *et al.* 2010). The metamorphic basement was nailed by the Eocene and Miocene granitoids (Altunkaynak & Yılmaz 1999; Karacık & Yılmaz 1998; Altunkaynak 2007; Akay 2009; Dilek & Altunkaynak 2007; 2009; Hasözbek *et al.* 2010a, b) which are suggested to have been emplaced either along detachment faults in an extension zone (Bozkurt & Oberhänsli 2001; Isik *et al.* 2003; Isik & Tekeli 2001; Jolivet & Brun 2010; Ring & Collins 2005; Seyitoglu *et al.* 2004; Stouraiti *et al.* 2010; Thomson & Ring 2006), or originated from a thickened crust resulting from a compression event (Akay 2009; Altunkaynak & Yilmaz 1999; Hasözbek *et al.* 2010a, b; Karacik & Yilmaz 1998; Yilmaz *et al.* 2001).

In NW Turkey, the Alaçam granite is exposed along the collision zone between the Sakarya continent and the Menderes platform. Four different tectonic zones of these two continents form imbricated nappe packages which were intruded by the Miocene Alaçam granite (Hasözbek *et al.* 2010b) (Figure 1 & 2). These four tectonic zones, from bottom to top, are: 1) Menderes metamorphics, which form the basement of the study area, characterized by a high - to medium- grade metapelite association, 2) a meta-ophiolitic nappe complex, similar in lithology to the late Cretaceous Selçuk Formation (Güngör & Erdoğan 2001; 2002) which tectonically overlays the Menderes metamorphics, 3) the Afyon Zone, which tectonically overlays both the Menderes Massif and the meta-ophiolitic nappe complex (greenschist facies low grade metamorphic rocks) mostly comprises gneissic granites, metapelites, metarhyolites, and recrystallized limestones, 4) the Bornova Flysch Zone, a non-metamorphic Late Cretaceous-Late Oligocene ophiolitic mélange, which tectonically overlies the Afyon Zone (Hasözbek *et al.* 2010b, and references therein). The Alaçam granite and its host rocks (tectonic package) are unconformably overlain by Middle-Upper Miocene continental-lacustrine sedimentary rocks, and an andesitic volcanic sequence (Figure 2).

The Alaçam granite cuts various units of the Menderes Massif, the Afyon Zone, and the Bornova Flysch Zone and its age was determined by U-Pb (zircon) method at 20.0 ± 1.4 Ma (Hasözbek *et al.* 2010b) (Figure 2). The granite displays characteristically steeply-dipping, sharp contacts with the country rocks. The inner contact zone consists of microgranite, which gradually passes inward into a coarse-grained holocrystalline phase. Abundant enclaves of Menderes metamorphics and Afyon Zone rocks are found along the contact zone. The granitic body is not deformed, except part of the contact zones, which probably arise from rapid cooling at a shallow crustal level during continuous emplacement (Hasözbek *et al.* 2010b).

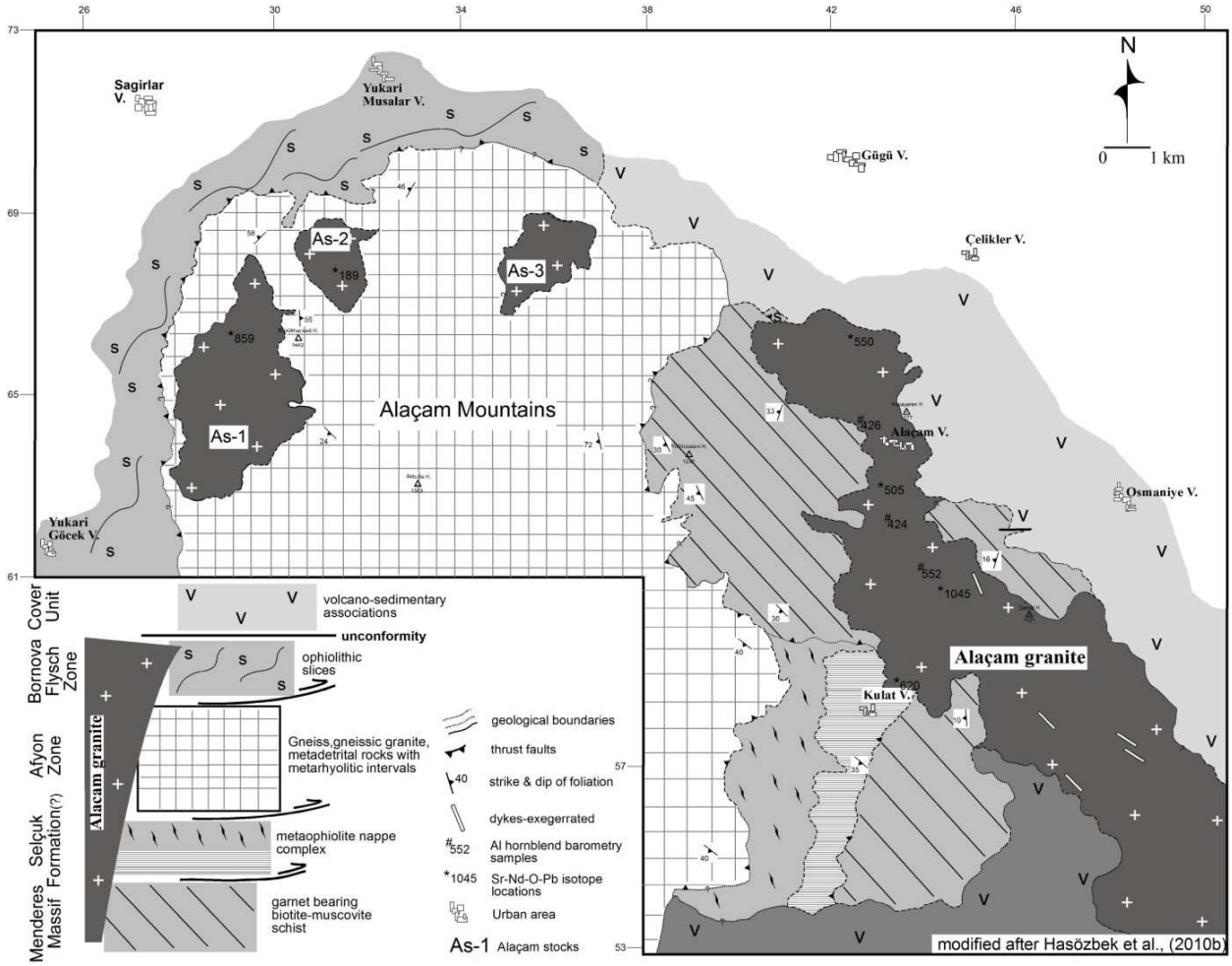

Figure 2. Geological map and columnar section of the study area (modified after Hasözbek et al. 2010b)

Analytical Methods

Geochemical analyses were carried out in Acme Analytical Laboratories Ltd (Vancouver, Canada) by ICP-AES (Inductively Coupled Plasma Atomic Emission Spectrometry) and ICP-MS (Inductively Coupled Plasma Mass Spectrometry). The data are published and discussed in detail in Hasözbek *et al*. (2010b). Thin section preparation and polishing for microprobe analysis were done in petrographical lab of Tübingen University. Chemical analysis of amphibole minerals from the Alaçam granite were carried out on a JEOL 8900 electron microprobe at the Institut für Geowissenschaften, Tübingen University, Germany (Table 2). (424a-UTM: 0643656;4362433; 426-UTM: 0642874;4364265; 552-UTM: 0644483;4361393). Raw data were corrected accuracy to Armstrong (1991). Both synthetic and natural standards were used. The emission current was 15 nA and the acceleration voltage 15 kV. Counting times were usually 10 s for each element. In order to avoid significant Al increase through contact with plagioclase and biotite, analyses were performed on amphibole minerals in contact with quartz. The Anderson and Smith (1995) calibration method with deriving the temperature from the plagioclase-hornblende geothermometer (reaction B) of Holland and Blundy (1994) was used where plagioclase was in contact with amphibole. Atomic proportions of amphiboles were taken from Holland and Blundy (1994). The analytical study by Hammarstrom and Zen (1986) and Hollister et al. (1987) suggest that the Al content of calcic amphibole led to evaluate the pressure attending to pluton crystallization. Moreover, other experimental studies confirmed an increase in Al content of hornblende while pressure increases (Schmidt 1992). Pressure calculations, were performed by using excel sheet from Anderson and Smith (1995). Plagioclase compositions were determined by standard petrographical method. According to our pressure calculations, we established that uncertainty in plagioclase concentrations in determined pressure was not more than 0.5 kbar. BSE images of the amphibole contacts with other minerals (quartz, plagioclase, and biotite) presented in this paper were taken by using the electron microprobe at the Institut für Geowissenschaften, Tübingen University, Germany.

Sr, Nd, Pb, O isotope analysis from 6 samples of the Alaçam granite (Table 3) (189-UTM: 0631536;4367877; 505-UTM: 0643100;4363201; 550-UTM: 0644210;4366460; 620-UTM: 0644460;4358460; 859-UTM: 0628932;4366465; 1045-UTM: 0644798;4360915) were performed at the Department of Geochemistry, Tübingen University. For Sr and Nd analyses, about 75-80 mg of whole-rock sample powder was spiked with mixed ^{84}Sr-^{87}Rb tracer. Samples were dissolved in concentrated HF acid in Teflon vials in poly-tetrafluor-ethylene (PTFE)

reaction bombs at 220 ^{0}C under high pressure for 4 days. Digested samples were dried and redissolved in 2.5 N HCL. Conventional cation exchange chromatography technique was used for separating Rb, Sr, Sm, Nd, U, Th and Pb. Sr was loaded with a Ta-HF activator and measured on a single W filament. Rb, Sm and Nd isotope compositions were measured in a double Re filament configuration mode and single Re filaments were used for Pb isotope measurements. Isotopic analyses were done using a Finnigan MAT 262 thermal ionization mass spectrometer (TIMS). For mass fractionation, Sr was normalized to $^{86}Sr/^{88}Sr = 0.1194$ and Nd was normalized to $^{146}Nd/^{144}Nd = 0.7219$. During this study, measurement of the La Jolla Nd standard gave a mean $^{143}Nd/^{144}Nd$ ratio of 0.511820 ± 10 (certified value of 0.511850) and NBS-987 Sr standard yielded a $^{87}Sr/^{86}Sr$ ratio of 0.710240 ± 11 (certified value of 0.710245). $^{87}Rb/^{86}Sr$ ratios for whole rock samples were calculated from the $^{87}Sr/^{86}Sr$ ratios and the Rb and Sr concentrations taken from the ICP/ES measurements. The thermal fractionation of Pb isotopes was determined by measuring of Pb standard NBS981 and the isotopic ratios were corrected for 0.11% fractionation per atomic mass unit.

For the measurement of O isotopes, a conventional extraction method of oxygen and BrF_5 reagent was used, according to a method of Clayton and Mayeda (1963). About 7 mg of sample was converted into CO_2. Reaction was performed at 550ºC for 16-18 h. Isotope measurements were made using a Finnigan MAT 252. Oxygen isotope compositions are given in the standard δ-notation and expressed relative to VSMOW in permil (‰). The precision of $\delta^{18}O$ values was better than ±0.2‰, as compared with accepted $\delta^{18}O$ values for NBS-28 of 9.64‰.

Petrography, Geochemistry and Isotopic data

The detailed petrographical characteristics and whole rock geochemistry of the Alaçam pluton have been given in Hasözbek *et al.* (2010b). The pluton is mostly granite in composition except few samples showing granodiorite composition. The Alaçam granite generally exhibits a moderate coarse-grained holocrystalline texture. In places where the margin of the granite is well exposed however, the texture is fine-grained due to rapid cooling (Hasözbek *et al.* 2010b). The mineral assemblage is quartz, albite, orthoclase, hornblende, biotite, and minor zircon, titanite, sphene, apatite, and magnetite (Figure 3). Plagioclases generally exhibit albite twinning and normal oscillatory zoning due to changes in composition from core to rim. Small hornblende and biotite inclusions are also found in plagioclase crystals. Few plagioclases are altered into sericite. Alkali feldspars are mostly microcline or microperthite

and may display a cloudy appearance due to sericitization. Most of the quartz minerals exhibit polygonal structure and vary in size. Amphiboles occur in euhedral-subhedral prismatic or rhombic forms with lamella twinning (Figure 3a - d).

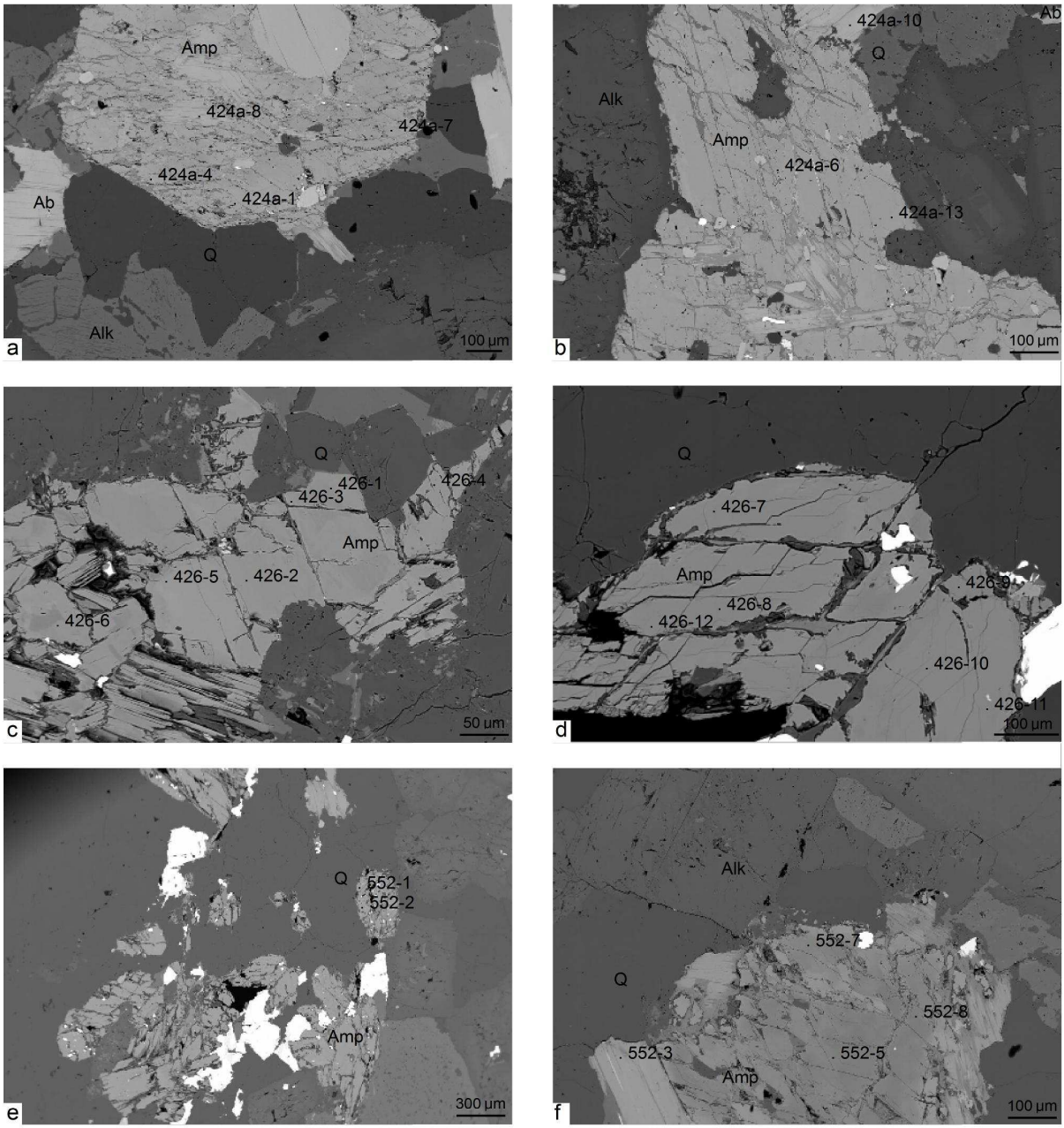

Figure 3. BSE images of mineral textures and spots of microprobe analysis from the Alaçam granite. (a-b) 424a, (c-d) 426, (e-f) 552. Q, quartz, Ab, albite; Alk, alkali feldspar; Amp, amphibole.

The Alaçam granite is subalkaline, high-K calc-alkaline in composition. With A / CNK values< 1.1. Ba (288-1330 ppm), La (23-64 ppm), and Th (9-48 ppm) concentrations indicate enrichment in incompatible elements. The chondrite- and primitive mantle-normalized element patterns also show enrichment in incompatible elements (Figure 4a - b). High field strength elements such as Pb and low field strength elements such as Rb display negative anomalies (Figure 4b). Negative anomalies in Sr are also significant. Enrichment in large ion lithophile elements ($[La/Yb]_N$ = 6 - 17), as compared to high field strength elements ($[Gd/Yb]_N$ = 1 - 1.6) is significant in the chondrite-normalized patterns (Hasözbek *et al.* 2010b).

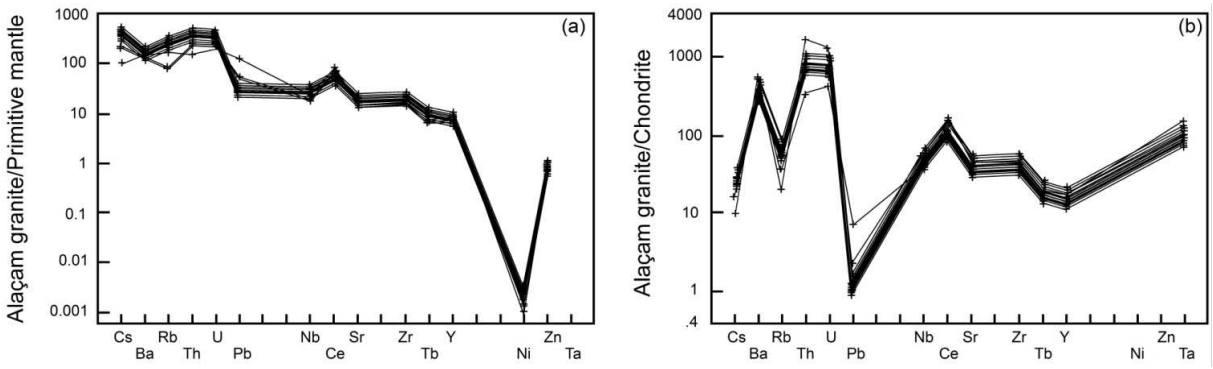

Figure 4. (a) Primordial mantle-, (b) Chondrite-normalized multielement diagrams (spider diagram) for the Alaçam granite. Normalized values are after Taylor and McLennan (1985).

Mineral chemistry

Three samples were chosen from the main body of the Alaçam granite for Al-in-hornblende barometry (Figure 2). Results of the microprobe analysis are presented in Table 1. Chemical compositions of the rims and cores of the analyzed amphiboles do not differ from each other (Figure 5) and do not show any systematic variation in the amphibole classification diagrams of Leake (1997) (Figure 5). Amphiboles are all calcic in nature and range from pargasite to edenite in the calcic-a classification (Figure 5a). In the calcic-b classification diagram of Leake (1997), they are gathered in the magnesiohornblende field (Figure 5b). Fe^{3+}/Fe^* ratio ranges from 0.20 to 0.37. The total Al content is between 0.942 and 1.609 cations per formula unit and all cores and rims of the A-site occupancy range from 0.295 to 0.555. Pressure calculations for amphibole compositions (rim and core) are given in Table 1, in which all data

fall in the same range between 0.60 and 2.07 kbar. By using a conversion factor of 1 kbar = 3.7 km of crust (Tulloch & Challis 2000), the intrusion depth of the Alaçam granite is between 2-7 km.

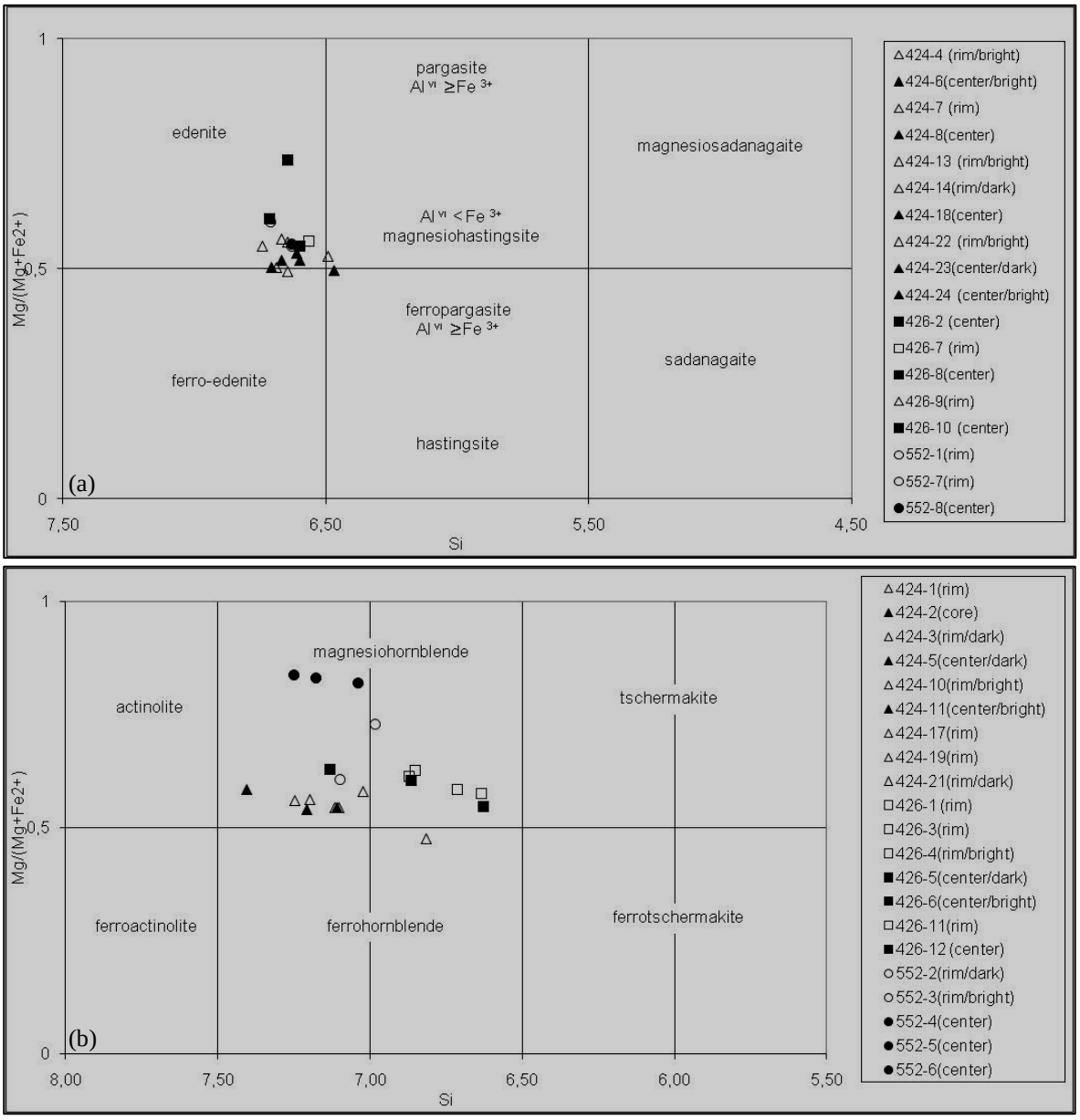

Figure 5. Amphibole classification diagrams of Leake (1997) for the Alaçam granite based on (a) calcic-a, and (b) calcic- b

Table 1. Microprobe analyses of hornblende rims and cores from the Alaçam granite and calculated

Sample	**424a-1**	**424a-7**	**424a-8**	**424a-4**	**424a-6**	**424a-10**	**424a-13**	**426-1**	**426-2**	**426-3**	**426-4**	**426-5**	**426-6**	**426-7**	**426-8**	**426-9**	**426-10**	**426-11**	**426-12**	**552-1**	**552-2**	**552-3**	**552-5**	**552-7**	**552-8**
	r	r	c	r/b	c/b	r/b	r	r	c	r	r/b	c/d	c/b	r	c	r	c	r	c	r	r/d	r/b	c	r	c
SiO2	47,51	45,37	44,7	44,15	44,78	45,26	43,73	45,06	45,34	46,52	46,43	48,44	46,43	44,06	44,05	44,81	44,49	44,58	44,48	45,07	48,16	47,97	49,35	44,33	44,45
TiO2	0,43	1,245	1,247	1,325	1,086	1,186	1,508	1,483	1,502	0,603	0,586	0,767	0,917	1,72	1,68	1,443	1,425	1,531	1,74	1,304	0,872	0,687	0,625	1,478	1,413
Al2O3	6,11	7,99	8,47	8,36	8,11	7,56	9,19	8,11	7,97	6,95	6,88	5,26	6,93	8,84	8,69	8,18	8,55	8,32	8,34	7,95	6,38	5,4	6,7	8,5	8,39
FeO*	20,19	19,49	20,23	20,9	21,32	21,48	21,16	17,87	17,32	18,34	18,19	17,22	18,41	18,87	18,88	18,52	18,87	18,87	19,72	18,01	14,33	17,87	10,57	19,42	19,56
MgO	10,78	10,21	9,55	8,99	9,05	8,59	9,39	10,92	11,54	11,57	11,4	12,46	11,2	10,3	10,14	10,46	10,22	10,49	9,98	11,08	14,38	11,99	16,5	9,97	10,12
MnO	0,979	0,674	0,723	0,851	0,925	1,032	0,678	0,595	0,534	0,785	0,754	0,804	0,841	0,648	0,614	0,711	0,749	0,712	0,737	0,769	0,677	0,983	0,266	0,794	0,743
CaO	10,83	11,12	11,29	11,22	10,88	10,83	11,05	11,4	11,51	11,81	11,93	11,62	11,59	11,39	11,39	11,38	11,29	11,39	11,16	11,19	11,32	11,49	11,73	11,13	11,19
Na2O	1,233	1,77	1,76	1,72	1,77	1,58	1,86	1,59	1,68	1,154	1,245	1,034	1,235	1,74	1,7	1,58	1,65	1,51	1,64	1,72	1,56	1,285	1,66	1,72	1,79
K2O	0,533	0,882	1,003	1,024	0,894	0,823	1,018	0,937	0,922	0,633	0,638	0,499	0,756	1,054	1,082	0,97	1,025	0,992	0,913	0,881	0,539	0,518	0,485	1,012	0,944
F	0,102	0,133	0,162	0,161	0,155	0,164	0,144	0,152	0,135	0,067	0,068	0,064	0,075	0,165	0,185	0,149	0,153	0,154	0,13	0,147	0,05	0,049	0,041	0,16	0,149
Cl	0,224	0,334	0,276	0,32	0,342	0,247	0,35	0,214	0,223	0,17	0,202	0,17	0,19	0,2	0,183	0,155	0,165	0,18	0,149	0,32	0,365	0,259	0,458	0,274	0,274
Sum	98,92	96,10	99,41	99,02	99,31	98,75	100,08	98,33	96,10	98,60	98,32	98,34	98,57	98,99	98,59	98,36	98,59	98,73	98,99	98,44	96,10	98,50	98,39	98,79	99,02
Fe2O3,calc	5,93	4,65	4,51	4,73	5,37	4,75	6,31	4,25	4,36	6,56	6,03	3,89	5,68	4,71	4,28	4,45	4,66	5,39	5,17	5,05	4,49	3,55	4,32	4,90	5,20
FeO,calc	14,86	15,30	16,17	16,65	16,49	17,21	15,49	14,04	13,40	12,44	12,77	13,72	13,30	14,63	15,03	14,52	14,68	14,02	15,07	13,46	10,29	14,68	6,68	15,01	14,88
H2O,calc	1,89	1,85	1,84	1,81	1,82	1,83	1,83	1,87	1,88	1,93	1,91	1,94	1,92	1,86	1,85	1,88	1,87	1,87	1,89	1,84	1,93	1,92	1,95	1,83	1,84
O=F, Cl	0,09	0,13	0,13	0,14	0,14	0,12	0,14	0,11	0,11	0,07	0,07	0,07	0,07	0,11	0,12	0,10	0,10	0,11	0,09	0,13	0,10	0,08	0,12	0,13	0,12
SUM	101,32	101,40	101,57	101,17	101,52	100,93	102,40	100,51	100,89	101,12	100,77	100,61	100,98	101,20	100,75	100,58	100,82	101,03	101,31	100,65	100,91	100,70	100,64	100,99	101,26
Fe3/Fe*	**0,26**	**0,21**	**0,20**	**0,20**	**0,23**	**0,20**	**0,27**	**0,21**	**0,23**	**0,32**	**0,30**	**0,20**	**0,28**	**0,22**	**0,20**	**0,22**	**0,22**	**0,26**	**0,24**	**0,25**	**0,28**	**0,18**	**0,37**	**0,23**	**0,24**
Formula per Holland and Blundy, 1994																									
T-sites																									
Si	7,022	6,742	6,669	6,646	6,705	6,814	6,493	6,714	6,712	6,853	6,871	7,132	6,866	6,565	6,597	6,694	6,645	6,635	6,626	6,709	6,985	7,100	7,039	6,631	6,629
Aliv	0,978	1,258	1,331	1,354	1,295	1,186	1,507	1,286	1,288	1,147	1,129	0,868	1,134	1,435	1,403	1,306	1,355	1,365	1,374	1,291	1,015	0,900	0,961	1,369	1,371
Al(total)	1,065	1,400	1,490	1,484	1,432	1,342	1,609	1,425	1,391	1,207	1,200	0,913	1,208	1,553	1,534	1,441	1,505	1,460	1,465	1,395	1,091	0,942	1,127	1,499	1,475

Table 1. continued

M1,2,3 sites																									
Alvi	0,086	0,142	0,159	0,129	0,137	0,156	0,101	0,138	0,103	0,060	0,072	0,045	0,074	0,118	0,132	0,135	0,150	0,095	0,091	0,104	0,076	0,042	0,165	0,129	0,104
Ti	0,048	0,139	0,140	0,150	0,122	0,134	0,168	0,166	0,167	0,067	0,065	0,085	0,102	0,193	0,189	0,162	0,160	0,171	0,195	0,146	0,095	0,076	0,067	0,166	0,158
Fe3+	0,659	0,520	0,506	0,535	0,605	0,538	0,704	0,477	0,486	0,727	0,671	0,431	0,632	0,528	0,482	0,500	0,524	0,604	0,579	0,566	0,490	0,395	0,464	0,552	0,584
Mg	2,374	2,261	2,123	2,017	2,020	1,927	2,078	2,425	2,546	2,540	2,514	2,734	2,468	2,287	2,263	2,329	2,275	2,327	2,216	2,458	3,108	2,645	3,507	2,222	2,249
Mn	0,123	0,085	0,091	0,109	0,117	0,132	0,085	0,075	0,067	0,098	0,095	0,100	0,105	0,082	0,078	0,090	0,095	0,090	0,093	0,097	0,083	0,123	0,032	0,101	0,094
Fe2+	1,710	1,852	1,980	2,060	1,999	2,112	1,863	1,719	1,631	1,508	1,580	1,606	1,618	1,792	1,856	1,784	1,796	1,712	1,826	1,628	1,147	1,718	0,764	1,829	1,810
Ca	0,000	0,000	0,000	0,000	0,000	0,000	0,000	0,000	0,000	0,000	0,003	0,000	0,000	0,000	0,000	0,000	0,000	0,000	0,000	0,000	0,000	0,000	0,000	0,000	0,000
	5,000	5,000	5,000	5,000	5,000	5,000	5,000	5,000	5,000	5,000	5,000	5,000	5,000	5,000	5,000	5,000	5,000	5,000	5,000	5,000	5,000	5,000	5,000	5,000	5,000
M4 site																									
Fe	0,127	0,049	0,038	0,036	0,066	0,054	0,060	0,031	0,028	0,025	0,000	0,084	0,027	0,032	0,027	0,030	0,037	0,032	0,052	0,047	0,101	0,099	0,033	0,048	0,046
Ca	1,715	1,771	1,805	1,810	1,746	1,747	1,758	1,820	1,826	1,864	1,889	1,833	1,836	1,819	1,828	1,822	1,807	1,817	1,781	1,785	1,759	1,822	1,793	1,784	1,788
Na	0,158	0,180	0,157	0,155	0,188	0,198	0,182	0,149	0,146	0,111	0,111	0,083	0,137	0,150	0,145	0,148	0,156	0,151	0,167	0,168	0,140	0,079	0,175	0,168	0,166
	2,000	2,000	2,000	2,000	2,000	2,000	2,000	2,000	2,000	2,000	2,000	2,000	2,000	2,000	2,000	2,000	2,000	2,000	2,000	2,000	2,000	2,000	2,000	2,000	2,000
A site																									
Ca	0,000	0,000	0,000	0,000	0,000	0,000	0,000	0,000	0,000	0,000	0,000	0,000	0,000	0,000	0,000	0,000	0,000	0,000	0,000	0,000	0,000	0,000	0,000	0,000	0,000
Na	0,195	0,330	0,352	0,347	0,326	0,263	0,354	0,310	0,336	0,218	0,246	0,212	0,217	0,353	0,349	0,309	0,322	0,285	0,307	0,329	0,299	0,290	0,284	0,331	0,352
K	0,100	0,167	0,191	0,197	0,171	0,158	0,193	0,178	0,174	0,119	0,120	0,094	0,143	0,200	0,207	0,185	0,195	0,188	0,174	0,167	0,100	0,098	0,088	0,193	0,180
Sum A	0,295	0,497	0,543	0,544	0,496	0,421	0,546	0,488	0,510	0,337	0,367	0,306	0,360	0,553	0,555	0,494	0,517	0,473	0,480	0,496	0,399	0,388	0,373	0,524	0,531
OH site																									
O	0,000	0,000	0,000	0,000	0,000	0,000	0,000	0,000	0,000	0,000	0,000	0,000	0,000	0,000	0,000	0,000	0,000	0,000	0,000	0,000	0,000	0,000	0,000	0,000	0,000
OH	1,895	1,852	1,852	1,840	1,838	1,857	1,842	1,873	1,880	1,925	1,916	1,927	1,916	1,870	1,865	1,889	1,885	1,881	1,900	1,848	1,886	1,911	1,869	1,853	1,859
F	0,048	0,063	0,077	0,078	0,074	0,079	0,069	0,072	0,064	0,032	0,032	0,030	0,036	0,079	0,089	0,071	0,073	0,073	0,062	0,070	0,023	0,023	0,019	0,077	0,071
Cl	0,057	0,085	0,071	0,083	0,088	0,064	0,089	0,055	0,057	0,043	0,051	0,043	0,048	0,051	0,047	0,040	0,042	0,046	0,038	0,082	0,091	0,066	0,112	0,070	0,070
	2,000	2,000	2,000	2,000	2,000	2,000	2,000	2,000	2,000	2,000	2,000	2,000	2,000	2,000	2,000	2,000	2,000	2,000	2,000	2,000	2,000	2,000	2,000	2,000	2,000
Sum cations	15,295	15,497	15,543	15,544	15,496	15,421	15,546	15,488	15,510	15,337	15,367	15,306	15,360	15,553	15,555	15,494	15,517	15,473	15,480	15,496	15,399	15,388	15,373	15,524	15,531
Mg/Fe2+	1,293	1,189	1,052	0,962	0,978	0,890	1,080	1,386	1,535	1,657	1,591	1,618	1,501	1,254	1,202	1,284	1,241	1,334	1,180	1,467	2,490	1,456	4,400	1,184	1,212

Table 1. continued

Thermobarometric results																								
Ps (kb)	2,06	3,65	4,08	4,05	3,80	3,38	4,65	3,77	3,61	2,74	2,70	1,34	2,74	4,38	4,29	3,85	4,16	3,94	3,96	3,63	2,18	1,48	2,35	4,12	4,01
Anderson and Smith (pressure at various thermometers)																									
T (C) HB1*	770,2	817,3	825,6	849,6	827,5	783,7	923,9	844,0	877,3	840,8	840,0	791,7	824,1	916,5	890,7	849,8	854,5	886,4	904,6	859,2	814,4	805,9	758,5	859,8	887,6
P(Kb) HB1*	0,86	1,15	1,27	0,54	1,00	1,73	-1,71	0,49	-0,69	-0,23	-0,23	-0,18	0,23	-1,59	-0,67	0,37	0,46	-0,77	-1,42	-0,09	0,02	-0,36	1,33	0,27	-0,76
T (C) HB2	**773,2**	**800,3**	**794,9**	**804,2**	**809,0**	**789,0**	**841,4**	**806,5**	**818,2**	**786,4**	**782,4**	**747,1**	**796,3**	**832,0**	**821,6**	**808,9**	**814,5**	**826,1**	**838,9**	**817,4**	**787,1**	**744,0**	**764,1**	**818,0**	**826,7**
P(Kb) HB2	**0,80**	**1,58**	**2,07**	**1,82**	**1,49**	**1,62**	**1,25**	**1,52**	**1,09**	**1,12**	**1,18**	**0,60**	**0,91**	**1,33**	**1,55**	**1,53**	**1,63**	**1,14**	**0,79**	**1,13**	**0,64**	**0,77**	**1,23**	**1,51**	**1,18**
T (C) BH	728,0	786,9	804,4	813,8	796,8	768,1	866,3	823,9	827,9	791,7	785,9	725,5	787,0	878,1	863,9	830,2	844,8	854,2	857,9	810,1	744,4	721,7	725,6	830,7	833,7
P(Kb) BH	1,53	1,90	1,84	1,57	1,79	2,06	0,45	1,07	0,83	1,01	1,11	0,89	1,11	-0,15	0,26	0,95	0,77	0,31	0,21	1,32	1,41	1,07	1,84	1,16	0,98

HB 1 refers to Holland and Blundy Hbld-Plag thermometry calibration reaction edenite + 4 quartz = tremolite + albite, HB 2 refers to Holland and Blundy Hbld-Plag thermometry calibration reaction edenite + albite = richterite + anorthite, BH refers to Blundy and Holland Hbld-Plag thermometry calibration reaction edenite + 4 quartz = tremolite + albite. Pressure by Schmidt (Ps), (1992), and Anderson and Smith, (1995). Cations based on 23O and summed to 13. (r:rim, c:core, b:bright, d:dark)

Sr-Nd-Pb-O Isotopes

Sr, Nd, Pb, and O isotope analyses are reported in Table 2. Different samples from the Alaçam granite show initial $^{87}Sr/^{86}Sr$ isotopic ratios ranging from 0.70865 to 0.70911. The samples have initial εNd values ranging from -5.3 to -6.3. Pb isotopic composition ranges from 18.87 to 18.89 for the initial $^{206}Pb/^{204}Pb$ ratio, from 15.69 to 15.70 for the initial $^{207}Pb/^{204}Pb$ ratio, and from 38.98 to 39.00 for the initial $^{208}Pb/^{204}Pb$ ratio. $\delta^{18}O$ values of the Alaçam granite range from 9.5 to 10.5 ‰. One sample (550) has a $\delta^{18}O$-value of 4.5, which is probably related to hydrothermal alteration at the contact with the Alaçam granite resulted in decrease of ^{18}O relative to ^{16}O or enrichment in ^{16}O (Table 2).

Discussion

Emplacement depth of the Alaçam granite

The emplacement depths of the Aegean and NW Anatolian Miocene granitoids are based on two main evidences: 1) geological features which mainly comprise contact relationships between granitoids and host rocks, occurrence of volcanic counterparts of the pluton, or caldera-type structures (Altunkaynak & Yilmaz 1999; Yilmaz *et al.* 2001; Akay 2009; Aydogan *et al.* 2008; Hasözbek *et al.* 2010a, b), 2) geodynamic observations indicating an emplacement depth, such as core complexes and syn-extension emplacement structures (Isik & Tekeli 2001; Jolivet & Brun 2010; Stouraiti *et al.* 2010, and references therein). Evidence based on geological features is as follows: Kozak, Evciler and Kestanbol granitoids crop out with their volcanic counterparts and these granitoids pass gradually into porphyritic volcanic associations which imply a shallow emplacement depth of these granitoids (Altunkaynak & Yilmaz 1998, 1999; Karacik & Yilmaz 1998; Yilmaz *et al.* 2001). The Eğrigöz and Alaçam granitic bodies exhibit wide microgranitic contact zone passing gradually inward into the coarser granitic body that indicates rapid cooling at shallow crustal levels. Rb-Sr biotite ages of 18.8 ± 0.2 Ma from the Eğrigöz granite and 20.01 ± 0.20 Ma from the Alaçam granite are almost concordant with the U-Pb zircon ages demonstrating that rapid cooling took place during emplacement (Hasözbek *et al.* 2010a, b). Besides, the emplacement depth of the granitoids was evaluated from geodynamic observation and various researchers suggest a large scale crustal extension related emplacement model for these granitoids (e.g. Cyclades Miocene plutonic suites, Eğrigöz, Alaçam granites in NW Anatolia) (Isik & Tekeli 2001;

Bozkurt 2004; Seyitoglu *et al.* 2004; Jolivet & Brun 2010; Stouraiti *et al.* 2010). The extension model gave rise to consider an intrusion depth between brittle-ductile transition zone. In general, these types of fault zones can form and evolve in the middle to lower crust (Ramsay 1980; Coward 1984). The location of the transition zone between elastico-frictional (ductile) and quasi-plastic (brittle) behavior, defines an emplacement depth of these granitoids between ca. 15-20 km (Sibson 1977). However, our new Al-in-hornblende thermobarometry from amphiboles of the Alaçam granite is inconsistent with this geodynamic model. Geochronological data indicate a rapid cooling of the granitic body by close consistency between U-Pb zircon age (20.0 ± 1.4 Ma) and Rb-Sr biotite age (20.01 ± 0.20 Ma) (Hasözbek *et al.* 2010b). Therefore, the emplacement mode of the Alaçam granite is inconsistent with the crustal scale extension model which requires deeply seated injection of about 15-20 km into the footwall of a regional detachment fault.

Petrogenesis of the Alaçam granite

Miocene granites of NW Anatolia are mostly peraluminous or slightly metaluminous I-type granitoids (Altunkaynak & Yilmaz 1999; Yilmaz *et al.* 2001; Akay 2009; Aydogan *et al.* 2008; Hasözbek *et al.* 2010a, b). Previous studies on both I-and S-type Miocene granitoids in the southern Aegean indicate a metasedimentary crustal source for their generation and suggests a heterogeneous crustal source rather than a mantle derived component (Stouraiti *et al.* 2010, and references therein).

According to initial $^{87}Sr/^{86}Sr$ versus Rb/Sr and initial $^{87}Sr/^{86}Sr$ versus 1000/Sr diagrams of the Alaçam granite, assimilation played an important role during the evolution of this granite (Figure 6a, b).

A clear distinctive pattern is observed for Pb isotopes when compared with Aegean islands granites. Samples of the Aegean islands show a wide range of $^{206}Pb/^{204}Pb$ (ca. 18.5-19.0) (Juteau *et al.* 1986) (Table 3, Figure 7). In $^{208}Pb/^{204}Pb$ versus $^{206}Pb/^{204}Pb$, $^{207}Pb/^{204}Pb$ versus $^{206}Pb/^{204}Pb$, and $^{87}Sr/^{86}$ Sr versus $^{206}Pb/^{204}Pb$ plots (Figure 7a-c) the Alaçam granite exhibits Pb isotope ratio values than Aegean granitoids indicating more crustal contribution in magma source.

Table 2. Sr-Nd-Pb-O isotope composition of whole rock samples from the Alaçam granite.

A L A C A M G R A N I T E

Sample	Sr(ppm)	Rb(ppm)	$^{87}Rb/^{86}Sr$	$^{87}Sr/^{86}Sr$	$^{87}Sr/^{86}Sr(i)$	Sm(ppm)	Nd(ppm)	$^{147}Sm/^{144}Nd$	$^{143}Nd/^{144}Nd$	$^{143}Nd/^{144}Nd$ (i)	eNd	$^{206}Pb/^{204}Pb$	$^{207}Pb/^{204}Pb$	$^{208}Pb/^{204}Pb$	$\delta\ ^{18}O_{SMOW}$
550	254	163,8	1,866	0,70963	0,70910	4,69	25,4	0,1121	0,51234	0,51233	-5,8	18,873	15,7	39,003	4,5
620	261	188,9	2,094	0,70974	0,70915	5,48	29,4	0,1132	0,51237	0,51235	-5,3	18,89	15,696	38,988	9,5
189	343,5	145,3	1,224	0,70900	0,70865	5,3	31	0,1038	0,51234	0,51233	-5,8	18,896	15,71	39,002	10,5
1045	309,9	124,1	1,159	0,70939	0,70906	6,4	36,2	0,1073	0,51232	0,51231	-6,2	18,902	15,699	39,017	10,3
859	316,6	135,4	1,238	0,70931	0,70895	4,9	23,7	0,1255	0,51231	0,5123	-6,4	18,891	15,698	39,007	10,3
505	260	164	1,825	0,70963	0,70911	5,33	30,3	0,1068	0,51234	0,51233	-5,8	18,879	15,702	38,997	9,9

Sr, Rb, Sm, Nd concentrations are in ppm. (i): initial. SMOW: Standard Mean Ocean Water. Pb is corrected by 0.8‰ mass unit

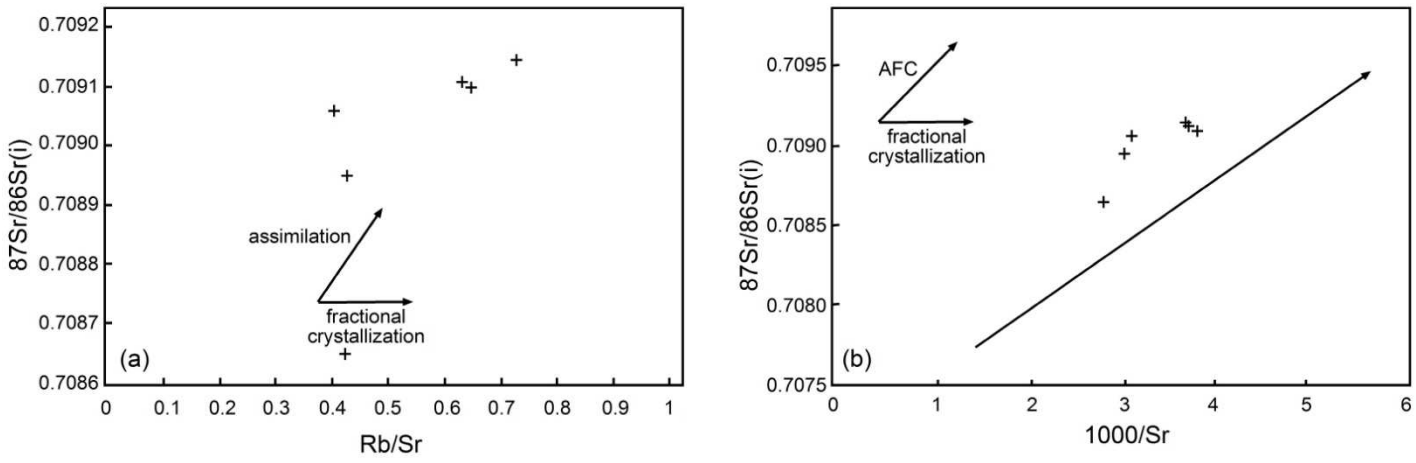

Figure 6. (a) Initial $^{87}Sr/^{86}Sr$ vs Rb/Sr, (b) Initial $^{87}Sr/^{86}Sr$ vs 1000/Sr ratios for the Alaçam granite (see Table 3) implying assimilation rather than fractional crystallization during magma genesis.

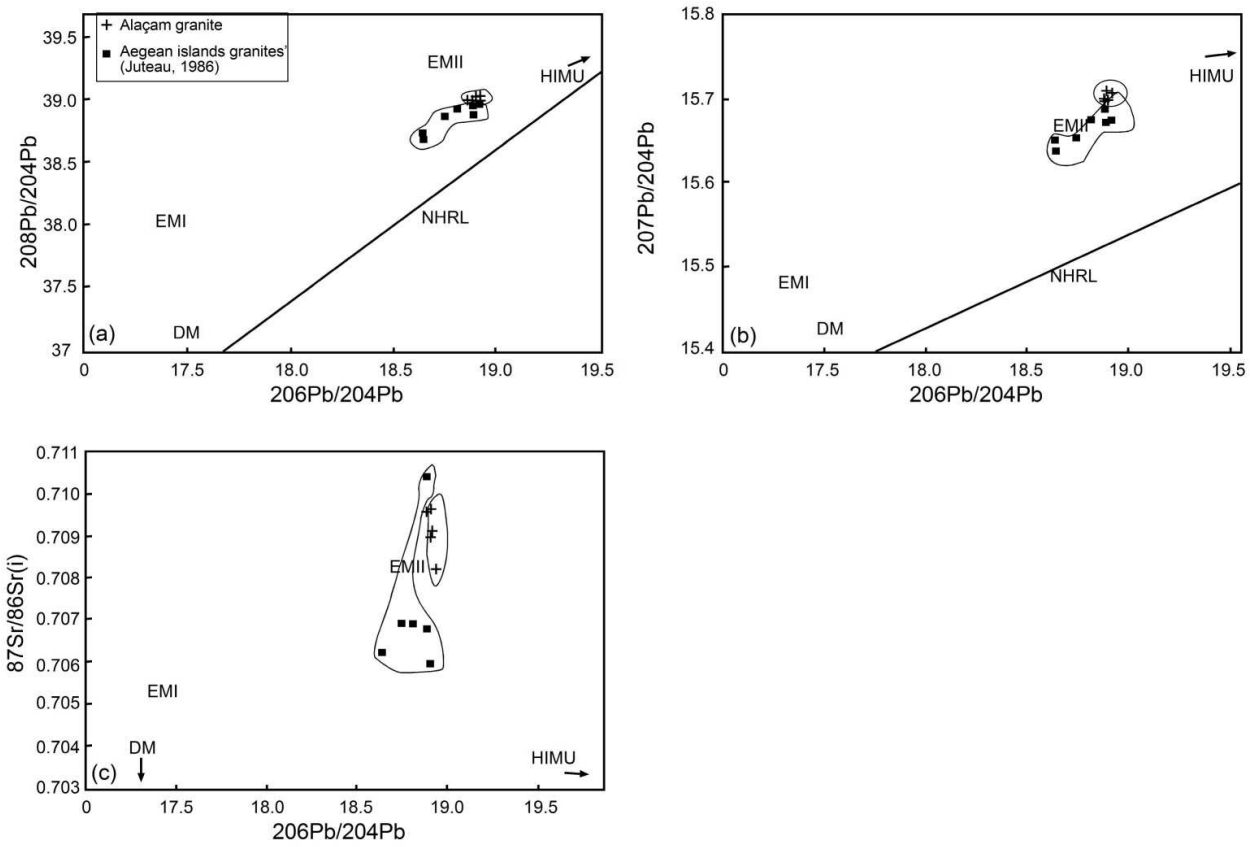

Figure 7. (a) $^{208}Pb/^{204}Pb$ vs $^{206}Pb/^{204}Pb$, (b) $^{207}Pb/^{204}Pb$ vs $^{206}Pb/^{204}Pb$, (c) initial $^{87}Sr/^{86}Sr$ vs $^{206}Pb/^{204}Pb$ ratios for the Alaçam granite and the Aegean islands granites' (Juteau et al. 1986). EM: Enriched Mantle, DP: Depleted Mantle, NHRL: Northern Hemisphere Reference Line, HIMU: high-μ (Hart, 1984; 1986; Hart et al. 1988).

The Alaçam granite displays lower initial $^{87}Sr/^{86}Sr$ and $\delta^{18}O$ values compared to the I-type granitoids of Tinos and Ikaria (Altherr *et al.* 1998) in central Aegean (Table 3, Figure 8). In this diagram, a remarkable distinction is observed between Aegean granites and Alaçam granite. Altherr *et al.* (1998) proposed the involvement of older recycled crustal material in order to explain the high initial $^{87}Sr/^{86}Sr$ and $\delta^{18}O$ values of the Aegean granites. Sr-Nd-O isotopic constraints support an older crustal source (Menderes Massif) for the Alaçam granite as well, rather than a mantle contribution to the source which was previously envisaged for the Aegean Miocene granitoids (Juteau *et al.* 1986; Dilek & Altunkaynak 2007). Additional evidence for an older crustal source can be gained from the U-Pb zircon upper intercept age of the Alaçam granite and adjacent granite bodies of 550-500 Ma ages. (Hasözbek *et al.* 2010a, b).

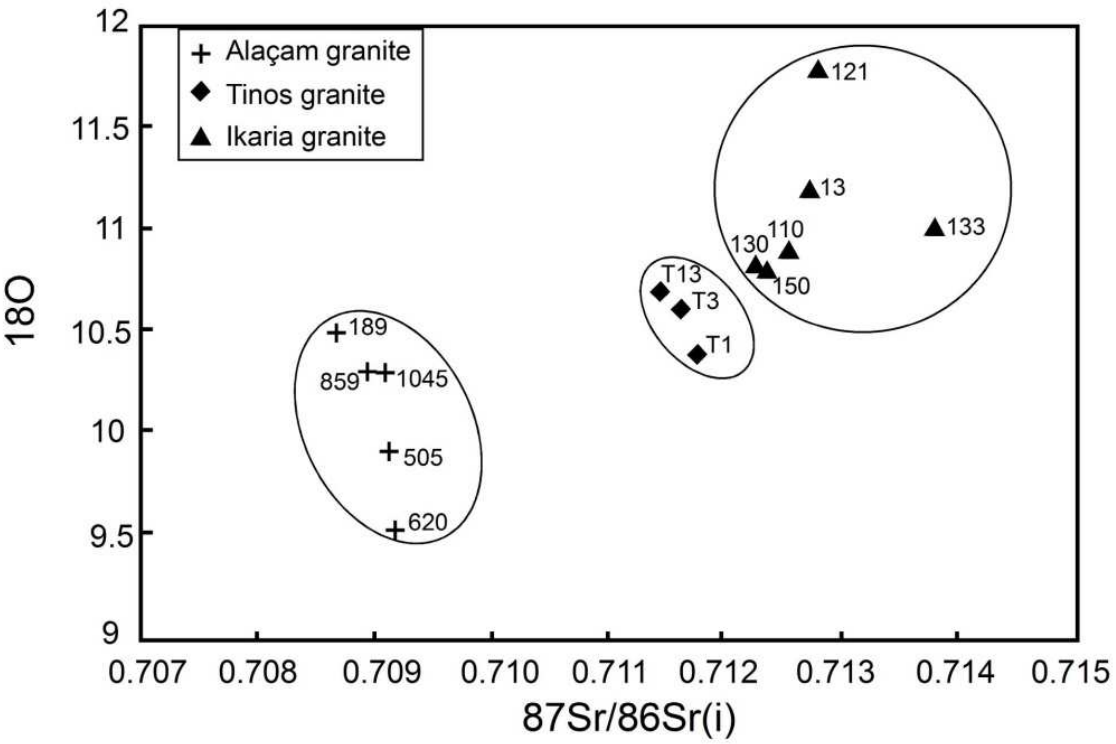

Figure 8. Whole rock $\delta^{18}O$ versus initial $^{87}Sr/^{86}Sr$ of the Alaçam granite (this study), Ikaria and Tinos granites (Altherr et al. 1998)

The $\varepsilon Nd_{(i)}$ versus $^{87}Sr/^{86}Sr_{(i)}$ diagram in Figure 9 shows the isotopic compositions of the Alaçam granite with Miocene granitoids of central Aegean (Ikera, Tinos) and meta-sedimentary rocks from both Aegean islands and the Menderes Massif. Again, the granite defines a distinct area in comparison to the granitoids of the Aegean islands (Ikera, Tinos).

Moreover, all granite samples from NW Anatolia and the Aegean islands plot in the crustal field.

Our Sr-Nd (Figure 6), Pb (Figure 7) and O (Figure 8) isotope data show that crustal assimilation played an important role on the generation of the Alaçam granite. We performed an AFC modeling by using $^{143}Nd/^{144}Nd(i)$ vs. $^{87}Sr/^{86}S(i)$ isotope data for demonstrating this process. We selected representative basalt composition from Brique (1986) for mantle end-member and granite as a contaminant from Juteau (1986). This modeling reveals that the "r"-ratio (assimilation/fractional crystallization) is between 0.20-0.35 (Figure 10) which implies that the mixing processes only exhibit between 20-35% during crystallization.

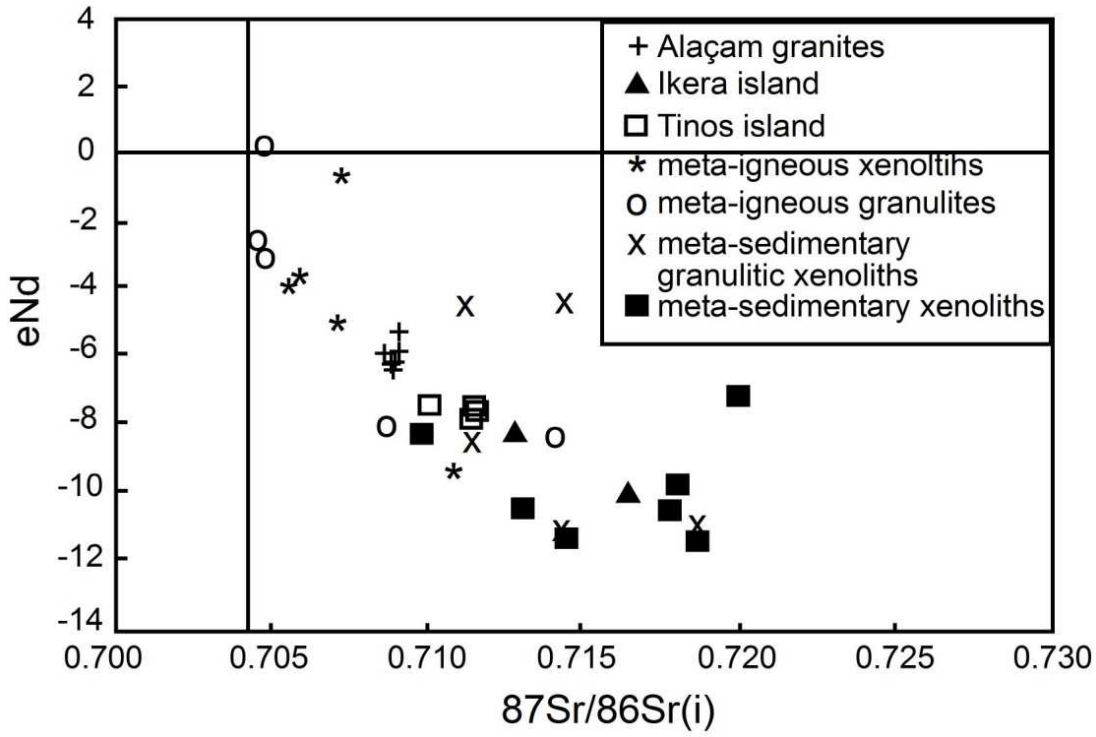

Figure 9. $\mathcal{E}Nd_{(i)}$ versus $^{87}Sr/^{86}Sr_{(i)}$ ratios for the Alaçam granite (see Table 3) and various Miocene granitoids (Tinos, Ikaria) (Stouraiti et al. 2010, and and references therein) from the Aegean islands and basement rocks (metagranite

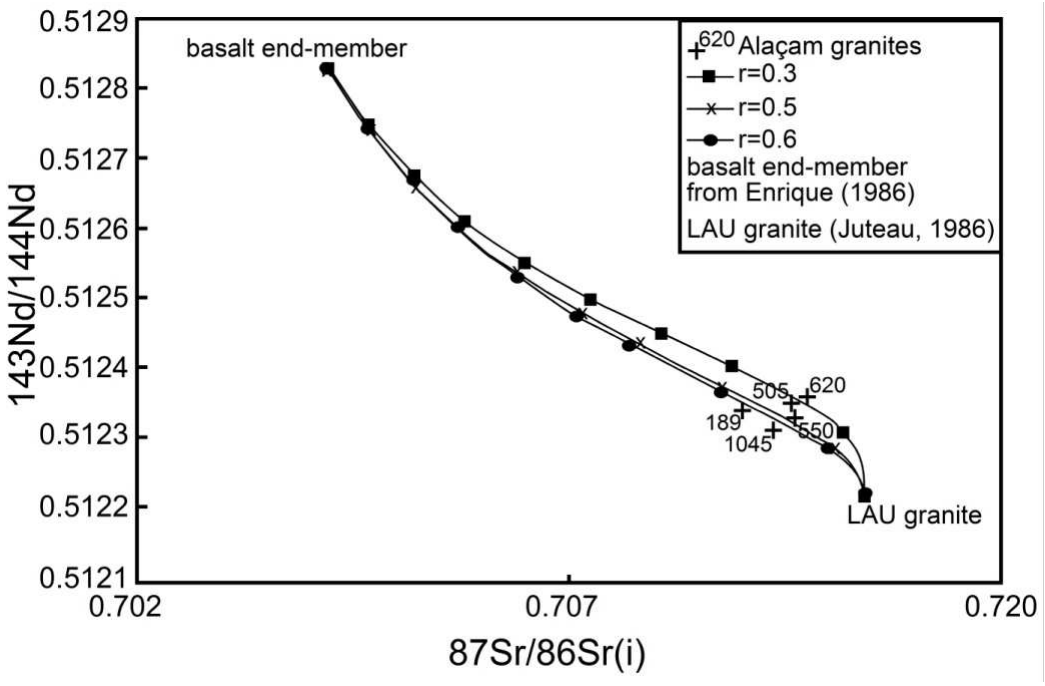

Figure 10. AFC modeling of ^{143} Nd/^{144}Nd (i) vs. ^{87}Sr/^{86}Sr(i) ratios for the Alaçam granite. End member (A) is basalt average from (Briqueu 1986) composition, ^{87}Sr/^{86}Sr(i)=0,70420, ^{143}Nd/^{144}Nd(i)=0,51283, Sr=200 ppm, Nd=10 ppm. Contaminant (B) is granite from (Juteau 1986). ^{87}Sr/^{86}Sr(i)=0,71023, ^{143}Nd/^{144}Nd(i)=0,51222, Sr=335 ppm, Nd=34,4 ppm. DSr: 2, DNd: 1

Conclusions

The following conclusions about the Alaçam granite can be made based on new Al-in-hornblende barometry and isotopic data:

1) Estimated emplacement depth for the Alaçam granite is calculated as ca. 2-7 km by Al-in-hornblende barometry. This shallow crustal emplacement is compatible with geological and geochronological data. Such model does not support previously mentioned syn extension (low angle fault) related mechanism for the emplacement of the Alaçam granite, along a ductile-brittle transition zone (ca. 10-15km).

2) Sr-Nd-Pb-O isotopic compositions of the Alaçam granite point to derivation from a meta-sedimentary (metagreywacke type) source. Our new isotope results are with dehydration melting of metaluminous older crustal sources as previosly suggested by Stouraiti *et al.* (2010 and references therein). Furthermore, upper intercept age data of ca.500-550 Ma (U-Pb zircon age) from the Miocene Alaçam, Eğrigöz and Koyunoba granites support a derivation from similar older source (Hasözbek *et al.* 2000a, b).

3) Isotopic compositions of the Alaçam granite indicate a distinct isotopic ratio differences, however a common older crustal sources are observed for Aegean granites and the Alaçam granite.

4) AFC modeling points out an evolution by crustal assimilation during crystallization of the Alaçam granite which probably indicates that the crustal derived melt was also contaminated by other crustal source.

Acknowledgements

This study was financially supported by the DAAD, Scientific and Technical Research Council of Turkey (TUBITAK) and Dokuz Eylul University, Scientific Research Projects Foundation (project no: 2009. KB. FEN. 074). A. Okay, O. Candan, E. Koralay, G. Topuz, E. V. Muratçay and C. Pin are thanked for help and discussion. T. Wenzel, Institute of Geoscience, Tübingen is thanked for support during microprobe analyses. C. Shang, and E. Reitter, Department of Geochemistry, Tübingen University, are thanked for technical help.

REFERENCES

AKAL, C. 2003. Mineralogy and geochemistry of Melilite Leucitites,Balıkesir, Afyon (Turkey). *Turkish Journal of Earth Sciences, **12*** 215-239

AKAY, E. 2009. Geology and petrology of the Simav Magmatic Complex (NW Anatolia) and its comparison with the Oligo-Miocene granitoids in NW Anatolia: implications on Tertiary tectonic evolution of the region. *International Journal of Earth Sciences, **98***, 1655-1675.

ALDANMAZ, E., PEARCE, J., THRIWALL, M. F., & MITCHELL, J. 2000. Petrogenetic evolution of late Cenozoic, post-collision volcanism in western Anatolia, Turkey. *Journal of Volcanology and Geothermal Research, **102***, 67-95.

ALTHERR, R., HENJES-KUNST, F., MATTHEWS, A., FRIEDRICHSEN, H., & HANSEN, B. T. 1998. O-Sr isotopic variations in Miocene granitoids from the Aegean: evidence for an origin by combined assimilation and fractional crystallization. *Contributions to Mineralogy and Petrology, **100***, 528-541.

ALTHERR, R., & SIEBEL, W. 2002. I-type plutonism in a continental back-arc setting: Miocene granitoids and monzonites from the central Aegean Sea, Greece. *Contributions to Mineralogy and Petrology, **143***, 397-415.

ALTHERR, R., TOPUZ, G., MARSCHALL, H., ZACK, T., & LUDWIG, T. 2004. Evolution of a tourmaline-bearing lawsonite eclogite from the Elekdag area (Central Pontides, N Turkey): evidence for infiltration of slab-derived B-rich fluids during exhumation. *Contributions to Mineralogy and Petrology, **148***, 409-425.

ALTUNKAYNAK, S. 2007. Collision-driven slab breakoff magmatism in northwestern Anatolia, Turkey. *Journal of Geology, **115***, 63-82.

ALTUNKAYNAK, S., & YILMAZ, Y. 1998. The Mount Kozak magmatic complex, western Anatolia. *Journal of Volcanology and Geothermal Research, **85*** 1-4, 211-231.

ALTUNKAYNAK, S., & YILMAZ, Y. 1999. The Kozak Pluton and its emplacement. *Geological Journal, **34***, 257-274.
ANDERSON, J. L. & SMITH, D. R. 1995. The effect of temperature and oxygen fugacity on Al-in-hornblende barometry. *American Mineralogist*, **80**, 549-559.
ARMSTRONG. J.T., 1991. Quantitative elemental analysis of individual microparticles with electron beam instruments. In: Heinrich, K.F.J. and Newbury, D.E., Editors, 1991. *Electron Probe Quantitation*, Plenum, New York, 261–315.
AYDOGAN, M. S., COBAN, H., BOZCU, M., & AKINCI, O. 2008. Geochemical and mantle-like isotopic (Nd, Sr) composition of the Baklan Granite from the Muratdagi Region (Banaz, Usak), western Turkey: Implications for input of juvenile magmas in the source domains of western Anatolia Eocene-Miocene granites. *Journal of Asian Earth Sciences*, ***33***, 155-176.
BECCALUVA, L., DI GIROLAMO, P. & SERRI, G. 1991. Petrogenesis and tectonic setting of the Roman volcanic province, Italy. *Lithos* **26**, 191–221
BLUNDY, J. D. & HOLLAND, T. J. B. 1990. Calcic amphibole equilibria and a new amphibole-plagioclase geothermometer. *Contributions to Mineralogy and Petrology,* **104**, 208-224.
BOZKURT, E. 2004. Granitoid rocks of the southern Menderes Massif (southwestern Turkey): field evidence for Tertiary magmatism in an extensional shear zone. *International Journal of Earth Sciences, **93***, 52-71.
BOZKURT, E., & OBERHÄNSLI, R. 2001. Menderes Massif (Western Turkey): structural, metamorphic and magmatic evolution - a synthesis. *International Journal of Earth Sciences, **89***, 679-708.
BRICHAU, S., RING, U., CARTER, A., MONIE, P., BOLHAR, R., STOCKLI, D., & BRUNEL, M. 2007. Extensional faulting on Tinos island, Aegean sea, Greece: How many detachments? *Tectonics, **26,*** 4-16
BRIQUEU, L., JAVOY, M., LANCELOT, J. R., & TATSUMOTO, M. 1986. Isotope Geochemistry of Recent Magmatism in the Aegean Arc - Sr, Nd, Hf, and O Isotopic-Ratios in the Lavas of Milos and Santorini - Geodynamic Implications. *Earth and Planetary Science Letters*, ***80*** 1-2, 41-54
CANDAN, O., CETINKAPLAN, M., OBERHANSLI, R., RIMMELE, G., & AKAL, C. 2005. Alpine high-P/low-T metamorphism of the Afyon Zone and implications for the metamorphic evolution of Western Anatolia, Turkey. *Lithos, **84***, 102-124.
CLAYTON, R. N. & MAYEDA, T. K. 1963. The use of bromine pentafluoride in the extraction of oxygen from oxides and silicates for isotopic analysis. *Geochemica Cosmochimica Acta* **27**, 43-52.
COWARD, M. P. 1984. Precambrian crust: examples from NW Scotland and southern Africa and their significance, in Kröner, A., and Greiling, R., eds., Precambrian tectonics ilustrated. *Stuttgart, e., Schweizerbartische Verlangsbuchhandlung (Nägele u. Obermiller)*, 207-235.
DILEK, Y., & ALTUNKAYNAK, S. 2007. Cenozoic crustal evolution and mantle dynamics of post-collisional magmatism in western Anatolia. *International Geology Review, **49***, 431-453.
DILEK, Y., & ALTUNKAYNAK, S. 2009. Geochemical and temporal evolution of Cenozoic magmatism in western Turkey: mantle response to collision, slab breakoff, and lithospheric tearing in an orogenic belt. *Geol Soc London Spec Pub In: van Hinsbergen, D. J. J., Edwards, M. A. & Govers, R., (Eds), **311***, 213-234.

GÜNGÖR, T., & ERDOĞAN , B. 2001. Emplacement age and direction of the Lycian nappes in the Söke-Selçuk region, western Turkey. *International Journal of Earth Sciences*, **89**, 874-882.
GÜNGÖR, T., & ERDOĞAN, B. 2002. Tectonic significance of mafic volcanic rocks in a Mesozoic sequence of the Menderes Massif, West Turkey, *International Journal of Earth Sciences*, **91**, 386-397.
HAMMARSTROM, J. A., & ZEN, E. A. 1986. Aluminium in hornblende: an emprical igneous geobarometer. *American Mineralogist, **71***, 1297-1313.
HART, S.R., 1984. A large-scale isotope anomaly in the Southern Hemisphere mantle. *Nature* **309**, 753-757
HART, S.R., 1988. Heterogeneous mantle domains: signatures, genesis and mixing chronologies. *Earth and Planetary Science Letters* **90**, 273-296
HART, S.R., GERLACH, D.C., WHITE, W.M., 1986. A possible new Sr-Nd-Pb mantle array and consequences for mantle mixing. *Geochimica Cosmochimica Acta* **50**, 1551-1557.
HASÖZBEK, A., AKAY, E., ERDOGAN, B., SATIR, M., & SIEBEL, W. 2010a. Early Miocene granite formation by detachment tectonics or not? A case study from the northern Menderes Massif (Western Turkey). *Journal of Geodynamics-in press-*.
HASÖZBEK, A., SATIR, M., ERDOĞAN, B., AKAY, E., & SIEBEL, W. 2010b. Early Miocene post-collisional magmatism in NW Turkey: geochemical and geochronological constraints. *International Geology Review-in press-*.
HOLLAND, T. & BLUNDY, J. 1994. Non-ideal interactions in calcic amphiboles and their bearing on amphibole-plagioclase thermometry. *Contribution in Mineralogy and Petrology* **116**, 433-47.
HOLLISTER, L. S., GRISSOM, G. C., PETERS, E. K., STOWELL, H. H., & SISSON, V. B. 1987. Confirmation of the emprical correlation of Al in hornblende with pressure of solidification of calc-alkaline plutons. *American Mineralogist, **72***, 231-239.
ILBEYLI, N., & KIBICI, Y. 2009. Collision-related granite magma genesis, potential sources and tectono-magmatic evolution: comparison between central, northwestern and western Anatolia (Turkey). *International Geology Review, **51***, 252-278.
ISIK, V., SEYITOGLU, G., & CEMEN, I. 2003. Ductile-brittle transition along the Alasehir detachment fault and its structural relationship with the Simav detachment fault, Menderes Massif, western Turkey. *Tectonophysics, **374*** 1-2, 1-18.
ISIK, V., & TEKELI, O. 2001. Late orogenic crustal extension in the northern Menderes Massif (western Turkey): evidence for metamorphic core complex formation. *International Journal of Earth Sciences, **89***, 757-765.
JOLIVET, L., & BRUN, J. P. 2010. Cenozoic geodynamic evolution of the Aegean. *International Journal of Earth Sciences, **99***, 109-138.
JUTEAU, M., MICHARD, A., & ALBAREDE, F. 1986. The Pb-Sr-Nd isotope geochemistry of some recent circum-Mediterranean granites. *Contributions to Mineralogy and Petrology, **92***, 331-340.
KARACIK, Z., & YILMAZ, Y. 1998. Geology of the ignimbrites and the associated volcano plutonic complex of the Ezine area, northwestern Anatolia. *Journal of Volcanology and Geothermal Research, **85***, 251-264.

LEAKE, B.E., WOOLLEY, A. R., ARPS, C. E. S., BIRCH, W. D., GIBERT, M.C.,GRICE,J.D.,HAWTHORNE, F. C., KATO, A., KISCH, H. J., KRIVOVICHEV, V. G., LINTHOUT, K.,LAIRD, J., MANDARINO, J., MARESCH, W. V., NICKEL, E. H., ROCK, N., M., S.,SCHUMACHER, J. C., STEPHENSON, N. C. N., WHITTAKER, E. J. W. and YOUZHI,G., 1997. Nomenclature of Amphiboles: Report of the Subcomittee on Amphiboles of the International Mineralogical Association Commission on New Minerals and Mineral Names, *Mineralogical Magazine, 61*, 295-321.

NEUBAUER, F. & RAUMER, J.V. 1993. The Alpine basement-linkage between Variscides and east-Mediterranean mountain belt. In: RAUMER, J.F. & NEUBAUER, F. (eds), Pre Mesozoic Geology in the Alps. *Springer-Verlag*, 641–664.

OKAY, A. I. 1980. Lawsonite zone blueschists and a sodic amphibole producing reaction in the Tavsanli region, Northwest Turkey. *Contributions to Mineralogy and Petrology, **75***, 179-186.

OKAY, A. I. 1982. Incipient Blueschist Metamorphism and Metasomatism in the Tavsanli Region, Northwest Turkey. *Contributions to Mineralogy and Petrology, **79*** 4, 361-367.

RAMSAY, J. G. 1980. Shear zone geometry: a review. *Journal of Sructural Geology, **2***, 83-99.

RING, U., & COLLINS, A. S. 2005. U-Pb SIMS dating of synkinematic granites: timing of core-complex formation in the northern Anatolide belt of western Turkey. *Journal of the Geological Society London, **162***, 289-298.

SCHMIDT, M. W. 1992. Amphibole composition in tonalite as a function of pressure: an experimental calibration of the Al-in-hornblende barometer. *Contributions to Mineralogy and Petrology,* **110**, 304-310.

SEYITOGLU, G., ISIK, V., & CEMEN, I. 2004. Complete Tertiary exhumation history of the Menderes massif, western Turkey: an alternative working hypothesis. *Terra Nova, **16***, 358-364.

SIBSON, R. H. 1977. Fault rocks and fault mechanisms. *Journal of the Geological Society (London), **133***, 191-213.

STOURAITI, C., MITROPOULOS, P., TARNEY, J., BARREIRO, B., MCGRATH, A. M., & BALTATZIS, E. 2010. Geochemistry and petrogenesis of late Miocene granitoids, Cyclades, southern Aegean: Nature of source components. *Lithos, **114***, 337-352.

TAYLOR, S.R., MCLENNAN, S.M., 1985. The continental crust: Its composition and evolution. *Blackwell,* Oxford.

THOMSON, S. N., & RING, U. 2006. Thermochronologic evaluation of postcollision extension in the Anatolide orogen, western Turkey. *Tectonics, **25***, 1-20.

TULLOCH, A. J., & CHALLIS, G. A. 2000. Emplacement depths of Paleozoic-Mesozoic plutons from western New Zealand estimated by hornblende-Al geobarometry. *New Zealand Journal of Geology and Geophysics, **43***, 555-567.

WILSON M. 1989. Igneous Petrogenesis, Unwin Hyman Ltd., London, UK, 466p.

YILMAZ, Y., GENC, S. C., KARACIK, Z., & ALTUNKAYNAK, S. 2001. Two contrasting magmatic associations of NW Anatolia and their tectonic significance. *Journal of Geodynamics, **31***, 243-271.